

**A Numerical Investigation of the Effects of  
Freshwater Inflow on the Flushing in Boston's  
Inner Harbor**

by

Amy Betty Jo Chan

S.B., Environmental Engineering

S.B., Civil Engineering

Massachusetts Institute of Technology, 1993

Submitted to the Department of Civil and Environmental  
Engineering

in partial fulfillment of the requirements for the degree of  
Master of Science in Civil and Environmental Engineering

at the

MASSACHUSETTS INSTITUTE OF TECHNOLOGY

September 1995

© Massachusetts Institute of Technology 1995. All rights reserved.

Author .....  
Department of Civil and Environmental Engineering  
15 August 1995

Certified by .....  
E. Eric Adams  
Senior Research Engineer  
Thesis Supervisor

Accepted by .....  
Joseph M. Sussman  
Chairman, Departmental Committee on Graduate Students

MASSACHUSETTS INSTITUTE  
OF TECHNOLOGY

OCT 25 1995

Barker Eng

# A Numerical Investigation of the Effects of Freshwater Inflow on the Flushing of Boston's Inner Harbor

by

Amy Betty Jo Chan

Submitted to the Department of Civil and Environmental Engineering  
on 15 August 1995, in partial fulfillment of the  
requirements for the degree of  
Master of Science in Civil and Environmental Engineering

## Abstract

Contaminant transport within an estuarine environment is usually dominated by two mechanisms: oscillatory tidal forcing and freshwater flow into the estuary. It is these two forces that govern the residence time and flushing rate of a coastal embayment. However, there often is little known about the actual flushing rates and how these rates may vary under different conditions. Estimates can be determined through field experiments and numerical studies.

Two field studies that evaluated the residence time of freshwater in Boston's Inner Harbor. Between 1951 and 1952, Bumpus *et al.* measured the amount of freshwater in the Inner Harbor and the mean freshwater runoff from its rivers in order to calculate the residence time. During July 1992 Adams *et al.*, conducted a fluorescent tracer experiment in Boston's Inner Harbor. A 5.5 hour discharge of freshwater from the Charles River, which is the major freshwater source in the Harbor, was marked with a conservative tracer and then monitored for one week. Based on the time rate of change of the total tracer mass, a residence time of 3.75 days was calculated.

A 3-D numerical model was used to simulate effects of extreme freshwater inflow, which are expected to transport the majority of the pollutants from storm water and combined sewer overflows, and the effects of various freshwater input scenarios, and to determine the effects of these conditions on the residence time of the discharged freshwater. The model included the relevant physical factors involved with estuarine circulation. It was calibrated to the 1992 field study and was used to establish a relationship between the simulated residence time and freshwater inflow conditions. Model results were in agreement with the field study data, and indicated that the magnitude of the average freshwater flow rate had more significant effects on the residence time than the time sequence of freshwater discharge into the Inner Harbor.

Thesis Supervisor: E. Eric Adams  
Title: Senior Research Engineer

# Acknowledgments

So many people have been a great help to me throughout my entire thesis process, from my introduction to the project until the last page was printed out.

I'd like to thank my advisor, Dr. Adams, for his guidance, feedback and support during my project and writing process. My research group and other members of Parsons Lab have also helped me at different stages: Xue-Yong Z., Ling T., Scott S., Jennifer C., Seizo U., and Chin W. Their advice and insights have been life-savers to me!

My family has been a warm and continuous source of support. understanding and love. To my grandparents, Thomas and Po Yee Lee, Aunt Marie, Uncle Tony, cousin Josie, Uncle Pak Soon, and Grandma and Grandpa Raush, thank you for your love and support and for always caring for me. And to my parents, Pak Tung and Jane Chan, thank you for always being there for me and for providing me the love and encouragement that has always guided me.

Most of all, a huge thanks to my husband and best friend, Edgar, who is always in my cheering section. Thank you for putting up with my hours, and sometimes days, of stress, frustration and impatience. You have always been an inspiration to me. I thank you for all of your support, knowledge, understanding and love.

This is dedicated to my parents and to my husband.

Support for this research was provided by the Massachusetts Water Resources Authority and administered through the MIT Sea Grant College Program.

## **Biographical note**

Amy B. Chan was born in Boston, Massachusetts. She grew up in Miami, Florida, where she lived since a toddler. She graduated with honors from Miami Killian Senior High School in June 1989. She received her undergraduate education from the Massachusetts Institute of Technology, where in May 1993 she received dual S.B. degrees in Environmental Engineering and Civil Engineering with a minor in Music.

Amy was married in June 1995. Her name has been changed to Amy Chan Hilton, and all future publications and work will be signed under this name.



# Contents

- 1 Introduction 13**
  - 1.1 Motivation for study . . . . . 13
  - 1.2 The problem . . . . . 14
  
- 2 Theory 18**
  - 2.1 Flushing parameters . . . . . 18
    - 2.1.1 Residence time . . . . . 18
    - 2.1.2 Flushing rate . . . . . 20
  - 2.2 Mixing in estuaries . . . . . 21
    - 2.2.1 Causes of mixing . . . . . 21
    - 2.2.2 Components of estuarine mixing . . . . . 22
  
- 3 Field studies 25**
  - 3.1 Bumpus *et al.* . . . . . 25
    - 3.1.1 Background . . . . . 25
    - 3.1.2 Results . . . . . 26
  - 3.2 Boston Inner Harbor dye study . . . . . 28
    - 3.2.1 Background . . . . . 28
    - 3.2.2 Results . . . . . 30
  
- 4 Numerical Modeling 33**
  - 4.1 The model, ECOM-si . . . . . 33
    - 4.1.1 Model features . . . . . 34

4.1.2	Methods and schemes . . . . .	35
4.2	Model formulation . . . . .	37
4.2.1	The domain . . . . .	37
4.2.2	Boundary conditions . . . . .	41
4.2.3	Initial conditions and forcings . . . . .	42
4.2.4	Parameter values . . . . .	42
4.3	Model Simulations . . . . .	44
4.3.1	Base case . . . . .	44
4.3.2	Test scenarios . . . . .	46
4.3.3	Summary of simulations . . . . .	49
4.4	Modeling Results . . . . .	49
4.4.1	Base case . . . . .	50
4.4.2	Test Scenarios . . . . .	53
4.4.3	Summary . . . . .	68
<b>5</b>	<b>Discussion</b>	<b>71</b>
5.1	Calibration of numerical model . . . . .	71
5.2	Comparison between field studies and model . . . . .	82
5.3	Effects of freshwater inflow on flushing . . . . .	83
5.3.1	Varying continuous freshwater flow rates . . . . .	83
5.3.2	Varying freshwater input sequence . . . . .	83
5.3.3	Vertical diffusivity model sensitivity . . . . .	87
<b>6</b>	<b>Conclusion</b>	<b>95</b>
<b>7</b>	<b>Further study</b>	<b>98</b>
<b>A</b>	<b>Dye study concentration contours</b>	<b>99</b>
<b>B</b>	<b>Model simulation plots</b>	<b>104</b>
B.1	Base case . . . . .	104
B.1.1	Base case velocity vectors . . . . .	104

B.1.2	Base case concentration contours . . . . .	112
B.2	Variation in vertical diffusivity . . . . .	119
<b>Bibliography</b>		<b>126</b>

# List of Figures

1-1	Map of Boston Harbor and locations of CSOs . . . . .	15
1-2	Map of Boston Inner Harbor. . . . .	16
3-1	Flushing time as a function of mean runoff, after Bumpus <i>et al.</i> . . . .	27
3-2	New Charles River Dam flow rates as a function of time after high tide.	29
3-3	Fitting a line through $\ln(\text{mass})$ vs. time for dye study data . . . . .	31
3-4	Tracer mass as a function of time for dye study . . . . .	32
4-1	Features of the model domain. . . . .	38
4-2	Plan view of the model grid. . . . .	40
4-3	Time variation of freshwater flow rate at the Charles River Dam and Mystic River for the model base case. . . . .	45
4-4	Freshwater flow rate variation over time for Charles River Dam during the 2 hours around each high tide. . . . .	48
4-5	Tracer mass varying with time for the base case. . . . .	51
4-6	Fitting a line through $\ln(\text{mass})$ vs. time for the base case. . . . .	52
4-7	Tracer mass extrapolated to zero for the base case . . . . .	53
4-8	Tracer mass varying with time for continuous discharge with half of freshwater volume as base case. . . . .	54
4-9	Fitting a line through $\ln(\text{mass})$ vs. time for continuous discharge with half of freshwater volume as base case. . . . .	55
4-10	Tracer mass extrapolated to zero for continuous discharge with half of freshwater volume as base case . . . . .	55

4-11	Tracer mass varying with time for continuous discharge with same freshwater volume as base case. . . . .	56
4-12	Fitting a line through $\ln(\text{mass})$ vs. time for continuous discharge with same freshwater volume as base case. . . . .	57
4-13	Tracer mass extrapolated to zero for continuous discharge with same freshwater volume as base case . . . . .	57
4-14	Tracer mass varying with time for constant discharge with twice the freshwater volume as base case. . . . .	58
4-15	Fitting a line through $\ln(\text{mass})$ vs. time for constant discharge with twice the freshwater volume as base case. . . . .	59
4-16	Tracer mass as a function of time for twice freshwater volume . . . . .	59
4-17	Tracer mass varying with time for five times the freshwater volume as base case. . . . .	60
4-18	Fitting a line through $\ln(\text{mass})$ vs. time for five times the freshwater volume as base case. . . . .	61
4-19	Tracer mass as a function of time for five time freshwater volume . . . . .	61
4-20	Tracer mass varying with time for ten times the freshwater volume as base case. . . . .	62
4-21	Fitting a line through $\ln(\text{mass})$ vs. time for ten times the freshwater volume as base case. . . . .	63
4-22	Tracer mass as a function of time for ten times freshwater volume . . . . .	63
4-23	Tracer mass varying with time for discharge during the 2 hours around each high tide . . . . .	64
4-24	Fitting a line through $\ln(\text{mass})$ vs. time for discharge during the 2 hours around each high tide, with the same freshwater volume as base case. . . . .	65
4-25	Tracer mass as a function of time for discharge around high tide . . . . .	65
4-26	Tracer mass varying with time for the $u_{m01}=2.5 \times 10^{-5} \text{ m}^2/\text{s}$ case. . . . .	66
4-27	Fitting a line through $\ln(\text{mass})$ vs. time for the $u_{m01}=2.5 \times 10^{-5} \text{ m}^2/\text{s}$ case. . . . .	67

4-28	Tracer mass extrapolated to zero for the $umol=2.5 \times 10^{-5} \text{ m}^2/\text{s}$ case .	67
4-29	Tracer mass varying with time for the $umol=7.5 \times 10^{-5} \text{ m}^2/\text{s}$ case. . .	68
4-30	Fitting a line through $\ln(\text{mass})$ vs. time for the $umol=7.5 \times 10^{-5}$ $\text{m}^2/\text{s}$ case. . . . .	69
4-31	Tracer mass extrapolated to zero for the $umol=7.5 \times 10^{-5} \text{ m}^2/\text{s}$ case .	69
4-32	Summary of residence times as a function of average Charles River flow rate from model simulations. . . . .	70
5-1	Comparison of tracer concentration vertical profile at 34 hrs, upstream	73
5-2	Comparison of tracer concentration vertical profile at 34 hrs, down- stream . . . . .	74
5-3	Comparison of tracer concentration vertical profile at 84 hrs, upstream	75
5-4	Comparison of tracer concentration vertical profile at 84 hrs, down- stream . . . . .	76
5-5	Comparison of tracer concentration vertical profile at 115 hrs, upstream	77
5-6	Comparison of tracer concentration vertical profile at 115 hrs, down- stream . . . . .	78
5-7	Comparison of tracer concentration vertical profile at 134 hrs, upstream	79
5-8	Comparison of tracer concentration vertical profile at 134 hrs, down- stream . . . . .	80
5-9	A comparison of dye study data and model base case values of tracer concentration ( $\mu\text{g}/\text{l}$ ) in the Inner Harbor as a function of time . . . .	81
5-10	Residence time as a function of average flow rate from field study and model results. . . . .	84
5-11	Time variation of tracer concentration ( $\mu\text{g}/\text{l}$ ) in the Inner Harbor for various constant freshwater discharge rates. . . . .	85
5-12	Time variation of tracer concentration ( $\mu\text{g}/\text{l}$ ) in the Inner Harbor for the base case, continuous discharge, high tide simulations. . . . .	86
5-13	Time variation of tracer concentration ( $\mu\text{g}/\text{l}$ ) in the Inner Harbor for various $umol$ values. . . . .	88

5-14	$K_h$ variation with time for base case. . . . .	89
5-15	$K_h$ variation with time for ten times the base case average flow rate. . . . .	90
5-16	Vertical profiles of $K_h$ and $u$ at model time $t = 8$ hrs. . . . .	91
5-17	Vertical profiles of $K_h$ , $u$ , and tracer concentration at model time $t = 72$ hrs. . . . .	92
5-18	Vertical profiles of $K_h$ , $u$ , and tracer concentration at model time $t = 80$ hrs. . . . .	93
A-1	Ccontours of tracer concentration ( $\mu\text{g/l}$ ) for dye study at 34 hours after the initial release of tracer . . . . .	100
A-2	Ccontours of tracer concentration ( $\mu\text{g/l}$ ) for dye study at 84 hours after the initial release of tracer . . . . .	101
A-3	Ccontours of tracer concentration ( $\mu\text{g/l}$ ) for dye study at 115 hours after the initial release of tracer . . . . .	102
A-4	Ccontours of tracer concentration ( $\mu\text{g/l}$ ) for dye study at 140 hours after the initial release of tracer . . . . .	103
B-1	Velocity vectors for the base case at model time $t = 32$ hrs (11 hrs after initial injection of tracer) . . . . .	106
B-2	Velocity vectors for the base case at model time $t = 56$ hrs (35 hrs after initial injection of tracer) . . . . .	107
B-3	Velocity vectors for the base case at model time $t = 72$ hrs (51 hrs after initial injection of tracer) . . . . .	108
B-4	Velocity vectors for the base case at model time $t = 104$ hrs (83 hrs after initial injection of tracer) . . . . .	109
B-5	Velocity vectors for the base case at model time $t = 136$ hrs (115 hrs after initial injection of tracer) . . . . .	110
B-6	Velocity vectors for the base case at model time $t = 168$ hrs (147 hrs after initial injection of tracer) . . . . .	111
B-7	Tracer concentration ( $\mu\text{g/l}$ ) contours for the base case at model time $t = 32$ hrs (11 hrs after initial injection of tracer) . . . . .	113

B-8	Tracer concentration ( $\mu\text{g}/\text{l}$ ) contours for the base case at model time $t = 56$ hrs (35 hrs after initial injection of tracer) . . . . .	114
B-9	Tracer concentration ( $\mu\text{g}/\text{l}$ ) contours for the base case at model time $t = 72$ hrs (51 hrs after initial injection of tracer) . . . . .	115
B-10	Tracer concentration ( $\mu\text{g}/\text{l}$ ) contours for the base case at model time $t = 104$ hrs (83 hrs after initial injection of tracer) . . . . .	116
B-11	Tracer concentration ( $\mu\text{g}/\text{l}$ ) contours for the base case at model time $t = 136$ hrs (115 hrs after initial injection of tracer) . . . . .	117
B-12	Tracer concentration ( $\mu\text{g}/\text{l}$ ) contours for the base case at model time $t = 168$ hrs (147 hrs after initial injection of tracer) . . . . .	118
B-13	Tracer concentration ( $\mu\text{g}/\text{l}$ ) contours for $u_{m01}=7.5 \times 10^{-5} \text{ m}^2/\text{s}$ at model time $t = 32$ hrs (11 hrs after initial injection of tracer) . . . . .	120
B-14	Tracer concentration ( $\mu\text{g}/\text{l}$ ) contours for $u_{m01}=7.5 \times 10^{-5} \text{ m}^2/\text{s}$ at model time $t = 56$ hrs (35 hrs after initial injection of tracer) . . . . .	121
B-15	Tracer concentration ( $\mu\text{g}/\text{l}$ ) contours for $u_{m01}=7.5 \times 10^{-5} \text{ m}^2/\text{s}$ at model time $t = 72$ hrs (51 hrs after initial injection of tracer) . . . . .	122
B-16	Tracer concentration ( $\mu\text{g}/\text{l}$ ) contours for $u_{m01}=7.5 \times 10^{-5} \text{ m}^2/\text{s}$ at model time $t = 104$ hrs (83 hrs after initial injection of tracer) . . . . .	123
B-17	Tracer concentration ( $\mu\text{g}/\text{l}$ ) contours for $u_{m01}=7.5 \times 10^{-5} \text{ m}^2/\text{s}$ at model time $t = 136$ hrs (115 hrs after initial injection of tracer) . . . . .	124
B-18	Tracer concentration ( $\mu\text{g}/\text{l}$ ) contours for $u_{m01}=7.5 \times 10^{-5} \text{ m}^2/\text{s}$ at model time $t = 168$ hrs (147 hrs after initial injection of tracer) . . . . .	125



# Chapter 1

## Introduction

Contaminant transport within an estuarine environment is usually dominated by two mechanisms: oscillatory tidal forcing and freshwater flow into the estuary. It is these two forces that govern the residence time and flushing rate of a coastal embayment, and the transport of contaminants in the estuary. However, there often is little known about the actual residence times and how these rates may vary under different conditions. Estimates can be determined through field experiments and numerical studies.

### 1.1 Motivation for study

Boston Harbor is comprised of the Inner Harbor and the Outer Harbor. Both the Inner Harbor and Outer Harbor have been the focus of attention because of the chemical and biological contaminants that are present in these waters. The Inner Harbor extends from the mouths of the Mystic and Chelsea Rivers to its confluence to the Outer Harbor. It receives freshwater discharged from the Charles, Mystic, and Chelsea Rivers. See Figure 1-1. The Charles River is the primary source of freshwater to the Inner Harbor. The drainage areas of the Charles, Mystic and Chelsea Rivers are 82, 17 and 1 percent of the total areas, respectively. [2] [7] The annual average flow, calculated from 1931-1992 data, at the Waltham U. S. Geological Survey (USGS) gage on the Charles River is  $8.6 \text{ m}^3/\text{s}$ . The summertime

average of July through September data from that same period at the Waltham gage is  $3.4 \text{ m}^3/\text{s}$ . [28]

The Mystic and Charles Rivers have dams near their mouths to the Inner Harbor: the New Charles River Dam at the basin of the Charles River and the Amelia Earhart Dam upstream of the mouth of the Mystic. In addition, there are two small channels along the Inner Harbor, between its intersection with the Charles River and with the Outer Harbor, Fort Point Channel and Reserved Channel, as shown in Figure 1-2.

There exist combined sewer overflows (CSOs) along the Charles, Mystic and Chelsea Rivers, as indicated in Figure 1-1. There are also numerous CSOs along the Inner Harbor that drain directly into the harbor. These CSOs discharge stormwater, and raw sewage at times of heavy rainfall, into the rivers and harbor.

Because of the presence of contaminants in the Inner Harbor and its rivers, it is important to understand the transport of pollutants in the estuary. The residence time and flushing rate of the Inner Harbor are two parameters which describe the Inner Harbor that are vital to determining the degree of contamination in the harbor. It is also important to understand how the residence time and flushing rate can be affected by various conditions in the Inner Harbor, such as the variation of freshwater input from rivers. Understanding these relationships can help bring about solutions to the remediation efforts in the Inner Harbor.

## **1.2 The problem**

There are two major components of this investigation of the effects of freshwater inflows on the flushing of Boston's Inner Harbor. The first is to estimate of flushing rate and residence time of freshwater from the Charles River in Boston's Inner Harbor. And the second part is to determine what effect, if any, the quantity of freshwater discharged and the time sequence of the discharge has on its residence time in the Inner Harbor.

This investigation will begin by reviewing two previous field studies on residence

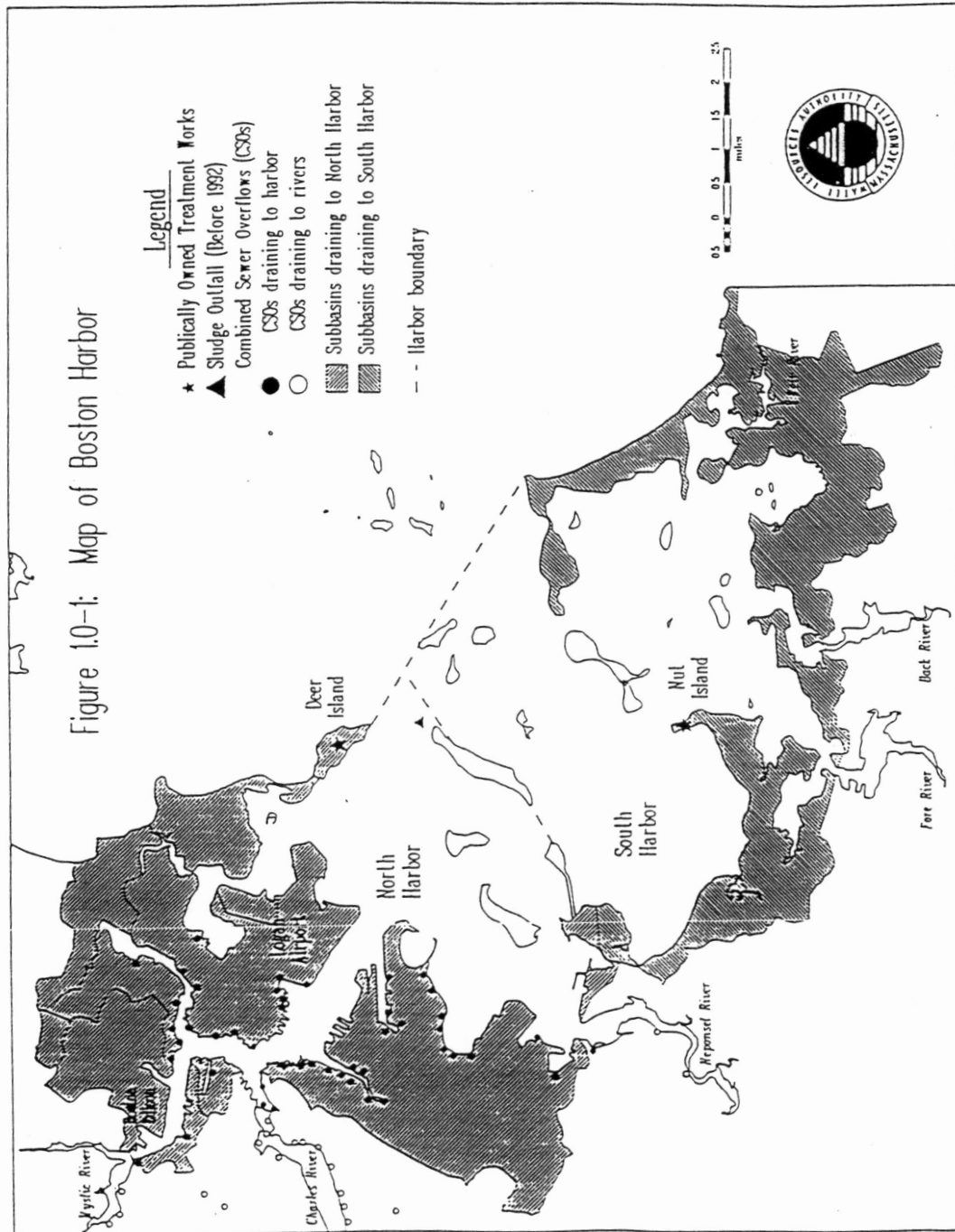


Figure 1-1: Map of Boston Harbor and the locations of CSOs in the Harbor.

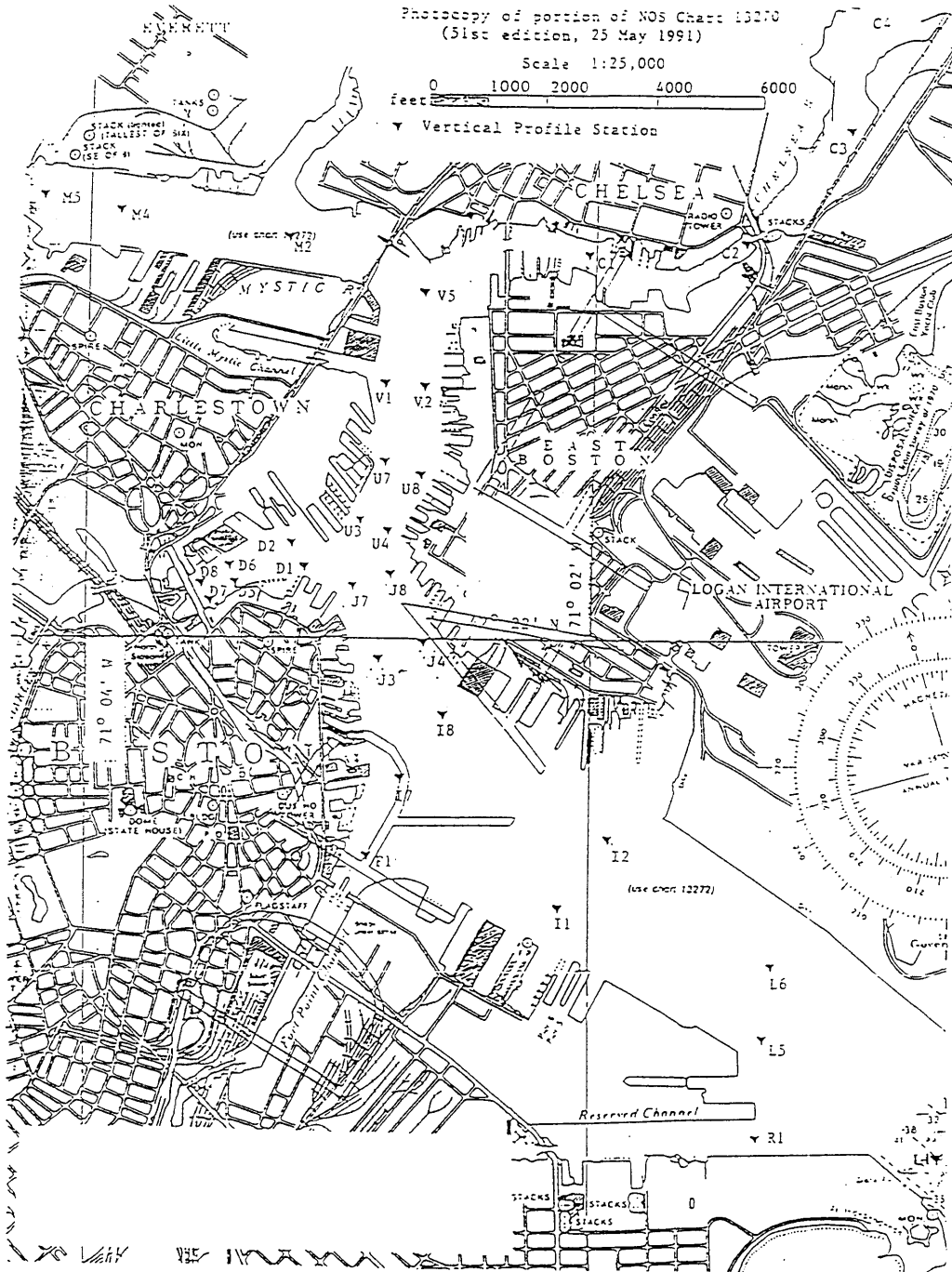


Figure 1-2: Map of Boston Inner Harbor.

time of freshwater in Boston's Inner Harbor. Next, the problem will be formulated for a numerical hydrodynamic model, using the more recent dye study data to help calibrate model. A residence time will be calculated for this base case model. Then the numerical model will be used to explore different cases of freshwater input from the Charles River, such as the variation in volumes of freshwater and discharge scenarios. The goal is to determine a relationship between freshwater inflow conditions and the residence time of the freshwater, and thus the residence time of any conservative contaminant associated with the freshwater discharge, in the Inner Harbor. This will aid in determining how much of the flushing can be controlled, such as by regulating the amount and the time sequence of freshwater discharged into the harbor. Additionally, this will help determine how long non-conservative contaminants have to decay, settle, react or volatilize in the Inner Harbor before they reach the Outer Harbor.

# Chapter 2

## Theory

This chapter will introduce the definitions and theories relevant to estuarine flushing. It will also briefly discuss mixing processes within an estuarine environment.

### 2.1 Flushing parameters

The residence time and flushing rate are important parameters which describe the flushing of an estuary. This section will describe how these parameters are defined.

#### 2.1.1 Residence time

Fischer *et al.* describes the “flushing time,” or mean detention time, as the “mean time that a particle of tracer remains inside an estuary.” They present a calculation for the mean detention time, based on one-dimensional analysis. The total volume of freshwater in an estuary between the mouth ( $x = 0$ ) and a given cross section location ( $x = L$ ) is given by Fischer *et al.* by

$$V = \int_0^L \int_A f dA dx, \quad (2.1)$$

where  $dA$  is the cross section area of the section,  $dx$  is the length of the section along the estuary, and  $f$  is the freshness, defined as the fraction of freshwater that a sample of water contains,

$$f = \frac{(S_o - S)}{S_o}, \quad (2.2)$$

where  $S_o$  is the salinity of ocean water and  $S$  is the salinity of the sample of water. Therefore pure freshwater has a freshness of one, and pure ocean water has a freshness of zero. So then the residence time,  $T_f$ , may be calculated by

$$T_f = \frac{V}{Q_f}, \quad (2.3)$$

where  $V$  is the freshwater volume and  $Q_f$  is the volume flow rate of freshwater in the estuary. [10]

Adams and Stolzenbach demonstrated that the mean Boston Inner Harbor residence time of dye can be estimated by extrapolating the dye recovery to zero at  $t = \infty$  and integrating over time. So then the residence time,  $\tau$ , for an instantaneous injection may be estimated by

$$\tau = \frac{\int_0^{\infty} M(t) dt}{M_0}, \quad (2.4)$$

where  $M(t)$  is the mass of dye in the harbor as a function of time and  $M_0$  is the initial dye mass.

While Equations 2.3 and 2.4 are experimental methods for calculating the residence time, the tidal prism method is a theoretical estimation of residence time. Residence time,  $\tau$ , is calculated by

$$\tau = \frac{VT}{P}, \quad (2.5)$$

where  $V$  is the volume of the estuary during high tide,  $T$  is the tidal period, and  $P$  is the intertidal or tidal prism volume, which is the total change in estuary water volume between low and high tide. This is often used as a lower bound of the  $\tau$  estimate since it assumes that the water entering the estuary on flood tide is entirely of oceanic salinity and that the estuary water is well-mixed throughout. In addition, this assumes that none of the mass that leaves the estuary on ebb tide will return

on the following flood tide. [1] [21]

A theoretical method presented by Ketchum [17] is the modified tidal prism technique. The estuary is divided into segments in which there is complete mixing at high tide, instead of the usual assumption that there is complete mixing over the entire length of the estuary during each tidal cycle. [21] The length of each segment is determined by the average length of the tidal excursion, which would be the longest segment over which well-mixed conditions can be assumed. The tidal excursion is defined as the average distance traveled by a particle of water during flood tide. [15]

Another variation of the tidal prism method is presented by Sanford *et al.* This tidal prism model is for a small well-mixed tidal embayment. They account for the fact that some of the mass that leaves the embayment during ebb tide does in fact return on the following flood tide by introducing the return flow factor. This return flow factor is the “fraction of water leaving during ebb that returns during flood tide.” So then the expression for the residence time,  $T_f$ , becomes

$$T_f = \frac{V}{(1 - b)Q + I} \quad (2.6)$$

where  $V$  is the average volume of the embayment,  $b$  is the return flow factor in which  $0 < b < 1$ ,  $Q$  is the volume flow rate of the tidal prism, and  $I$  is the volume flow rate of a stream or tributary discharging into the embayment. For the case of tidal flushing only, the expression becomes

$$T_f = \frac{VT}{(1 - b)P}, \quad (2.7)$$

where  $T$  is the period of the tide and  $P$  is the tidal prism. [26]

### 2.1.2 Flushing rate

The flushing rate is defined as the rate at which freshwater or a contaminant leaves an estuary or embayment. It is related to the residence time by



$$Q_f = \frac{V}{T_f}. \quad (2.8)$$

## 2.2 Mixing in estuaries

Mixing in estuaries is caused primarily by three forces: wind, tides and tributary flow. A combination of these sources of energy may act on the estuary although not all three may dominate. In addition, the mixing that is created can be separated into three components: vertical, lateral, and longitudinal mixing. This section will describe how these three forces cause mixing and how the three components of mixing are affected.

### 2.2.1 Causes of mixing

Mixing in estuaries is caused by a combination of small-scale turbulence and larger-scale advection. The small-scale turbulence has fluctuations with a period of less than a few minutes, whereas advective transport has longer periods. Advective velocities in an estuary are not constant in time, space, nor direction. The interaction between the three sources of mixing (wind, tides, and river flows) is complicated. The isolated effects of each source will be described.

#### Mixing by wind

Wind may not be as dominant a source of energy in estuaries, as it generally is in large lakes and the open ocean. The flow is mostly tidal in long, narrow estuaries, and wind has little opportunity to generate a significant current. However, this may not be the case in wide estuaries. Dissolved particles and slugs of less dense or warmer liquid floating on the water surface will be moved in the direction of the wind since the wind exerts a drag force on the water surface. Nevertheless, the effect of the wind on mixing depends on the currents that are induced in the estuary. [10]

## Mixing by tides

Tides cause mixing in estuaries in two ways, one small-scaled and the other larger-scaled. Turbulence is generated when tidal flow moves over the estuary bottom, which then leads to turbulent mixing. Larger scale currents are created by the interaction between the tidal wave and the estuary bathymetry. Examples of this larger scale mixing include shear flow dispersion, and other circulations, defined by tidal “pumping” and “trapping.” Tidal “trapping” refers to the results of side embayments and small branching channels in estuaries. [10]

Sanford *et al.* describes tidal flushing, which causes mixing, as the result of the “repeated exchange of the tidal prism between the embayment and its receiving water body.” When water enters the embayment during flood tide, the new water mixes with the existing water in the embayment. And “when the tide falls, the intertidal volume of water flows out of the embayment as an ebb tidal current. A fraction of this water is lost by advection or mixing into the receiving water body, and the remainder returns to the embayment on the following flood tide.” Therefore, the tidal return factor, in addition to the embayment geometry and the tidal range, affect tidal flushing. [26]

## Mixing by tributaries

Rivers discharge freshwater into the estuary, which is a body of denser saltwater. The gradient in the densities of water cause density currents, which affect mixing. These internal flows driven by density gradients are known as baroclinic circulation, whereas flows of constant density and pressure are barotropic circulations, such as that caused by tide-driven flows.

### 2.2.2 Components of estuarine mixing

The cross-sectional mixing coefficients for an estuary is often difficult to define, measure and estimate. This is due to the irregular cross-sections that an estuary may have and the complex processes that govern the mixing. The following sections

will describe a few definitions used for mixing coefficients and some measured values of these coefficients.

### Vertical Mixing

For the simple case of constant-density tidal flow in which vertical mixing is due mostly to bottom shear stress turbulence, the vertical mixing coefficient,  $\varepsilon_v$ , may be defined as

$$\varepsilon_v = 0.067du^*, \quad (2.9)$$

where  $d$  is the depth and  $u^*$  is the shear velocity. However,  $u^*$  may vary from approximately zero at slack tide to some maximum, and therefore the average value of  $u^*$  is often used. Because it is often difficult to measure shear in an unsteady flow, a relationship between shear velocity and mean velocity must be assumed. Bowden [6] proposed that at middepth,

$$\varepsilon_v = 0.0025dU_a, \quad (2.10)$$

where  $U_a$  is the depth mean amplitude of the current.

For stably stratified waters, Munk and Anderson [20] used

$$\varepsilon_v = \varepsilon_0(1 + 3.33Ri)^{-1.5}, \quad (2.11)$$

where  $\varepsilon_v$  is the value of  $\varepsilon_v$  for neutral stability and  $Ri$  is the gradient Richardson number given by  $Ri = \frac{g(\partial\rho/\partial z)}{\rho(\partial u/\partial z)^2}$ . The values of  $\varepsilon_v$  range from  $5 \times 10^{-4}$  m<sup>2</sup>/s at the surface and  $7.1 \times 10^{-3}$  m<sup>2</sup>/s at middepth found by Bowden [5] in the Mersey, and  $5 \times 10^{-5}$  m<sup>2</sup>/s to  $5 \times 10^{-4}$  m<sup>2</sup>/s in the Duwanish Waterway near Seattle, Washington, by Partch and Smith [22].

## Lateral Mixing

For a channel with a straight, rectangular cross-section with bottom-generated turbulence, the lateral, or transverse, mixing coefficient,  $\varepsilon_t$  can be approximated by

$$\varepsilon_t = 0.15du^*. \quad (2.12)$$

However, because of the curvatures in the channel and sidewall irregularities along with the complex mixing mechanisms found in estuaries, the values of  $\varepsilon_t$  may be much larger. Field measurements indicate values for  $\varepsilon_t/du^*$  range from 0.44 to 1.61.

## Longitudinal Mixing

It is common to combine the effects of all of longitudinal mixing into one dispersion coefficient,  $K$ . A “salt balance” equation for an estuary in steady state may be written as

$$U_f S = K(\partial S/\partial x), \quad (2.13)$$

where  $U_f$  is the net downstream velocity caused by freshwater discharge given by  $U_f = Q_f/A$ , in which  $Q_f$  is the freshwater volume flow rate and  $A$  is the cross-sectional area, and  $S$  is the water salinity. This balance equation states that the downstream advection of salt caused by the mean flow,  $U_f S$ , is balanced by the upstream transport caused by all other mechanisms. The value of  $K$  is commonly determined by measurements of variations of tracers or salinity.

The observed values of the longitudinal dispersion coefficient,  $K$ , vary depending on whether the salinity  $S$  is measured at high slack tide, low slack tide, or is an average over the tidal cycle. Values of  $K$  often range from 100 m<sup>2</sup>/s to 300 m<sup>2</sup>/s for moderately-sized estuaries. The observed values of  $K$  vary from approximately 50 m<sup>2</sup>/s to 1500 m<sup>2</sup>/s. [10]

# Chapter 3

## Field studies

There exist two field studies which explored the flushing of freshwater in Boston's Inner Harbor. The first is by D. F. Bumpus, Wm. S. Butcher, Wm. D. Atheran and C. G. Day (1953). The second is by E. E. Adams, D. L. McGillivary, S.-W. Suh and R. R. Luxenberg (1993). This chapter will give describe these two field studies and the results of these projects.

### 3.1 Bumpus *et al.*

A field study to estimate the residence time of freshwater within the Boston Inner Harbor was conducted as part of a survey project conducted by members of the Woods Hole Oceanographic Institution during the period of April 1951 to March 1953.

#### 3.1.1 Background

On ten occasions during the period between May 1951 and October 1952, water samples were collected with Nansen bottles at six locations in the Inner Harbor at three or four depths. The salinities of these water samples were determined by the Knudsen method. From these data, salinity distributions were formulated, and the fraction of freshwater was determined by these isohaline contours by Equation

2.2. A freshwater content of the Inner Harbor was calculated by summing up these freshwater portions over their respective volumes. [7]

The majority of the freshwater runoff into the Inner Harbor comes from the Charles River. Using data from the Waltham gage on the Charles River, where the drainage area above Waltham gage is 588 km<sup>2</sup> (227 square miles), runoff flow rates were calculated. These runoff rates were extrapolated to represent the drainage area of the Charles, Mystic and Chelsea Rivers, which have drainage areas of 774, 169, and 12.4 km<sup>2</sup> (299, 65.3, and 4.8 square miles), respectively, totaling to 996 km<sup>2</sup> (369 square miles). This represents the area above the mouths of the Charles, Mystic and Chelsea Rivers. Since the daily average flow rates at the Waltham gage on the Charles River were not steady during the field study and the monthly averages were not representative of the amount of runoff from one week, a cumulative method was used to determine the Waltham flow rates.

The flushing time, or residence time, was then estimated by dividing the estimated volume of freshwater entering the Inner Harbor by the mean freshwater runoff rate for the sampling day, as described in Equation 2.3

### **3.1.2 Results**

The calculated volume of freshwater in the Inner Harbor ranged from 1.1 km<sup>2</sup> to 4.6 km<sup>2</sup> (39.6 to 164 million ft<sup>3</sup>) during these ten observations. This represents 1.5 to 6 percent of the Inner Harbor water volume. The total quantity of water in the Inner Harbor at mean high water and mean low water was determined to be 77.9 km<sup>2</sup> and 56.4 km<sup>2</sup> (2,750 million ft<sup>3</sup> and 1,990 million ft<sup>3</sup>), respectively. The volume of freshwater estimated to enter the harbor in one day ranged from 0.16 km<sup>2</sup> to 2.9 km<sup>2</sup> (5.7 to 102 million ft<sup>3</sup>), or 0.2 to 4 percent of the Inner Harbor volume. [7]

As shown in Figure 3-1, the flushing times ranged from 1.6 days to 10.2 days, for mean runoff values from the Charles, Mystic and Chelsea Rivers of 33.6 m<sup>3</sup>/s and 1.9 m<sup>3</sup> (1,190 ft<sup>3</sup>/s and 66 ft<sup>3</sup>/s), respectively; with most of the estimated residence time between 2 and 5 days. The residence time for the Charles River mean flow of about 10 m<sup>3</sup>/s (350 ft<sup>3</sup>/s) was estimated to be about 2 days.

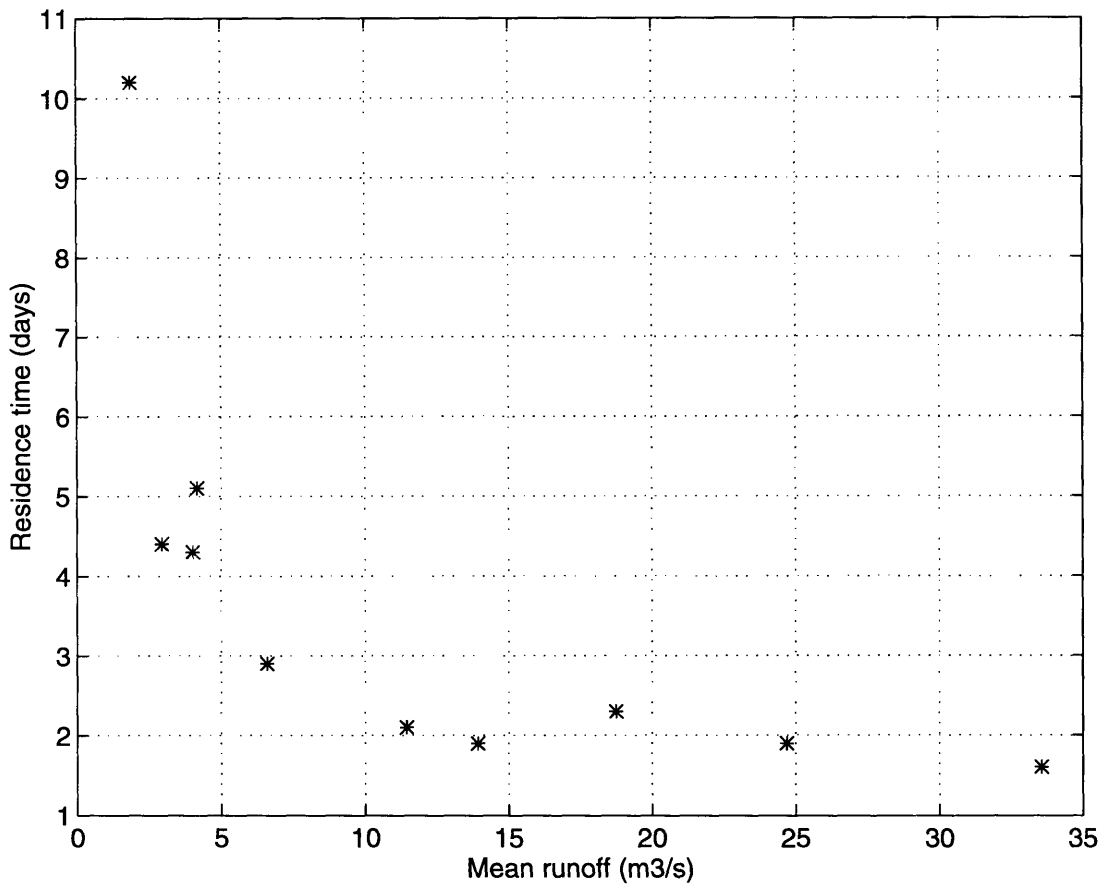


Figure 3-1: Flushing time as a function of mean runoff, after Bumpus *et al.*

## 3.2 Boston Inner Harbor dye study

During July 1992, a fluorescent tracer study was conducted in order to better understand the residence times and flushing rates of freshwater from the Charles River freshwater within Boston Inner Harbor. This was useful since little was known about the residence time of the Inner Harbor as compared to the residence times of the Outer Harbor and small headwater areas of the Inner Harbor, such as Fort Point Channel.

### 3.2.1 Background

Freshwater is released from the new Charles River Dam to maintain a nearly constant water level in the Charles River basin. The freshwater is usually released around low tide every tidal cycle through an upper or lower sluice gate, or through a combination of the two gates. Water is released through these sluice gates by gravity-driven flows. The flow rate at which freshwater is delivered depends on which gate is operating and the time after low tide at which the gates are lowered. Figure 3-2 indicates these relationships.

For the dye study, 227 kg (501 lb) of a 20 percent solution of Rhodamine WT, which has a specific gravity of 1.03, was released over a period of 5.5 hours into the Charles River just upstream of its entrance to the Inner Harbor at the Charles River Dam. This release of 45.5 kg (100 lb) of pure dye coincided with the freshwater release at the dam into the Inner Harbor, and therefore all of the freshwater released was tagged with the tracer. The dyed freshwater was released through the upper level sluice gate at a constant flow rate of  $20 \text{ m}^3/\text{s}$  (700 cfs) between 20:35 on the evening of 22 July 1992 and 02:00 on the morning of 23 July 1992. Low tide occurred at 23:37 on 22 July, and thus this tagged freshwater was released around low tide. A total of  $3.9 \times 10^5 \text{ m}^3$  ( $1.38 \times 10^7 \text{ ft}^3$ ) of freshwater was released over this 5.5 hour period.

Because there were dry conditions surrounding the period of the tracer experiment, freshwater was not released through the sluice gates at the Charles River Dam



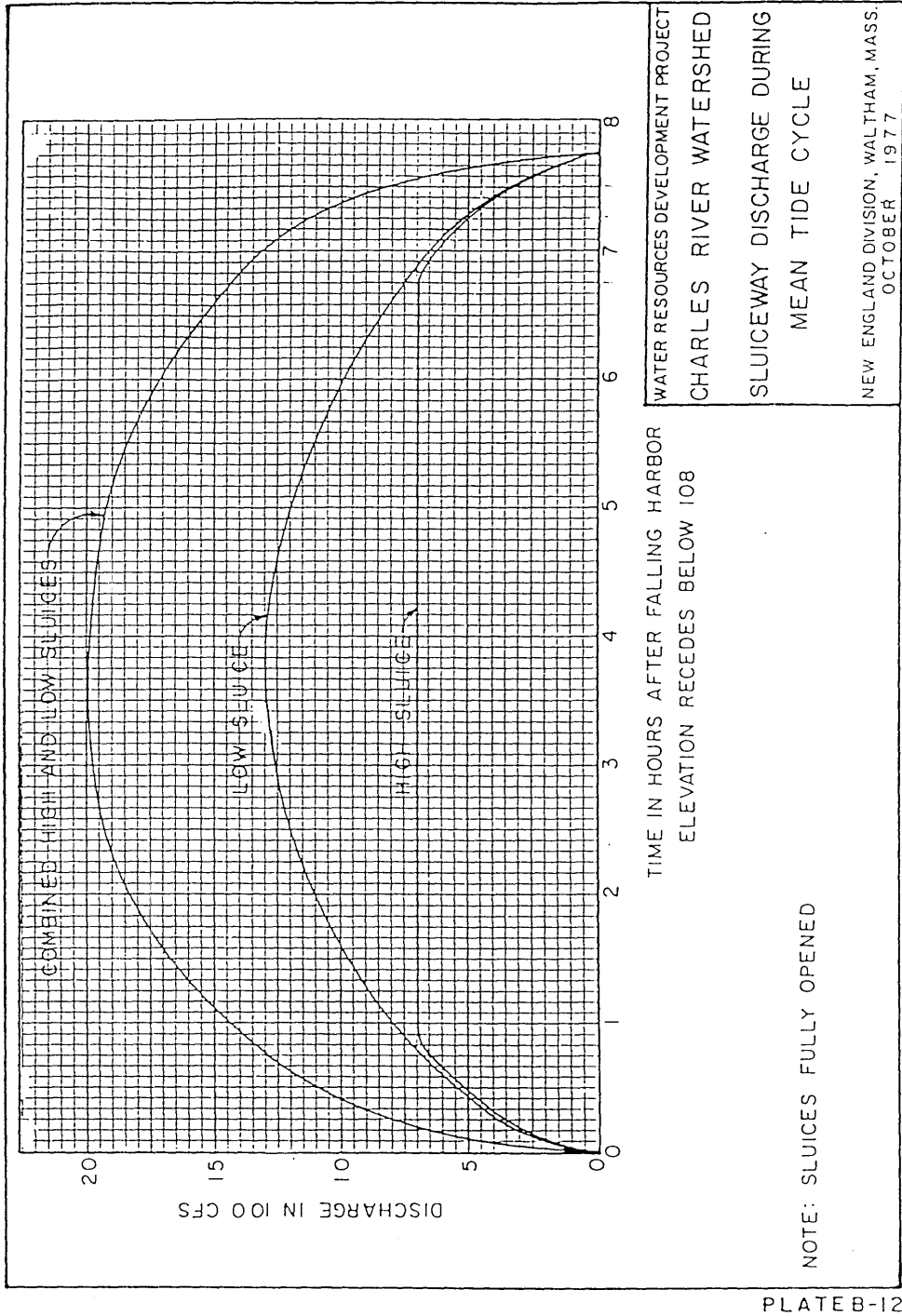


PLATE B-12

Figure 3-2: New Charles River Dam flow rates as a function of time after high tide.

during the tidal cycles immediately prior to and following the tracer release, with the exception of small quantities of Charles River water discharged into the Inner Harbor used to operate the fish ladder at the dam. Freshwater was last released through both sluice gates from 19:00 on 21 July to 02:30 on 22 July. The next freshwater discharge after the dye release occurred from 14:00 to 16:00 on 24 July. Therefore, there was an interval of about 18 hours with essentially no freshwater inflow to the Inner Harbor before the tracer release and an interval of about 36 hours with no freshwater discharge after the dye experiment. In total, there were five separate freshwater releases at the dam during this dye study, resulting in an average flow rate of  $3.2 \text{ m}^3/\text{s}$  ( $110 \text{ ft}^3/\text{s}$ ).

There were thirteen surveys for the next six days after dye release, from 23 July to 28 July. These took place around daytime high and low tides, for approximately two hours during each survey. These surveys were performed off of a 25-foot survey boat by Aquatec, Inc., of Colchester, Vermont, with a flow-through fluorometer which measured the temperature, fluorescence, and conductivity of the waters at depth intervals of approximately 0.3 m (1 ft), from the water surface to the bottom at about 30 locations throughout Inner Harbor. The labeled triangles in Figure 1-2 indicate the locations where samples were taken. Water salinity and tracer concentration were computed from the conductivity data.

### **3.2.2 Results**

Longitudinal-vertical contours of the tracer concentration indicate that the tracer dye is initially concentrated near the surface at the location of discharge at the dam and gradually spreads longitudinally and vertically. After approximately 40 hours, the data show that the dye was reasonably well-distributed laterally. It is also seen that the tracer concentration decreased towards the Inner Harbor mouth. These longitudinal-vertical cross-sections of tracer concentration contours are shown in Appendix A.

The total tracer mass was computed by spatially integrating the dye concentration data from each survey. In order to use Equation 2.4 to calculate the residence

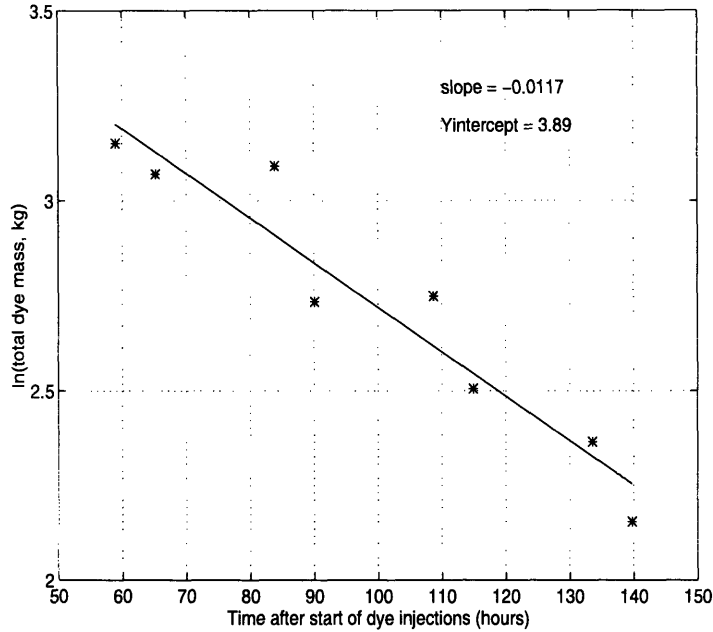


Figure 3-3: Fitting a line through  $\ln(\text{mass})$  vs. time for dye study data

time of the conservative tracer and its associated freshwater, the model data needed to be extrapolated. This was done by fitting a line through the data, with the natural log of the tracer mass versus time as the chosen form of the data. The data points starting from 59 hours after the beginning of the tracer release were used for line-fitting. The result was a line of slope -0.0117 and y-intercept 3.89. As shown in Figure 3-3, the Inner Harbor tracer mass data does decrease in an exponential form.

The residence time was calculated according to Equation 2.4. The numerator was estimated by using the trapezoidal method to integrate under the curve of total mass versus time, as shown in Figure 3-4. The calculated residence time from the dye study data was 3.75 days.

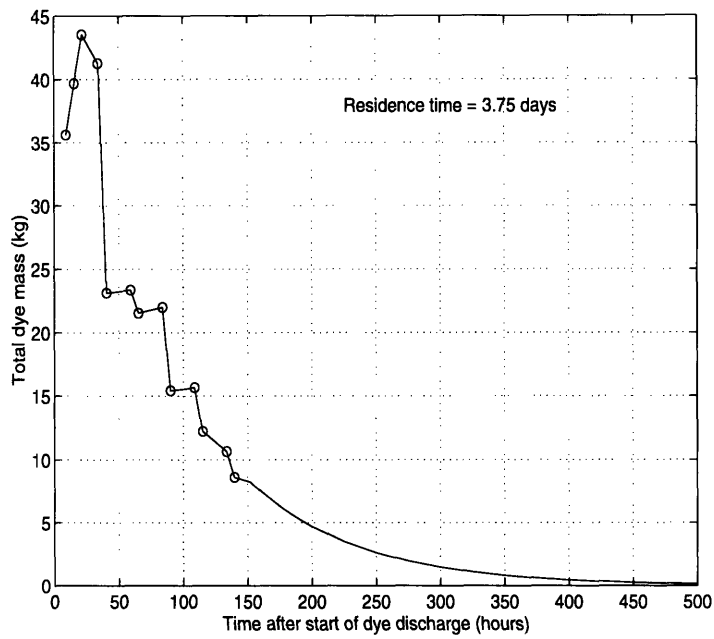


Figure 3-4: Tracer mass extrapolated to zero for the dye study. The circles indicate survey data, and the line beyond  $t = 140$  hours is extrapolated based on a line fit.

# Chapter 4

## Numerical Modeling

With the use of a numerical circulation model, the effects of freshwater inflow on the flushing of Boston's Inner Harbor may be explored. This chapter will first discuss the numerical model, ECOM-si, used to accomplish this. An explanation of the model formulation will follow, and then the modeling results will be presented.

### 4.1 The model, ECOM-si

The estuary, coastal and ocean model (ECOM) was first developed in 1975 by George L. Mellor. Since then, the model has been updated several times. A newer version of this model, ECOM-si, is based on ECOM, with many significant revisions included. This time-dependent, three-dimensional circulation model has been used in studies of estuarine and coastal environments, such as the South Atlantic Bight, the Hudson-Raritan estuary, the Gulf of Mexico, the Delaware Bay, River and adjacent continental shelf and the Massachusetts Bay. The model results have been extensively compared with data in these studies and indicate that the predominant physics have been realistically reproduced by the model. [16] The version of ECOM-si described in this section is the August 1991 revision.

### 4.1.1 Model features

ECOM-si uses fully non-linear momentum equations; however, it offers the option for linear momentum for debugging purposes. It includes Coriolis forcing, which is determined by the user specified latitude of the horizontal grid elements.

The model calculates the free surface elevation, the three components of velocity, temperature, salinity (which gives density through the equation of state), and turbulence kinetic energy and turbulence macroscale from the user-specified input information. The latter two turbulence-related variables are determined by the given horizontal and vertical eddy viscosity and the horizontal and vertical eddy diffusivity.

Variable grid spacing may be used in this model. The horizontal grid allows for an orthogonal, curvilinear coordinate system. When implementing this coordinate system, the governing equations are similar to the usual Cartesian equations and require only “marginally greater computer resources for their solution.”

“ECOM-si is a multi-level model whose equation set is obtained from the continuous governing equations by replacing the vertical derivatives by finite differences and locating the vertical grid level (or points) at  $\xi = \xi_k$ ,  $k = 0, 1, \dots, K$ , such that  $\xi_0 = 0$  (surface) and  $\xi_K = -1$  (bottom).” [16]

This model incorporates the  $\sigma$ -coordinate system in which the number of grid points in the vertical direction is independent of the water depth. The basic governing equations are set in a bottom-following,  $\sigma$ -coordinate system based on Phillips [23] and Blumberg and Mellor [3] [4]. The transformation is

$$x^* = x, \quad y^* = y, \quad \sigma = \frac{z - \eta}{H + \eta}, \quad t^* = t, \quad (4.1)$$

where  $x$ ,  $y$ ,  $z$  are the conventional Cartesian coordinates,  $\sigma$  is the transformed vertical coordinate,  $H(x, y)$  is the bottom topography,  $\eta(x, y)$  is the free surface elevation, and  $t$  is time. As a result,  $\sigma$  ranges from  $\sigma = 0$  at  $z = \eta$  to  $\sigma = -1$  at  $z = -H$ . The spacing on this transformed coordinate system may also be variable, as is allowed in the horizontal grid, so that surface and bottom boundary layers may be resolved. When the grid extends from a shallow region to a deep region, there

are sudden changes in the vertical dimension of the grid boxes that result from the use of the  $\sigma$ -coordinates. This causes some artificial numerical diffusion, vertically upward and downward on the grid. This artificial numerical diffusion is grid spacing dependent and is inherent in all numerical methods. Remedies for reducing this numerical diffusion are to implement a mathematically complete transformations over a finer grid spacing. [16]

ECOM-si allows for time variable onshore and offshore discharges. The flow rate, temperature, and salinity of the discharged water is specified at user-defined times. The offshore discharge also allows for a conservative tracer in the effluent. These discharges also may be distributed vertically at the specified grid points.

Additionally, a variety of other forcings may be included into the model. These include surface wind stress, atmospheric pressure gradients, heat flux (which is the total of the sensible, latent, long wave and net solar radiation components), salinity flux (which is evaporation minus precipitation), and tidal forcings. The model can produce computer generated data for up to six harmonic constituents according to

$$\eta = E_{mean} + \sum_{i=1}^6 a_i \cos(\omega_i t - \phi_i) \quad (4.2)$$

where  $E_{mean}$  is the mean water level with reference to a specified datum,  $a_i$  is the amplitude of the  $i^{th}$  tidal constituent,  $\omega_i$  is the frequency of the  $i^{th}$  tidal constituent, and  $\phi_i$  is the phase lag of the  $i^{th}$  tidal constituent. The six harmonic constituents are the solar semidiurnal  $S_2$  with a period of 12.00 hours, the lunar semidiurnal  $M_2$  with a period of 12.42 hours, the lunar semidiurnal  $N_2$  with a period of 12.66 hours, the lunar diurnal  $K_1$  with a period of 23.94 hours, the solar diurnal  $P_1$  with a period of 24.06 hours, and the lunar diurnal  $O_1$  with a period of 25.82 hours.

### 4.1.2 Methods and schemes

The equations and boundary conditions of the circulation model are solved by finite differences techniques. Computations are made using a horizontally and vertically staggered lattice of grid points. The model uses an implicit numerical scheme in

the vertical direction [25] and a semi-implicit scheme in the horizontal direction [8] for the barotropic mode. The finite difference equations inherently conserve energy, mass and momentum and introduce some amounts of artificial horizontal diffusion. [16]

The vertical mixing processes are modeled by a turbulence closure model of small scale turbulence. ECOM-si uses an imbedded second moment, level 2 1/2, turbulence closure sub-model by Mellor and Yamada [19], which has been modified by Galperin *et al.* [11] to provide vertical mixing coefficients. The vertical eddy viscosity and diffusivity are calculated from turbulence transport equations for the turbulence kinetic energy and the turbulence length scale. The vertical eddy mixing coefficients  $K_M$ ,  $K_H$ , and  $K_q$  are evaluated by

$$K_M = qlS_M, K_H = qlS_H \quad \text{and} \quad K_q = 0.2ql, \quad (4.3)$$

where  $S_M$  and  $S_H$  are stability functions that are analytically derived, algebraic relations.

Both land and open boundaries are given a no flux condition for the horizontal components of velocity, salinity, temperature, and conservative tracer. The open boundary condition is a simplification since the circulation processes in this region are complex and defining a boundary condition is still an unresolved topic.

The ramp function gradually increases all model forcing functions from zero to their full values at approximately three times the number of specified time steps. The ramp function is specified as

$$\text{ramp} = \frac{\tanh(dt_i)}{i_{ramp} + 1} \quad (4.4)$$

where  $dt_i$  is the current time step and  $i_{ramp}$  is the user-specified number of time steps for the ramp function.



## 4.2 Model formulation

The grid and input for the numerical model ECOM-si was formulated to simulate most of Boston's Inner Harbor features as closely as possible, while at the same time keeping the model representation simple in order to make it practical to implement. The volume and general shape of the Inner Harbor has been represented, as well as the dominant physical forces and attributes of the region. The following section will describe the domain of the model grid, the boundary and initial conditions, and parameter values used in the model simulations.

### 4.2.1 The domain

Boston's Inner Harbor and a portion of the Outer Harbor was represented in the model. The Outer Harbor region is necessary in order to provide a region into which the for the Inner Harbor waters may flush. The model domain is a three-dimensional, T-shaped volume with constant mean water level. The Inner Harbor was schematized by the long part of the T, with volume of Inner Harbor, including the Mystic River up to the Amelia Earhart Dam, the Chelsea River up to Chelsea Street-Eastern Avenue bridge and the area downstream of Charles River Dam, as well as the majority of Fort Point Channel and Reserved Channels. The Outer Harbor was represented by the cross of the T; the Harbor islands were not represented in order to keep the model grid simple. Figure 4-1 shows the main features of the model domain. The region of the Inner Harbor downstream of the Charles River Dam is indeed channel-like, with little meandering, and the expansion of the Inner Harbor into the Outer Harbor is sudden, with almost perpendicular corners. Therefore, the T-shape representation of Boston Inner and Outer Harbor is not too far from reality.

The area of the Inner Harbor was measured using a bathymetric chart of the region (Boston Inner Harbor, 1:10,000 scale, 27th edition, 1971). This was done by breaking up the Inner Harbor into rectangular sections to determine surface areas and then summing up these rectangular areas. A horizontal grid spacing system



then was devised such that the domain area matched the measured area as closely as possible. The Inner Harbor, its channels and the regions of the Charles, Mystic and Chelsea Rivers that directly discharge into the harbor were divided into eleven rectangles, totaling  $6.75 \times 10^6 \text{ m}^2$  ( $2.61 \text{ mi}^2$ ) in area. The total area representing the Inner Harbor in the model grid is  $6.72 \times 10^6 \text{ m}^2$  ( $2.39 \text{ mi}^2$ ), with constant grid spacings of 200 m (656 ft) in the longitudinal direction (the lengthwise direction of flow) and 160 m (525 ft) in the lateral direction (width of channel); this spans six grid cells wide and thirty-five grid cells long. The last column of nodes, which represents the area directly next to the Outer Harbor region, was expanded so that it is eight nodes wide rather than six. This was done to make the expansion to the outer region less sudden. Figure 4-2 shows the plan view (longitudinal and lateral directions) of the model grid.

The effects of Coriolis force were neglected because of the small scale of the Inner Harbor as compared to the scale over which Coriolis forces has significant effects and because dye study results show symmetry in the movement of the dye. Therefore the T-shaped domain was cut along its axis of symmetry to reduce the number of nodes and consequently the computation time, so that the shape of the domain region is a half-T, and only the lower half of the harbor is represented. In other words, Inner Harbor is thirty-five nodes long and three nodes wide (and four nodes wide in the last column near the outer region).

Since the treatment of the open boundary is still an unresolved topic at the moment, the Outer Harbor was treated as a reservoir for the water and mass from the Inner Harbor. As a result, the Outer Harbor was schematized as a large rectangular domain. The goal was to make this region large enough so that the majority of the mass does not reach the sides (lateral) nor the open boundary, while keeping practicality in mind, such as minimizing computation time. In order to reduce the number of nodes in this outer region, a variable horizontal grid spacing scheme was used. The areas of the grid cells increased with lateral and longitudinal distance from the mouth of the Inner Harbor (the location at which the Inner Harbor and Outer Harbor regions meet), so that the bottom downstream corner region of the domain

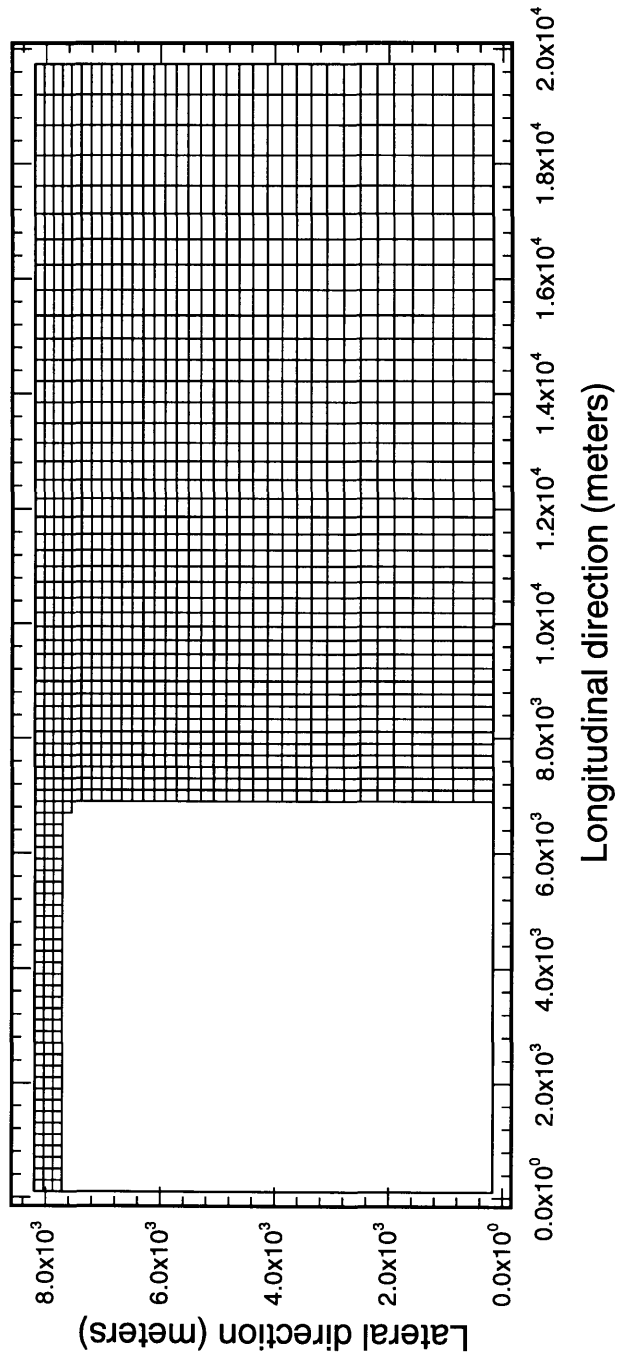


Figure 4-2: Plan view of the model grid.

had the largest grid size. In the longitudinal direction, the grid spacings increased by ten percent for the second and third groups of five nodes from the mouth, then fifteen percent for the next three groups of five nodes, and twenty percent for the last two groups, which are furthest away from the mouth. Starting from the mouth and moving outwards towards the right side of the domain, the longitudinal grid spacings are, 200.0, 220.0, 242.0, 278.3, 320.05, 368.05, 441.66, and 529.99 meters (656, 722, 794, 913, 1050, 1210, 1450, and 1740 ft). In the lateral direction, the grid spacings increased by ten percent for the second and third groups of five nodes from the mouth, then fifteen percent for the next three groups of five nodes, and twenty percent for the last group, which is furthest away from the mouth. Starting from the mouth and moving towards the side, the lateral grid spacings are 160.0, 176.0, 193.6, 222.64, 256.04, 294.44, and 353.33 meters (525, 577, 635, 730, 840, 966, 1150 ft). The Outer Harbor is 40 nodes long and 35 nodes wide. With the required dummy rows and columns at the outer edges, the total dimension of the grid is 78 nodes in the longitudinal and 39 nodes in the lateral direction.

The entire domain has a spatially-constant mean water depth of 10.0 meters (32.8 ft) in the vertical direction. There are ten equally-spaced layers. Because of the use of  $\sigma$ -coordinates, these ten layers vary with time in thickness and location in the vertical direction since there is tidal forcing. The bathymetric charts indicates a fairly constant depth within the Inner Harbor. This is due to the shipping channel in the center of the Inner Harbor. In addition, the horizontal areas of the various regions of the Inner Harbor take into account any large variation in depths, such as those that occur near the shores and in the Reserved and Fort Point Channels.

### **4.2.2 Boundary conditions**

The entire downstream face of the domain was represented as the open boundary, where there was tidal forcing, as shown in Figure 4-1. These 35 nodes received  $M_2$  tides, which have a period of 12.42 hours, with amplitudes of 1.5 m (4.9 ft) and no phase lag so that high tide occurred at  $t = 0$ . This means that the depth of the domain ranges from 8.5 meters (27.9 ft) to 11.5 meters (37.7 ft). All of the other

sides were dry cells, in which they were considered land.

### 4.2.3 Initial conditions and forcings

Coriolis force was neglected in the simulations since the area of the entire domain is 20,000 m ( $6.56 \times 10^4$  ft) long by 8280 m ( $2.72 \times 10^4$  ft) wide and the area of the Inner Harbor region is 7000 m ( $2.30 \times 10^4$  ft) long and 960 m wide (3150 ft); see Figure 4-2. And as explained in Section 4.2.1, this area is small compared to the distance over which Coriolis forces has significant effects. Additionally, precipitation, evaporation, heat flux, and wind were omitted in the simulations since these are also insignificant in affecting flushing in the Inner Harbor.

It was assumed that there is initially constant temperature of 17°C and salinity of 30 psu throughout entire domain. This assumption is a simplification since Boston Harbor is slightly stratified during the summer months due to the increased discharge from the rivers during the spring and the increased temperature gradients during the summer months. [7]

### 4.2.4 Parameter values

A time step of 60 seconds was chosen for the simulations. Each of the simulations was run for 10,080 time steps (168 hours), while printing velocity and tracer concentration data at every node and every layer every 480 timesteps (8 hours). The ramp function was given 90 time steps (1.5 hours) as its time constant,  $i_{ramp}$ , so that in approximately 4.5 hours, all the model forcing functions reached their full values.

Non-linear advection was used so that the momentum advection terms were included. The non-dimensional bottom friction coefficient (which is one-eighth of the Darcy-Weisbach friction factor) was chosen to be 0.0025 and the bottom roughness coefficient was 0.003 meters. The constant horizontal mixing coefficient was 2.0  $\text{m}^2/\text{s}$ . The horizontal Prandtl number, which is the ratio of horizontal viscosity to horizontal diffusivity (or the ratio of momentum mixing to dispersive mixing), was

1.0. A turbulent closure submodel (as described in Section 4.1.2) was used for the vertical mixing. The background mixing value was  $5 \times 10^{-5} \text{ m}^2/\text{sec}$ . This is 50 times greater than molecular mixing, and the value was chosen by roughly calibrating the amount of vertical mixing to that indicated by the Boston Inner Harbor dye study. The vertical Prandtl number was 1.0.

Freshwater discharges from the Mystic and Charles Rivers were simulated in the numerical model. It was assumed that the temperature of freshwater released was the same as that of harbor ( $17 \text{ }^\circ\text{C}$ ). The Mystic River discharge was represented by an offshore discharge at element (4, 36), which has its center at the coordinates (300.0 m, 8040 m), with all of the discharge occurring in the top surface layer. The daily average flow rates from the Winchester gage (#1025), which is about 0.8 km (0.5 mi) upstream of the Mystic Lakes, were adjusted by scaling these values by the ratio of the total drainage area to the gage drainage area. The total drainage area up to the Mystic bridge is  $171 \text{ km}^2$  ( $66 \text{ mi}^2$ ), and the drainage area at the gage is  $63.7 \text{ km}^2$  ( $24.6 \text{ mi}^2$ ). The adjusted daily average flow rates were used as the Mystic River freshwater discharge rates; so then the flow rates were nearly constant, varying every 24 hours. [28]

The Mystic River flow rates used in the model simulations ranged from 0.21 to  $0.70 \text{ m}^3/\text{s}$ . These values were calculated from the daily average flow rates at the Winchester gage, which were adjusted for the drainage areas. These flow rates represent half of the actual calculated values since the half-T grid, which represents half of the Inner Harbor, was used in the model simulations.

The Charles River Dam discharge location also was represented by an offshore discharge at element (13, 36), which was its center at the coordinates (2500 m, 8040 m), with all of the discharge occurring in the top surface layer. Since the Charles River flow rates vary with each model simulation, as does the freshwater input time sequence, further details on this freshwater discharge will be discussed in Section 4.3.

## 4.3 Model Simulations

A series of numerical simulations using the model ECOM-si were run to explore the effects of freshwater inflow on the flushing of Boston's Inner Harbor. All of these were run on a Unix DECstation 5000/25 workstation. First a base case was formulated and roughly calibrated, as described in the Section 4.2. Various scenarios were then tested using most of the input parameters from the base case. The following sections will describe the base case and these test scenarios in detail.

### 4.3.1 Base case

The base case simulation followed the time variation of freshwater discharge of the Charles River Dam from the Adams *et al.* dye study as closely as possible. The model ran for 168 hours (7 days), simulating from midnight (00:00) of 22 July 1992 until midnight of 28 July 1992. In order to allow all of the model parameters, such as the flow field, to reach "quasi-equilibrium," since the model simulation was starting from rest, the first freshwater injection did not occur until model time  $t = 20.7$  hours. This corresponds to 20:42 of 22 July in the dye study. This first slug of freshwater was injected over a period of 5.5 hours, from  $t = 20.7$  hours until  $t = 26.5$  hours, with a volume flow rate of  $10 \text{ m}^3/\text{s}$ . Because a true step function cannot be implemented in the model, the rectangular step input was simulated as a trapezoidal input. The flow rates at the sluice gates of the dam were determined from the calibration curves (Figure 3-2) for the Charles River Dam by using the daily logs which record the water elevations at the Charles River and the Boston Harbor sides of the dam every half hour.

A conservative tracer of concentration  $117 \mu\text{g}/\text{l}$  was also included with this initial freshwater injection. This first discharge corresponded to  $1.98 \times 10^5 \text{ m}^3$  of freshwater and 23.1 kg of a conservative tracer. The flow rates used in the model simulation for the Charles River Dam discharges represent half of the actual flow rates at the sluice gates because of the the half-T model grid used in the simulation. Similarly, the total mass injected represents half of the actual mass injected in the Boston



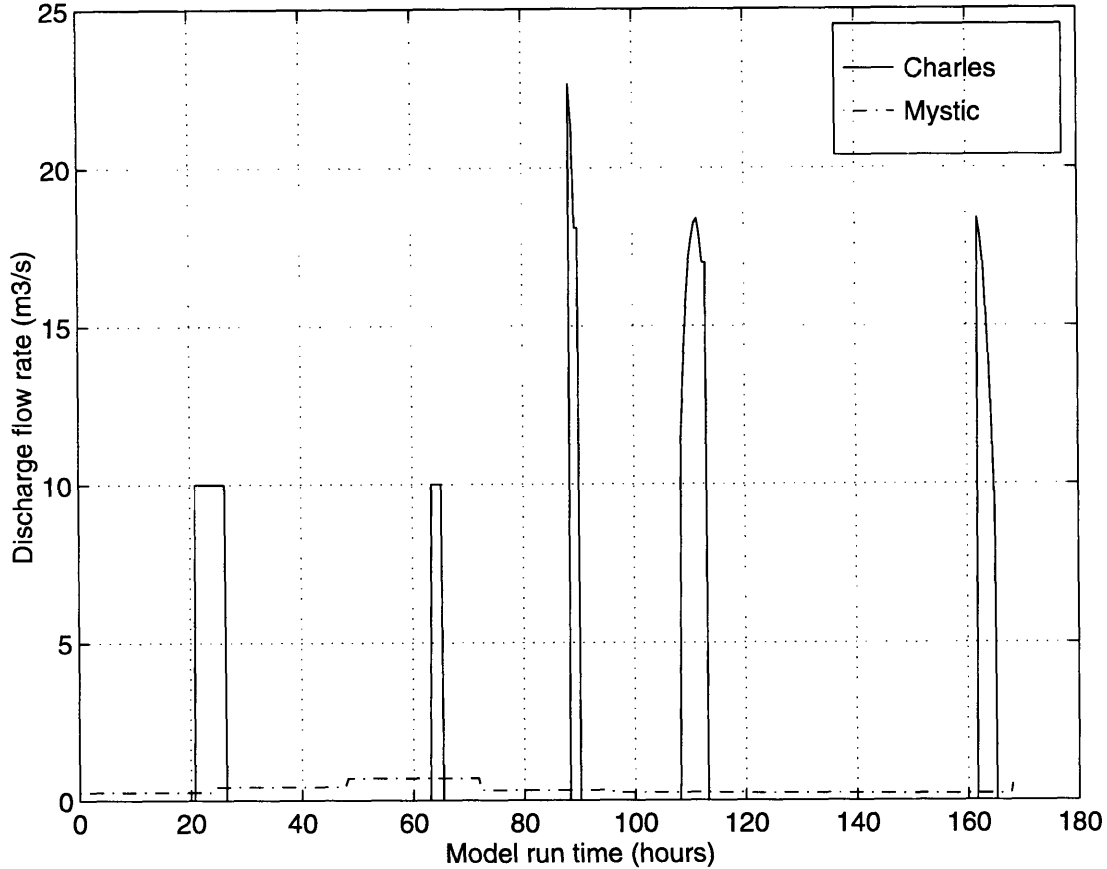


Figure 4-3: Time variation of freshwater flow rate at the Charles River Dam and Mystic River for the model base case.

Inner Harbor dye study by Adams *et al.*

The second discharge had a constant flow rate of 10 m<sup>3</sup>/s from model time  $t = 63.1$  to  $t = 65.5$  hours. The flow rate of the third discharge varied from 22.65 m<sup>3</sup>/s to 18.1 m<sup>3</sup>/s during model time  $t = 88.3$  to  $t = 90.2$  hours. The flow rate of the fourth discharged occurred at model time  $t = 108$  to  $t = 113$  hours with a flow rate from 11.4 m<sup>3</sup>/s to 18.4 m<sup>3</sup>/s. And the flow rate of the fifth discharged varied from 18.4 m<sup>3</sup>/s to 9.2 m<sup>3</sup>/s at model time  $t = 162$  to  $t = 165$  hours. Therefore, the total amount of freshwater released from the Charles River Dam during the model simulation was 851,000 m<sup>3</sup>, and the average freshwater flow rate over 147 hours is 1.61 m<sup>3</sup>/s. See Figure 4-3 for the time sequence of the freshwater discharge from the Charles River Dam and Mystic River used in the base case model simulation.

### 4.3.2 Test scenarios

Since the Charles River is the dominant source of freshwater inflow to the Inner Harbor, only the freshwater discharge of the Charles River was varied in the test scenarios. In all of these simulations, no freshwater was released from the Charles River Dam until at least 20.7 hours after the start of the model simulation (model time  $t = 20.7$  hours). Moreover, the same total mass of conservative tracer (23.1 kg) as in the base case was released in these simulations over the same period of time, 5.5 hours.

#### Continuous discharge

Rather than discharging freshwater in intermittent releases, as is usually done at the New Charles River Dam, freshwater from the river may be released continuously. Five simulations were carried out with constant and continuous freshwater discharges, each with different a flow rate, and thus a different total volume of freshwater, for each case.

**Half of total freshwater volume.** Half of the volume of freshwater as in the base case simulation ( $850,968 \text{ m}^3$ ) was released continuously over 147 hours. The Charles River freshwater flow rate in this simulation was  $0.80 \text{ m}^3/\text{s}$ . The concentration of tracer was  $1450 \text{ }\mu\text{g}/\text{l}$ , which was released over 5.5 hours, at  $t = 20.7 - 26.5$  hours.

**Same total freshwater volume.** The same volume of freshwater as in the base case simulation was released continuously over 147 hours. The Charles River freshwater flow rate in this simulation was  $1.61 \text{ m}^3/\text{s}$ . The concentration of tracer was  $726 \text{ }\mu\text{g}/\text{l}$ , which was released over 5.5 hours, at  $t = 20.7 - 26.5$  hours.

**Twice total freshwater volume.** Twice the total volume of base case Charles River freshwater was released continuously in this simulation with the constant flow rate of  $3.21 \text{ m}^3/\text{s}$ . The total freshwater released was  $3.96 \times 10^5 \text{ m}^3$ . The conservative tracer was again released over 5.5 hours, from model time  $t = 20.7$  hours to  $t = 26.5$

hours, with a concentration of  $363 \mu\text{g}/\text{l}$ .

**Five time total freshwater volume.** Five times the base case Charles River freshwater volume was released continuously in this simulation. The constant flow rate was  $8.03 \text{ m}^3/\text{s}$ , which discharged a total of  $9.9 \times 10^5 \text{ m}^3$  of freshwater over the 147-hour period. The tracer concentration was  $145 \mu\text{g}/\text{l}$ , which was discharged over 5.5 hours during model time  $t = 20.7 - 26.5$  hours.

**Ten times total freshwater volume.** Ten times the total volume of base case Charles River freshwater was released continuously in this simulation so that the constant flow rate was  $16.1 \text{ m}^3/\text{s}$ . The total freshwater released was  $1.98 \times 10^6 \text{ m}^3$ . The conservative tracer concentration was  $72.6 \mu\text{g}/\text{l}$ , which was discharged over 5.5 hours during model time  $t = 20.7 - 26.5$  hours.

### **Constant discharge around high tide**

Theoretically, freshwater released during high tide should be the most effective in transporting water out of the Inner Harbor. This simulation released Charles River freshwater periodically during the 2 hours around each high tide of the model simulation, starting from the high tide which  $t = 24.8$  hours in the model. Figure 4-4 shows the freshwater discharge patterns for the Charles River and the Mystic River for this simulation, as well as the times at which high tide occurs, which are signified by the asterisks (\*).

The flow rate of  $9.85 \text{ m}^3/\text{s}$  was constant and continuous during each of these 2-hour discharges, and the average flow rate over the 147 hours was  $1.61 \text{ m}^3/\text{s}$ , as was in the base case. Because it would not make sense to release the conservative tracer of 5.5 hours of freshwater discharge since that would take nearly three high tide cycles to release all of the tracer, the 23.1 kg of tracer was released during the first 2-hour interval, from  $t = 23.8 - 25.9$  hours.

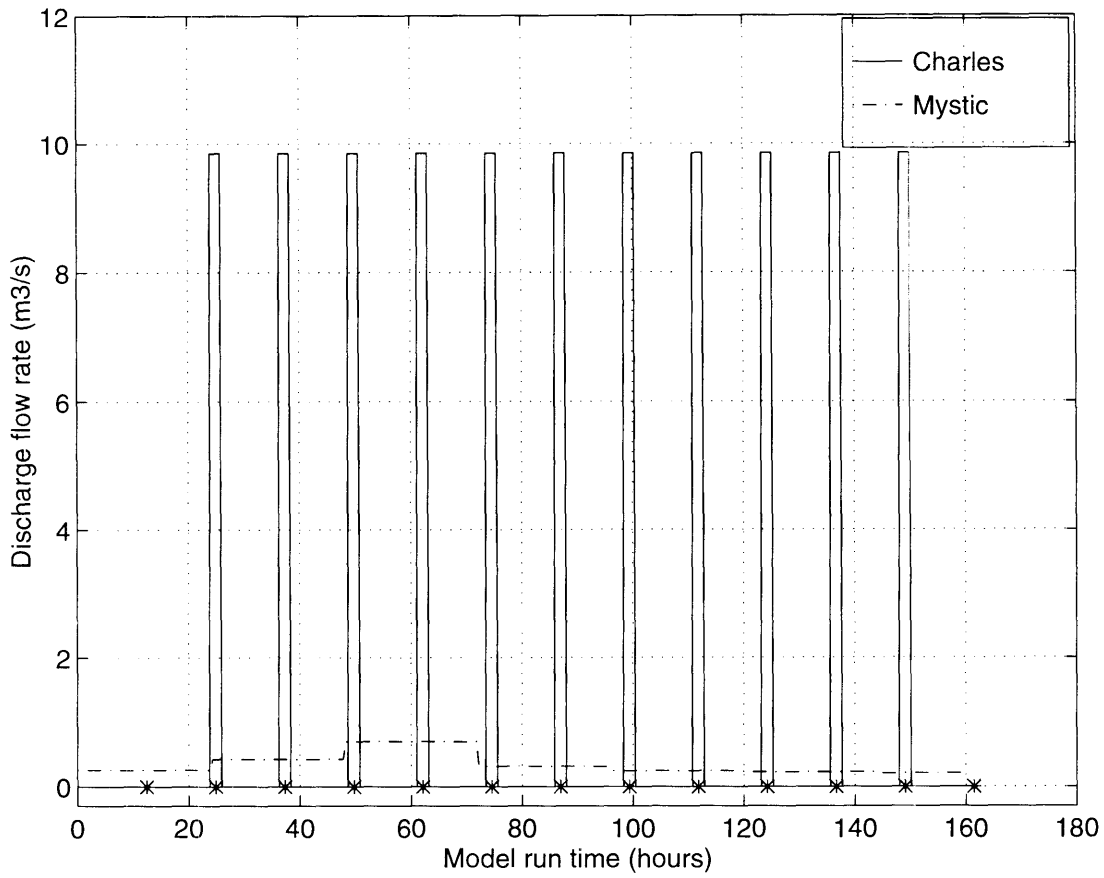


Figure 4-4: Freshwater flow rate variation over time for Charles River Dam during the 2 hours around each high tide.

### **Vertical diffusion model sensitivity**

The vertical mixing coefficient used in the circulation model ECOM-si is the sum of a user-specified background vertical diffusivity, `umo1`, and the coefficients calculated by the turbulence closure model. Changing the value of `umo1` is likely to have a noticeable effect on the vertical diffusion of the conservative tracer and also the residence time of the tracer and associated freshwater in the Inner Harbor. In order to test the sensitivity of the model to the background vertical mixing coefficient, `umo1`, two simulations were run in which the value of the molecular vertical diffusivity was changed from  $5 \times 10^{-5} \text{ m}^2/\text{s}$  in the base case to  $2.5 \times 10^{-5} \text{ m}^2/\text{s}$  and  $7.5 \times 10^{-5} \text{ m}^2/\text{s}$ , while keeping all the other inputs the same as the base case, including the Charles River Dam flow time sequence.

### **4.3.3 Summary of simulations**

The model simulations are summarized in Table 4.1. This table shows the type of discharge scenario (intermittent or continuous), the average flow rate of the Charles River discharge, and the `umo1` value used in the simulations. Note that the flow rates indicated are the values used in the simulations and are half of the actual flow rates at the Charles River since the half-T domain, which represents half of the river flows as well as half of the Inner and Outer Harbors, was used.

## **4.4 Modeling Results**

After each model simulation was completed, the model data was evaluated graphically and through some calculations of Charles River freshwater residence time in the Inner Harbor. As mentioned in Section 4.2, the model data were saved to an output file every 8 hours of simulation time. The parameters that were recorded at these times include the x, y, and z coordinates of each grid cell, the corresponding velocity components (u, v, and w) and the conservative tracer mass of each cell. In addition, the total mass in a region (the Inner Harbor, the Outer Harbor, or the

Discharge scenario	Avg. Charles River flow rate (m <sup>3</sup> /s)	umol (m <sup>2</sup> /s)
base-low tide	1.61	5 x 10 <sup>-5</sup>
hide tide	1.61	5 x 10 <sup>-5</sup>
continuous	0.803	5 x 10 <sup>-5</sup>
continuous	1.61	5 x 10 <sup>-5</sup>
continuous	3.21	5 x 10 <sup>-5</sup>
continuous	8.03	5 x 10 <sup>-5</sup>
continuous	16.1	5 x 10 <sup>-5</sup>
low tide	1.61	2.5 x 10 <sup>-5</sup>
low tide	1.61	7.5 x 10 <sup>-5</sup>

Table 4.1: Summary of model simulations. Note that the flow rates represent half of the actual values for the Charles River because of the half-T domain used in the simulations.

entire grid domain) was calculated every 8 hours by summing up the tracer mass in each grid cell of the desired region. The tracer mass in each grid cell was determined by the product of the tracer concentration of the cell and the cell volume. The volume in each cell varies with time because of the time-varying surface elevation, which is due to the tidal forcing. In the following sections, the relevant tracer mass data and the freshwater residence time calculations will be presented for each of the model simulations.

#### 4.4.1 Base case

Because a portion of the Charles River freshwater released is tagged with a conservative tracer, examining how the tracer mass varies with time within the Inner Harbor will lead to an understanding of the freshwater residence time. Figure 4-5 shows the time variation of tracer mass in the Inner and Outer Harbor, as schematized in the model grid, and the entire domain. Note that the total mass is twice the mass injected during the model simulation. This represents the mass in the entire Inner and Outer Harbor regions, as if the model grid was a full-T instead of the half-T that was used in the simulation.

In order to use Equation 2.4 to calculate the residence time of the conservative

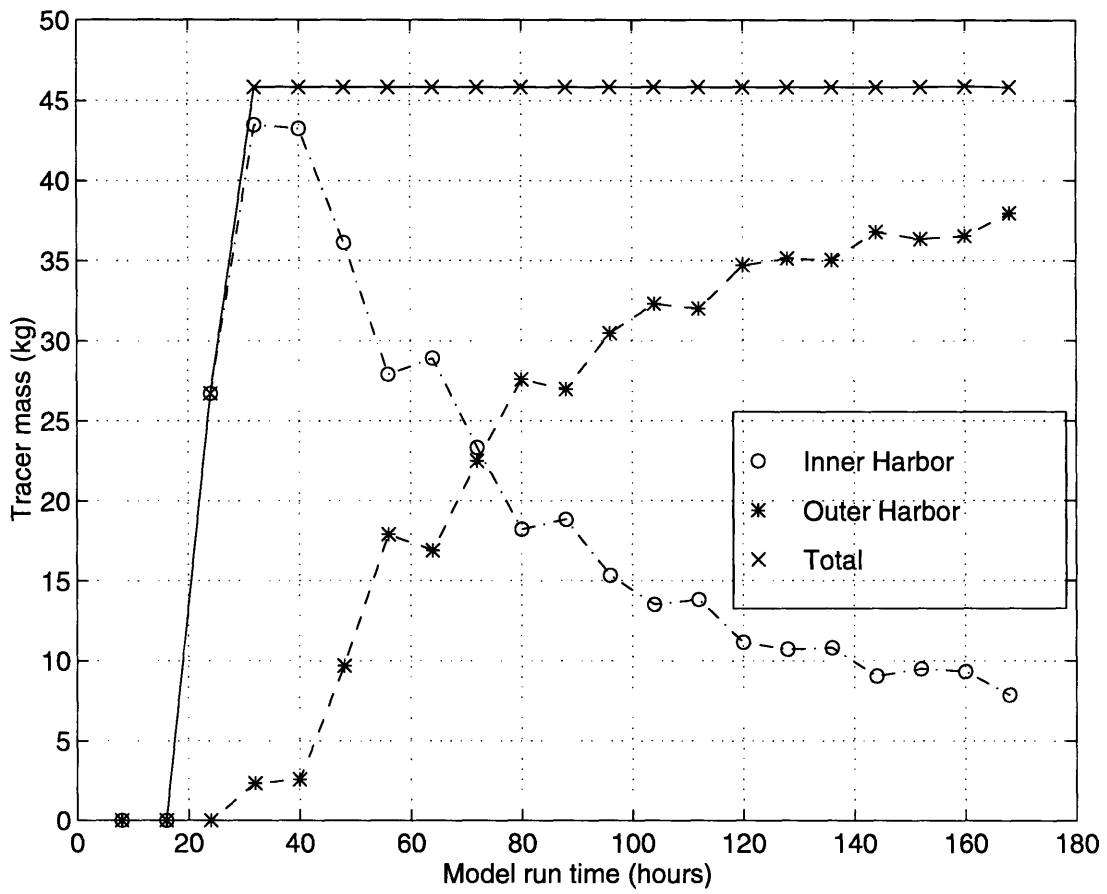


Figure 4-5: Tracer mass varying with time for the base case.

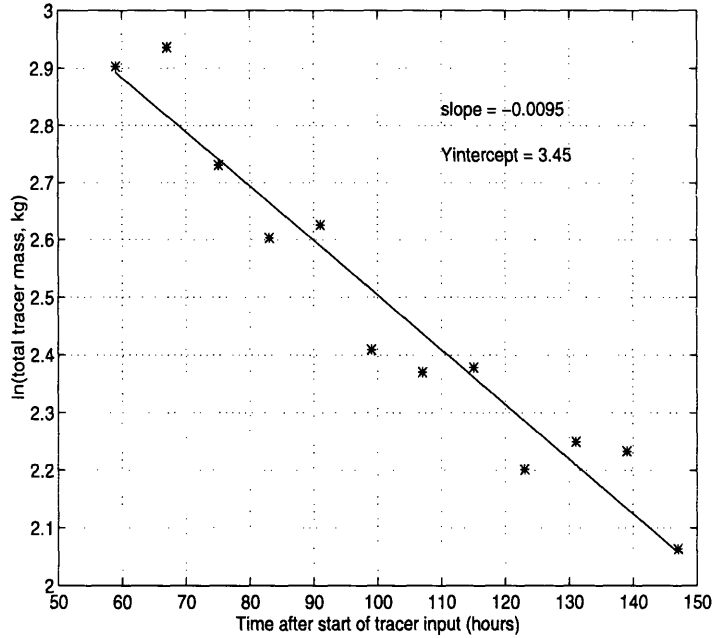


Figure 4-6: Fitting a line through  $\ln(\text{mass})$  vs. time for the base case.

tracer and its associated freshwater, the model data needed to be extrapolated. This was done by fitting a line through the data, with the natural log of the tracer mass versus time as the chosen form of the data. The data points starting from 59 hours after the beginning of the tracer release (model time  $t = 80$  hours) were used for line-fitting. The result was a line of slope  $-0.0095$  and  $y$ -intercept  $3.45$ . As shown in Figure 4-6, the Inner Harbor tracer mass data does decrease in an exponential form.

The residence time was calculated according to Equation 2.4 using the values extrapolated based on the line-fit. The numerator was estimated by using the trapezoidal method to integrate under the curve of total mass versus time. See Figure 4-7. The calculated residence time for the base case was 3.26 days.

Appendix Section B.1 shows the velocity vectors and the tracer concentration contours for the base case at several times during the simulation.



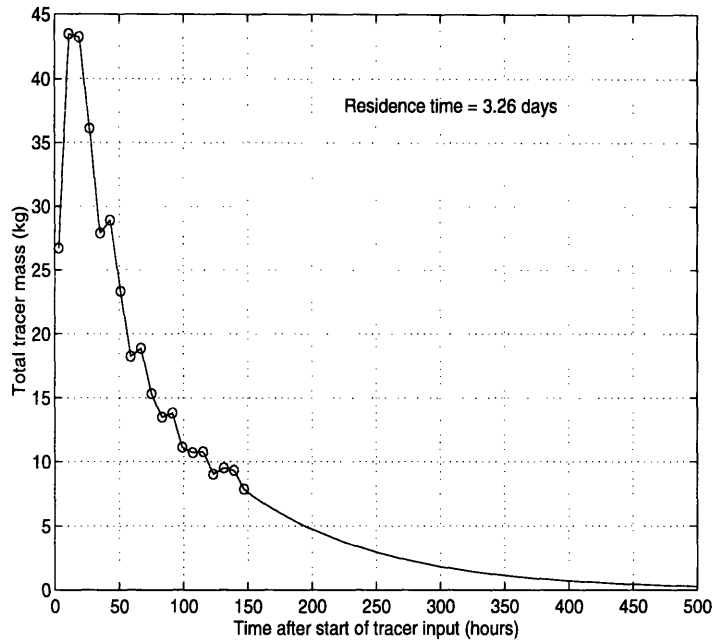


Figure 4-7: Tracer mass extrapolated to zero for the base case. The circles indicate the model data, and the line beyond  $t = 147$  hours is extrapolated based on a line fit.

#### 4.4.2 Test Scenarios

The results of the test scenarios described in Section 4.3.2 will be presented in this section.

##### Constant discharge

The following will describe the results of the model simulations in which the Charles River freshwater was discharged continuously at various flow rates.

**Half of total freshwater volume.** The mass variation with time in the Inner Harbor, Outer Harbor and the entire model grid for the simulation with continuous freshwater discharge, which has half of the total Charles River freshwater volume as the base case, is shown in Figure 4-8. Fitting a line through the data (natural log of Inner Harbor mass versus time) starting at 59 hours after the start of the tracer release gave a slope of -0.0080 and y-intercept of 3.58. See Figure 4-9. The calculated residence time from the mass-time curve in Figure 4-10 was 4.22 days.

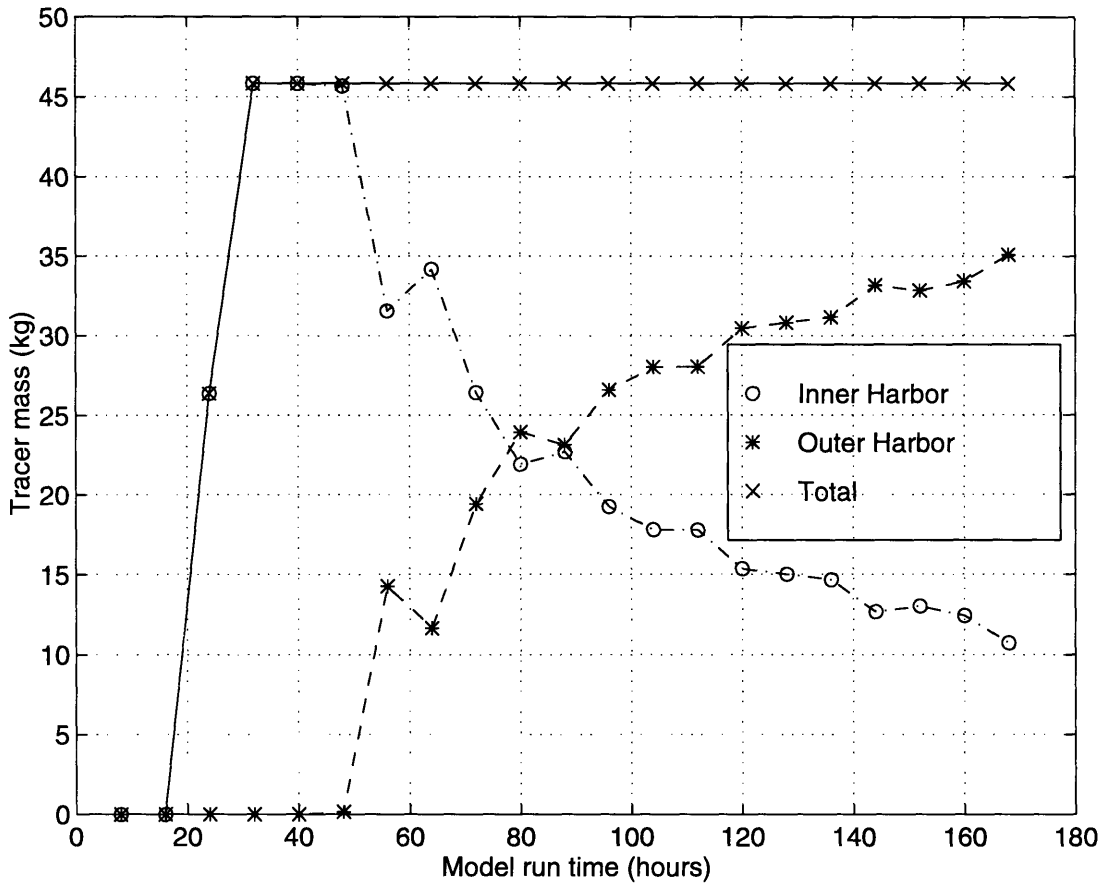


Figure 4-8: Tracer mass varying with time for continuous discharge with half of freshwater volume as base case.

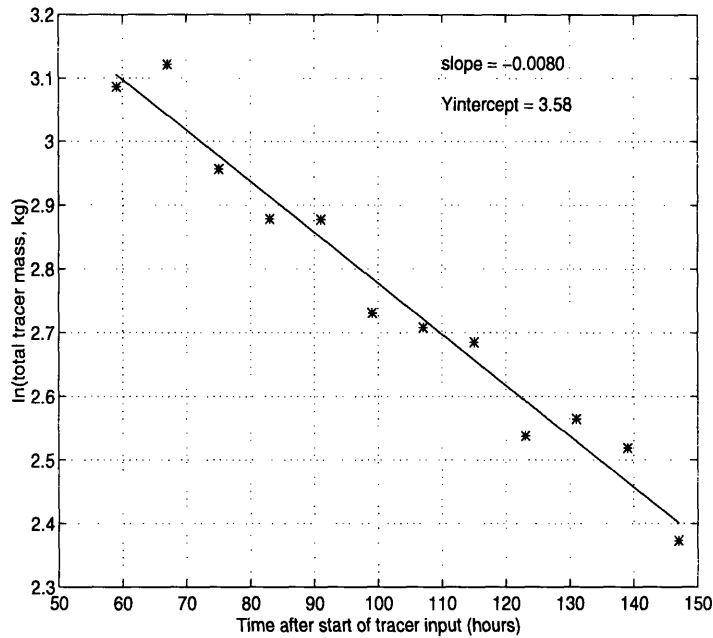


Figure 4-9: Fitting a line through  $\ln(\text{mass})$  vs. time for continuous discharge with half of freshwater volume as base case.

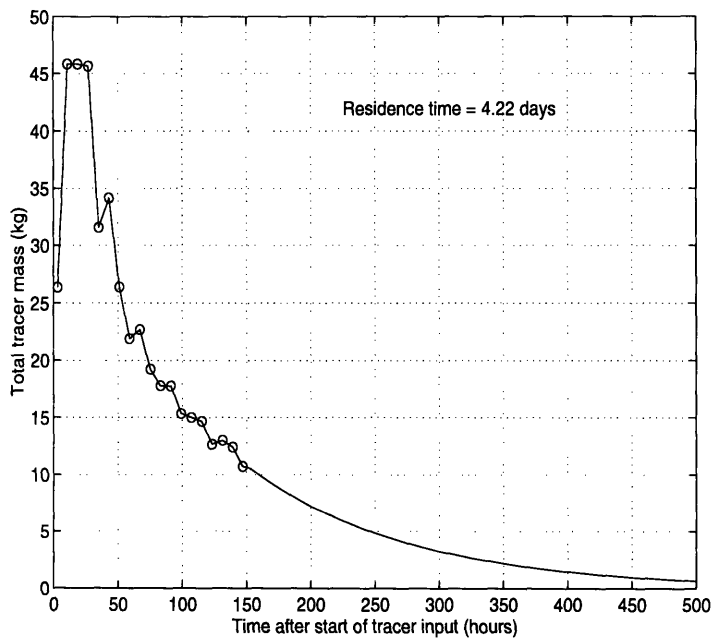


Figure 4-10: Tracer mass extrapolated to zero for continuous discharge with half of freshwater volume as base case. The circles indicate the model data, and the line beyond  $t = 147$  hours is extrapolated.

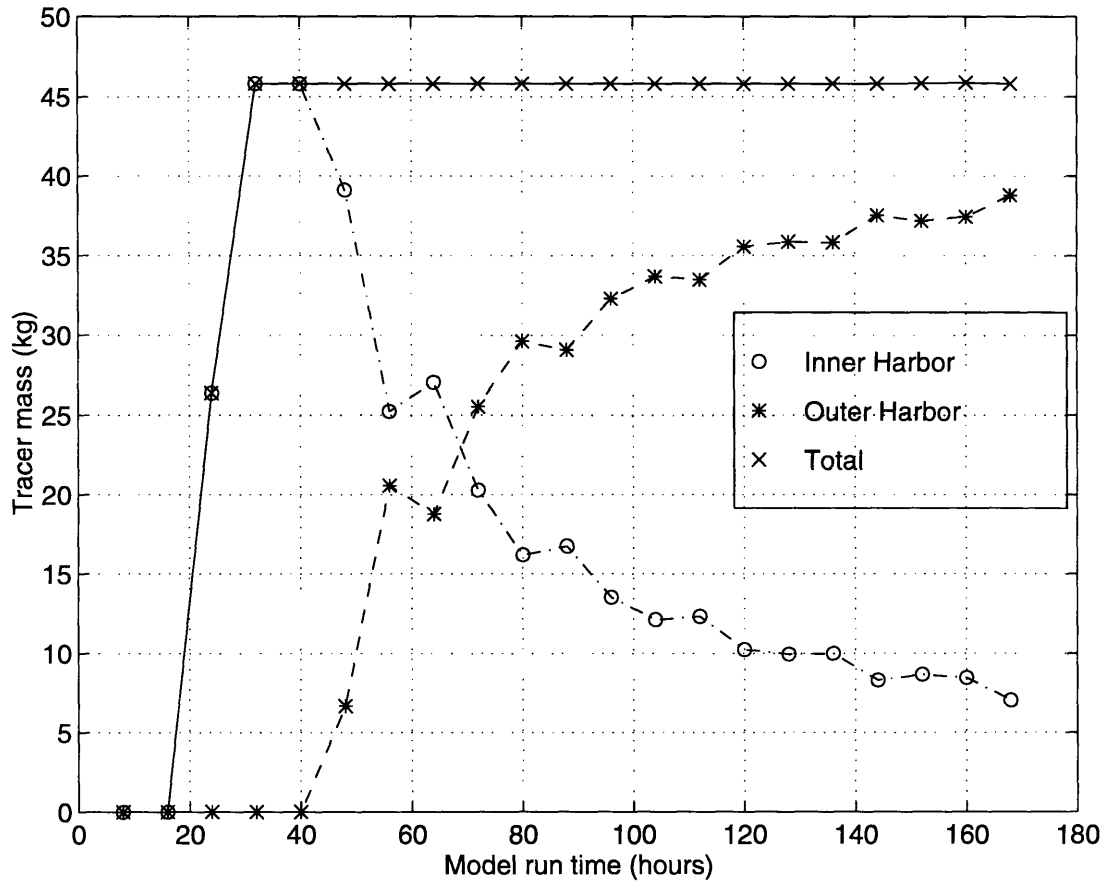


Figure 4-11: Tracer mass varying with time for continuous discharge with same freshwater volume as base case.

**Same total freshwater volume.** The mass variation with time in the Inner Harbor, Outer Harbor and the entire model grid for the simulation with continuous freshwater discharge, which has the same total Charles River freshwater volume as the base case, is shown in Figure 4-11. Fitting a line through the data (natural log of Inner Harbor mass versus time) starting at 59 hours after the start of the tracer release gave a slope of -0.0092 and y-intercept of 3.32. See Figure 4-12. The calculated residence time was 3.12 days. See Figure 4-13.

**Twice total freshwater volume.** The mass variation with time for the Inner Harbor, Outer Harbor and the entire model grid when twice the base case volume of Charles River freshwater is injected continuously is shown in Figure 4-14. Fitting a line through the data (natural log of Inner Harbor mass versus time) starting at

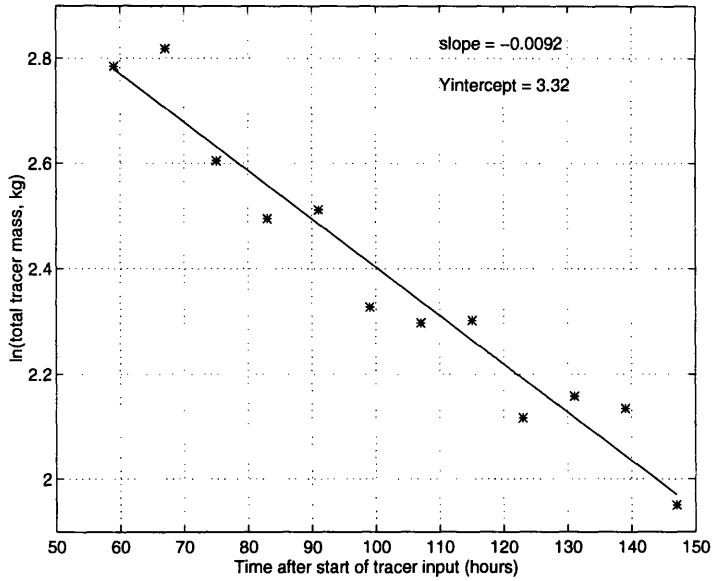


Figure 4-12: Fitting a line through  $\ln(\text{mass})$  vs. time for continuous discharge with same freshwater volume as base case.

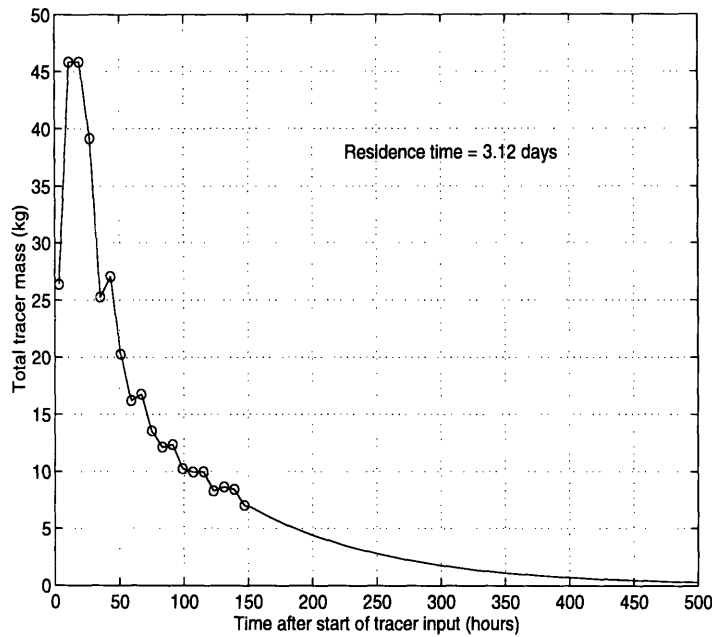


Figure 4-13: Tracer mass extrapolated to zero for continuous discharge with same freshwater volume as base case. The circles indicate the model data, and the line beyond  $t = 147$  hours is extrapolated.

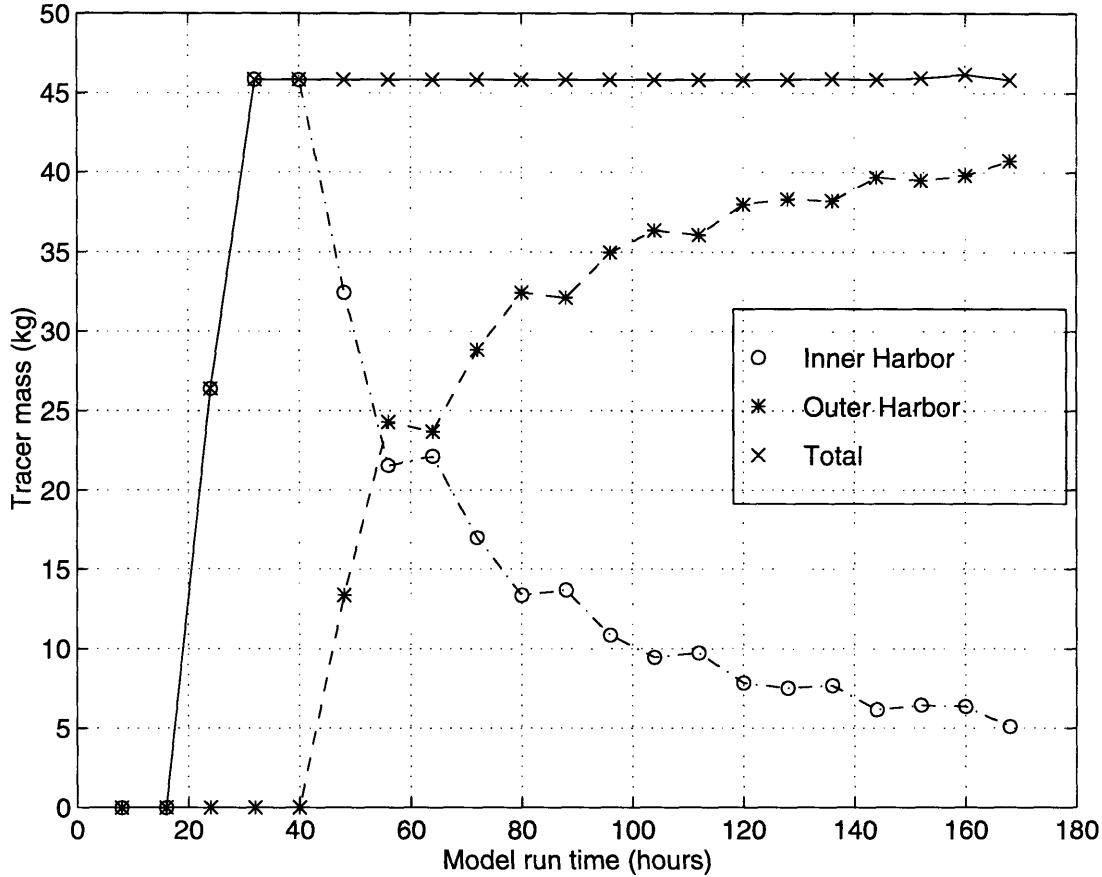


Figure 4-14: Tracer mass varying with time for constant discharge with twice the freshwater volume as base case.

59 hours after the start of the tracer release gave a slope of -0.0105 and y-intercept of 3.20, as shown in Figure 4-15. The calculated residence time was 2.54 days. See Figure 4-16.

**Five time total freshwater volume.** The mass variation with time for the Inner Harbor, Outer Harbor and the entire model grid when five times the base case volume of Charles River freshwater is injected continuously is shown in Figure 4-17. Note that the total tracer mass, and to some extent the Outer Harbor mass, increases after model time  $t = 128$  hours. This is due to the zero concentration gradient boundary condition imposed by the model ECOM-si for the open tidal boundary. Fitting a line through the data (natural log of Inner Harbor mass versus time) starting at 59 hours after the start of the tracer release gave a slope of -0.0126

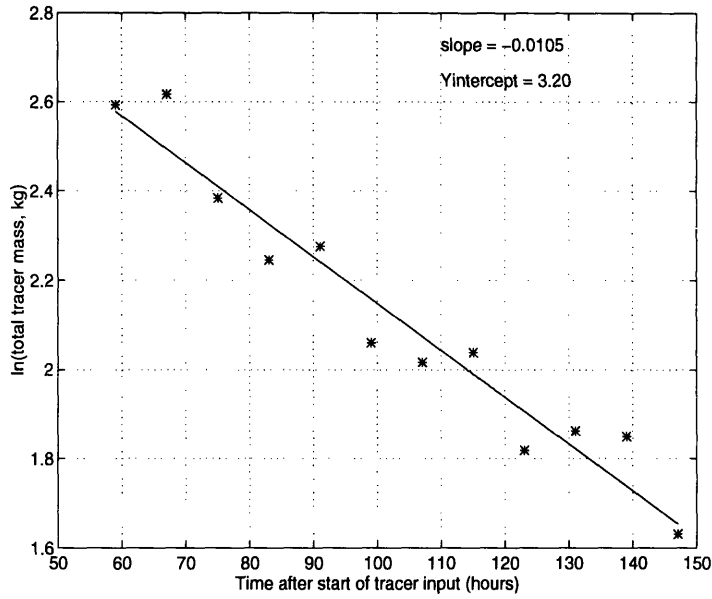


Figure 4-15: Fitting a line through  $\ln(\text{mass})$  vs. time for constant discharge with twice the freshwater volume as base case.

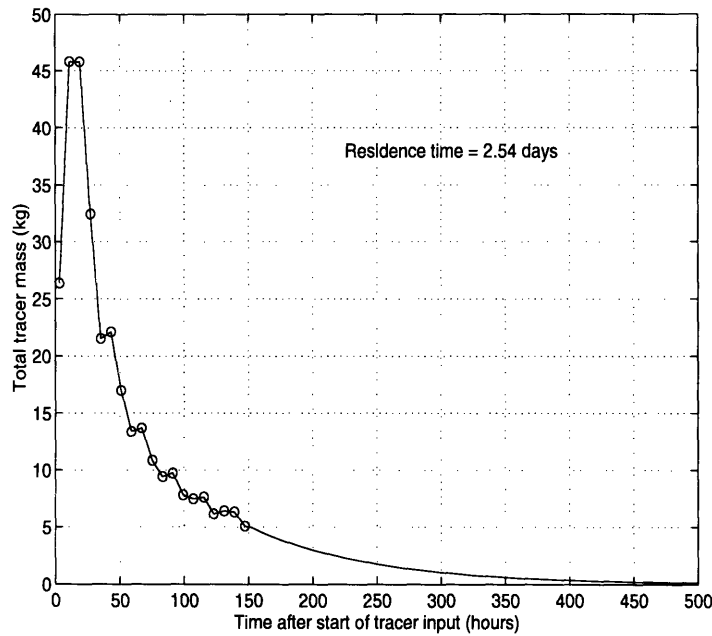


Figure 4-16: Tracer mass extrapolated to zero for constant discharge with twice the freshwater volume as base case. The circles indicate the model data, and the line beyond  $t = 147$  hours is extrapolated.

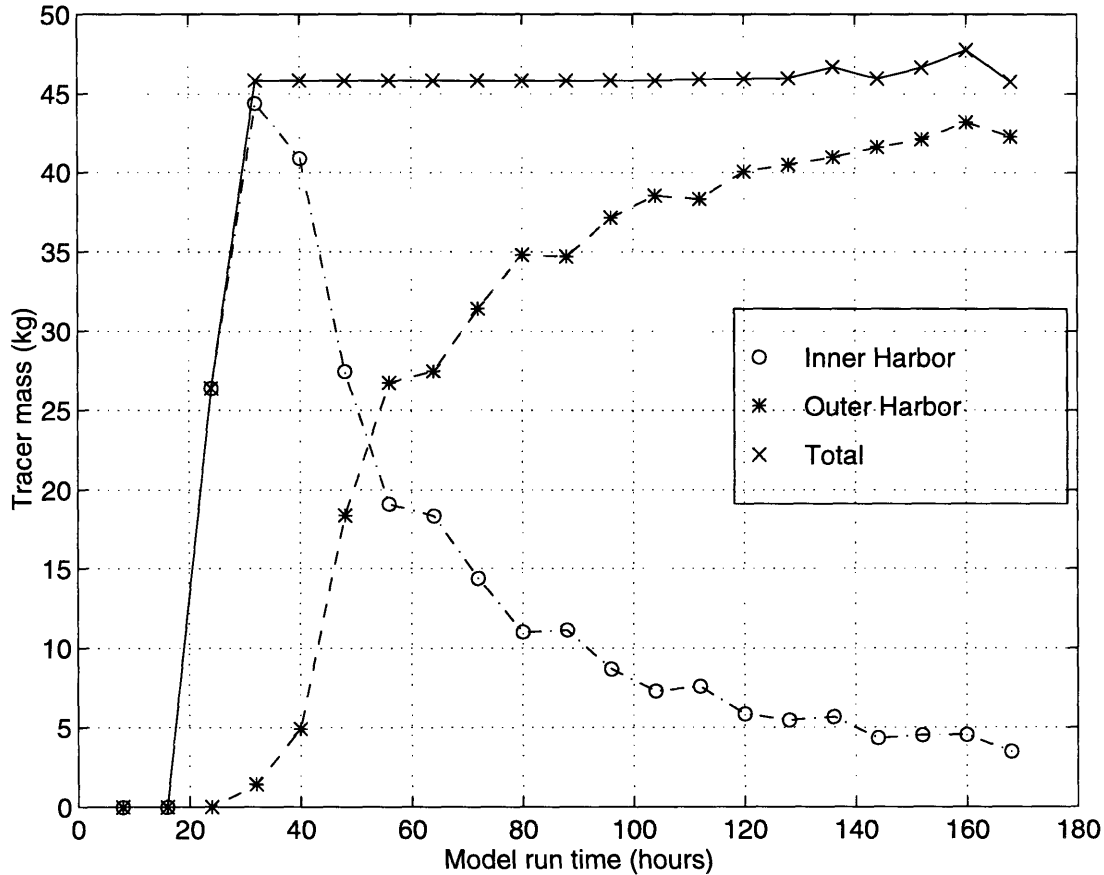


Figure 4-17: Tracer mass varying with time for five times the freshwater volume as base case.

and y-intercept of 3.13. See Figure 4-18. The calculated residence time was 2.04 days as shown in Figure 4-19.

**Ten times total freshwater volume.** The mass variation with time for the Inner Harbor, Outer Harbor and the entire model grid when twice the base case volume of Charles River freshwater is injected continuously is shown in Figure 4-20. Note that the Inner Harbor mass and total mass increases above the total input mass after model time  $t = 104$  hours. Again, this is due to the boundary condition imposed at the open tidal boundary by the model. Fitting a line through the data (natural log of Inner Harbor mass versus time) starting at 59 hours after the start of the tracer release gave a slope of -0.0128 and y-intercept of 2.81. See Figure 4-21. The calculated residence time calculated from integrating the mass versus time curve in



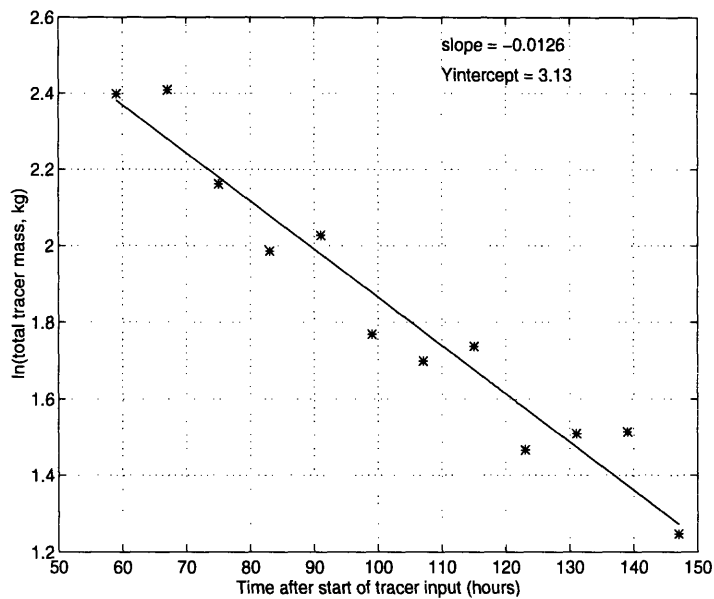


Figure 4-18: Fitting a line through  $\ln(\text{mass})$  vs. time for five times the freshwater volume as base case.

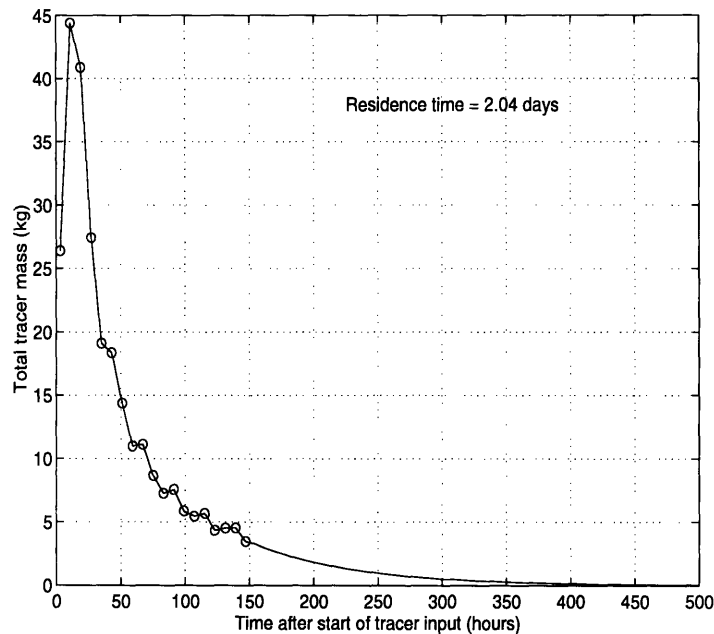


Figure 4-19: Tracer mass extrapolated to zero for five times the freshwater volume as base case. The circles indicate the model data, and the line beyond  $t = 147$  hours is extrapolated.

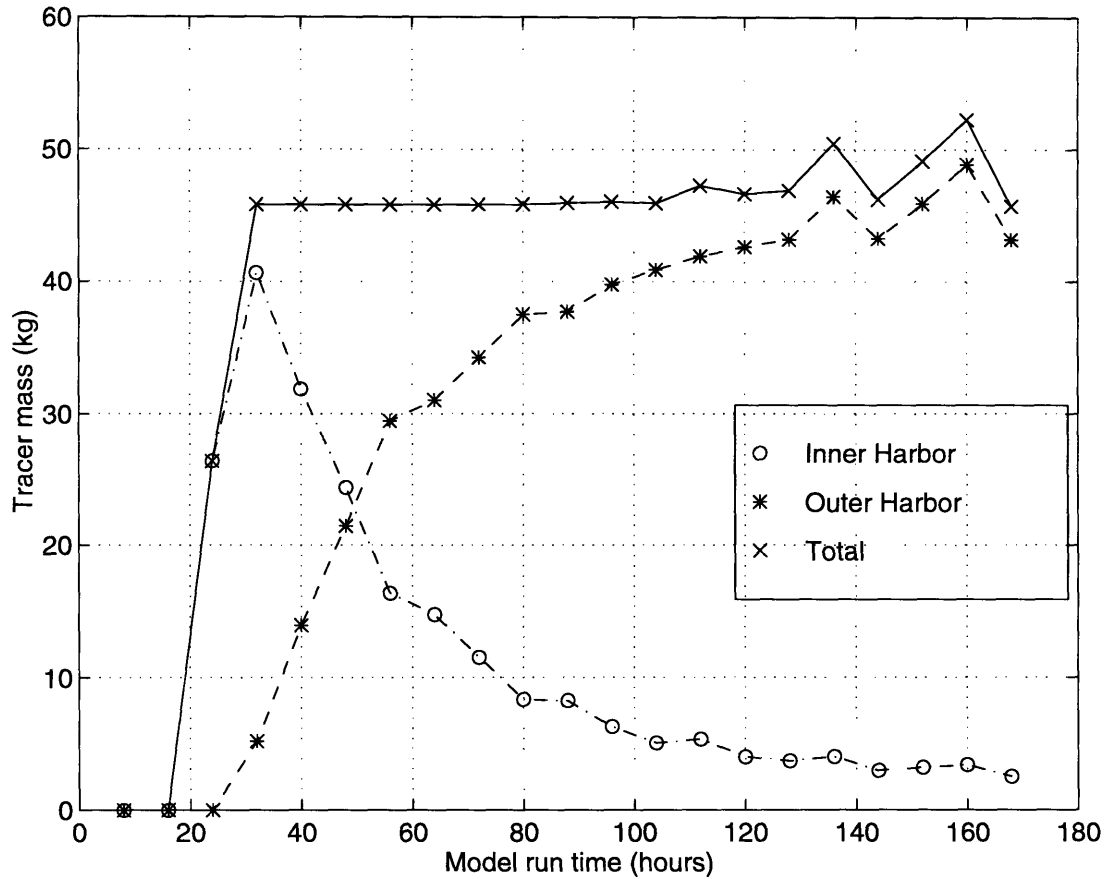


Figure 4-20: Tracer mass varying with time for ten times the freshwater volume as base case.

Figure 4-22 was 1.62 days.

### Constant discharge around high tide

The mass variation with time for the Inner Harbor, Outer Harbor and the entire model grid when freshwater is injected during the two hours surrounding each high tide is shown in Figure 4-23. Fitting a line through the data (natural log of Inner Harbor mass versus time) starting at 59 hours after the start of the tracer release gave a slope of -0.0098 and y-intercept of 3.45, as shown in Figure 4-24. The calculated residence time was 3.19 days. See Figure 4-25.

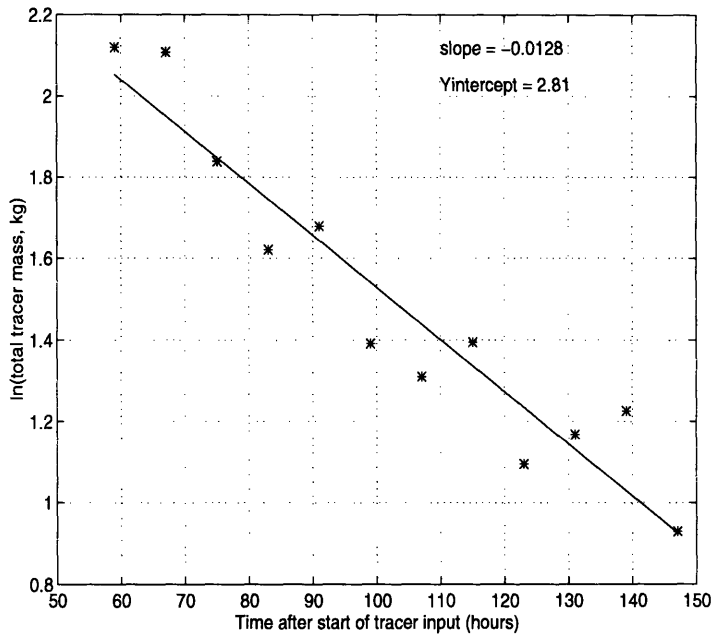


Figure 4-21: Fitting a line through  $\ln(\text{mass})$  vs. time for ten times the freshwater volume as base case.

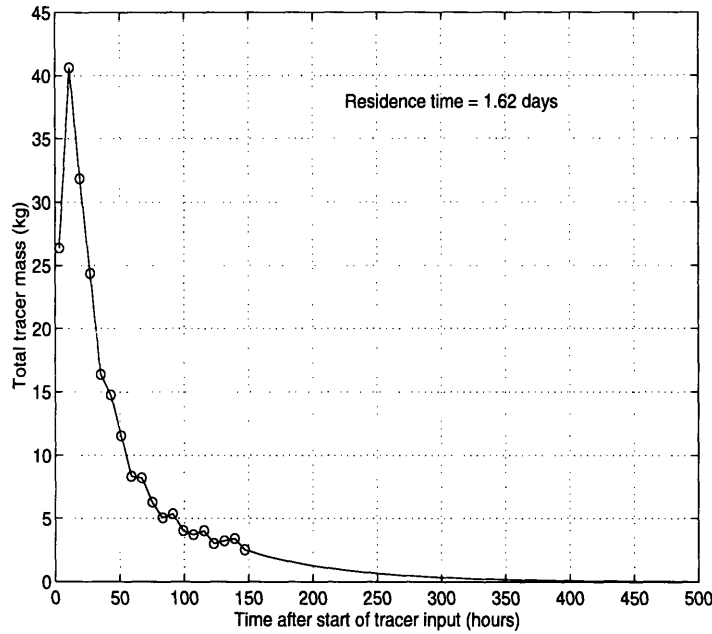


Figure 4-22: Tracer mass extrapolated to zero for ten times the freshwater volume as base case. The circles indicate the model data, and the line beyond  $t = 147$  hours is extrapolated.

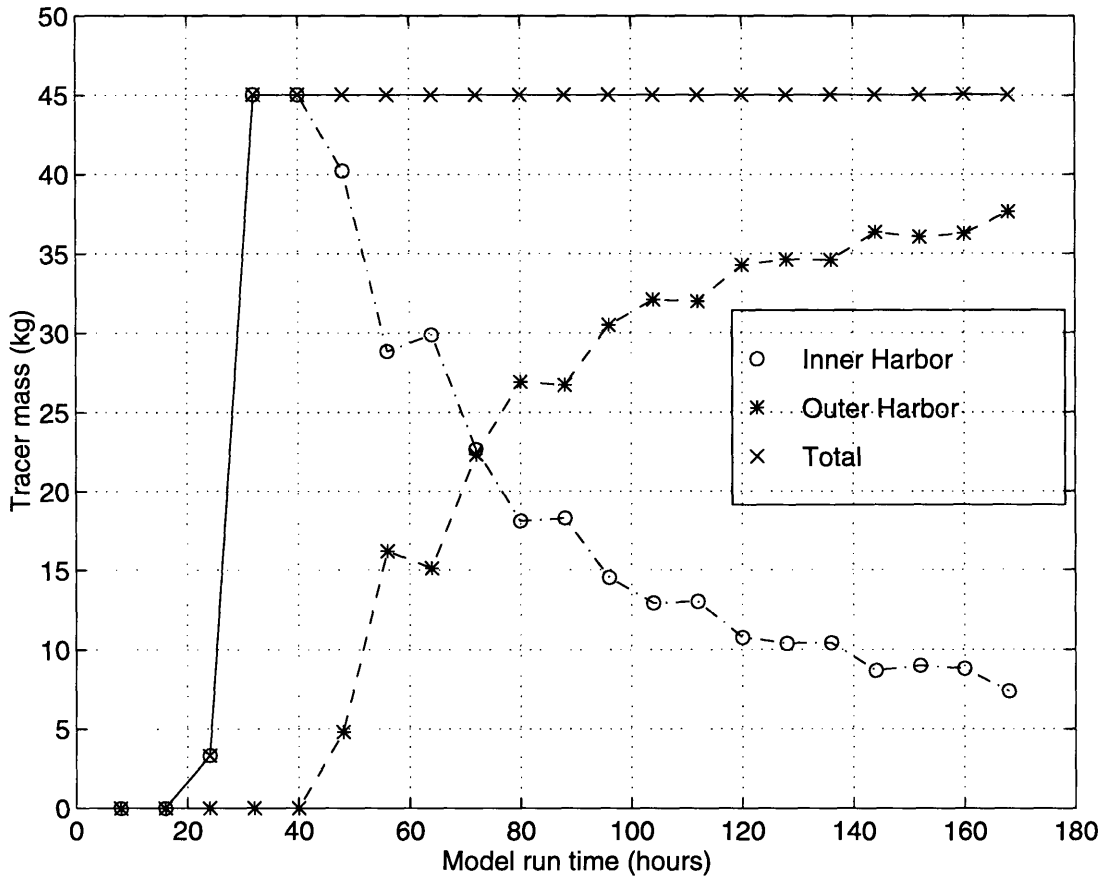


Figure 4-23: Tracer mass varying with time for discharge during the 2 hours around each high tide, with the same freshwater volume as base case.

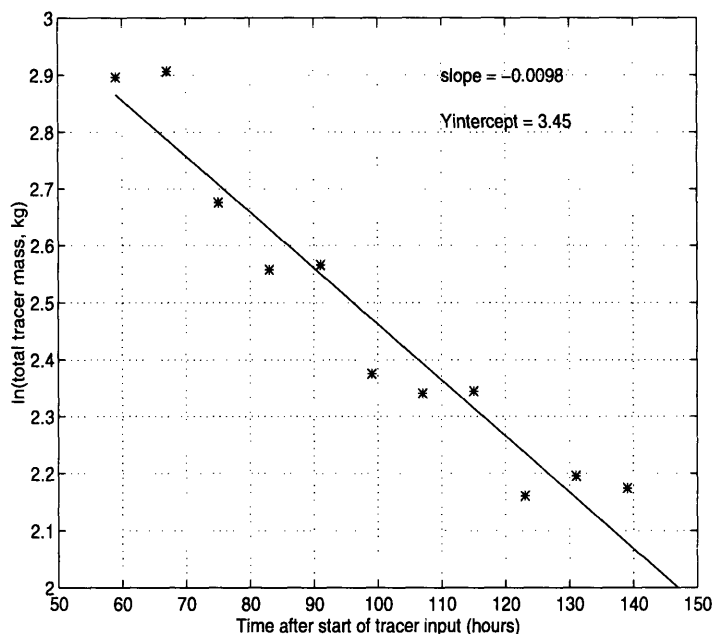


Figure 4-24: Fitting a line through  $\ln(\text{mass})$  vs. time for discharge during the 2 hours around each high tide, with the same freshwater volume as base case.

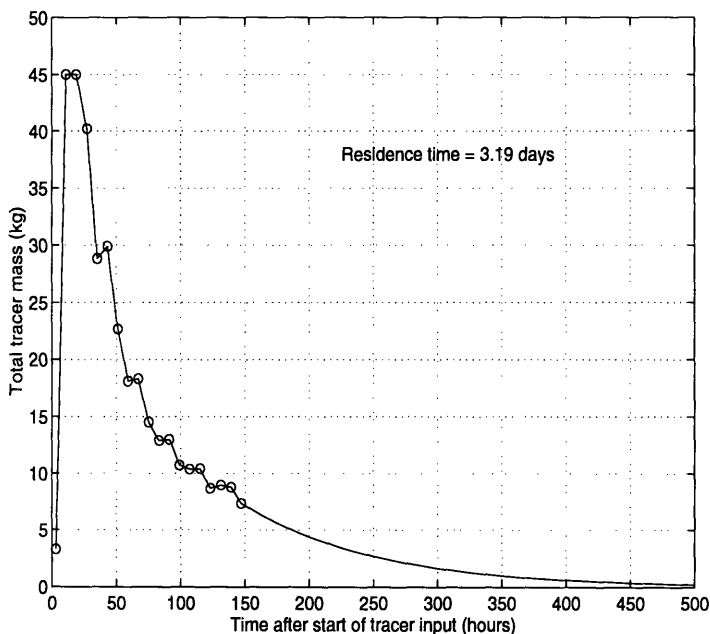


Figure 4-25: Tracer mass extrapolated to zero for discharge during the 2 hours around each high tide, with the same freshwater volume as base case. The circles indicate the model data, and the line beyond  $t = 147$  hours is extrapolated.

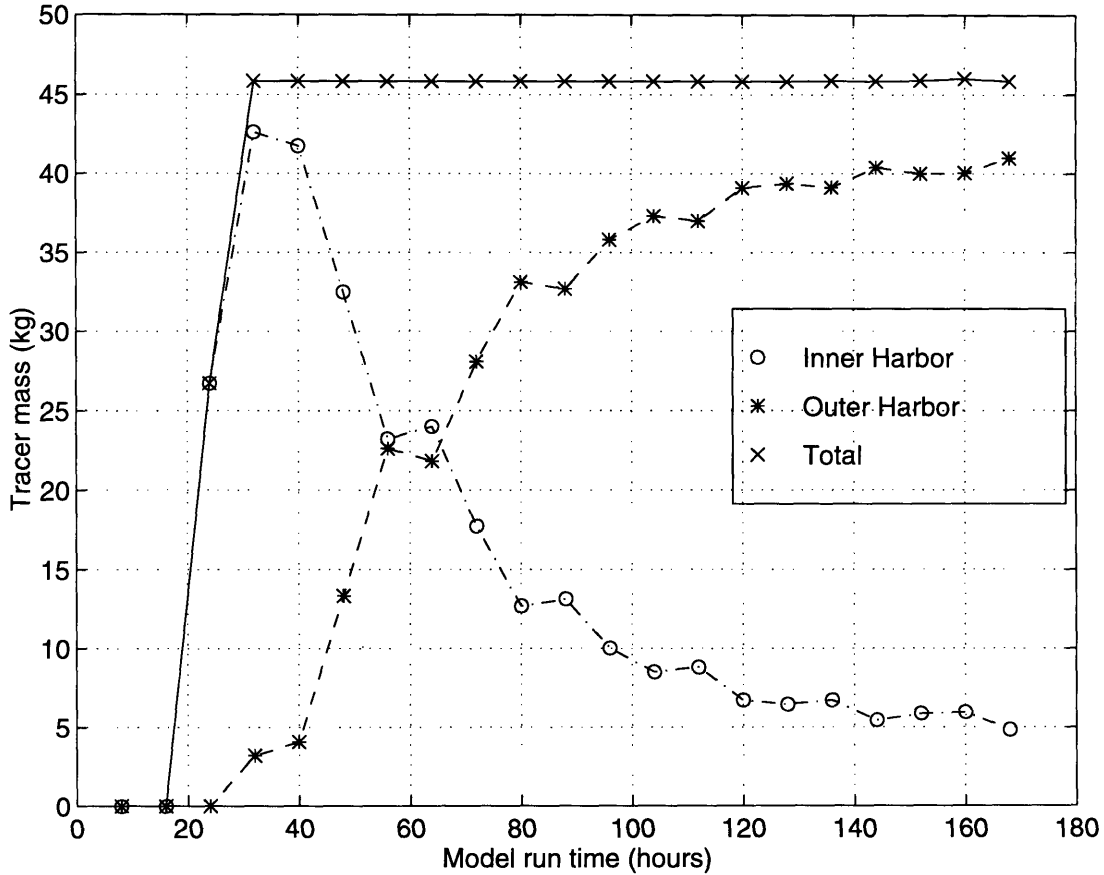


Figure 4-26: Tracer mass varying with time for the  $um_1=2.5 \times 10^{-5} \text{ m}^2/\text{s}$  case.

### Varying the vertical diffusion

The mass variation with time for the Inner Harbor, Outer Harbor and the entire model grid for the simulation in which the background molecular diffusivity value  $2.5 \times 10^{-5} \text{ m}^2/\text{s}$  is shown in Figure 4-26. Fitting a line through the data (natural log of Inner Harbor mass versus time) starting at 59 hours after the start of the tracer release gave a slope of -0.0107 and y-intercept of 3.13, as shown in Figure 4-27. The calculated residence time was 2.41 days, as calculated from the mass variation curve shown in Figure 4-28.

The mass variation with time for the Inner Harbor, Outer Harbor and the entire model grid when the conditions are the same as those in the base case with the exception of a high background molecular diffusivity of  $7.5 \times 10^{-5} \text{ m}^2/\text{s}$  is shown in Figure 4-29. Fitting a line through the data (natural log of Inner Harbor mass

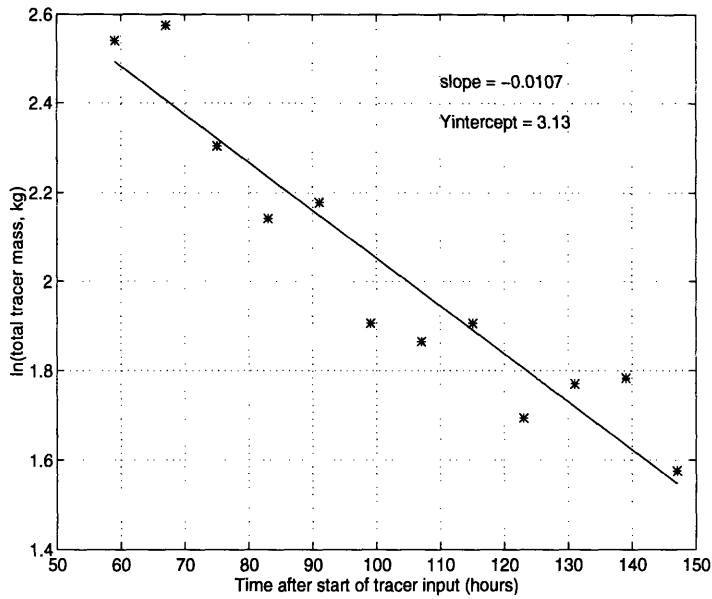


Figure 4-27: Fitting a line through  $\ln(\text{mass})$  vs. time for the  $u_{m01}=2.5 \times 10^{-5} \text{ m}^2/\text{s}$  case.

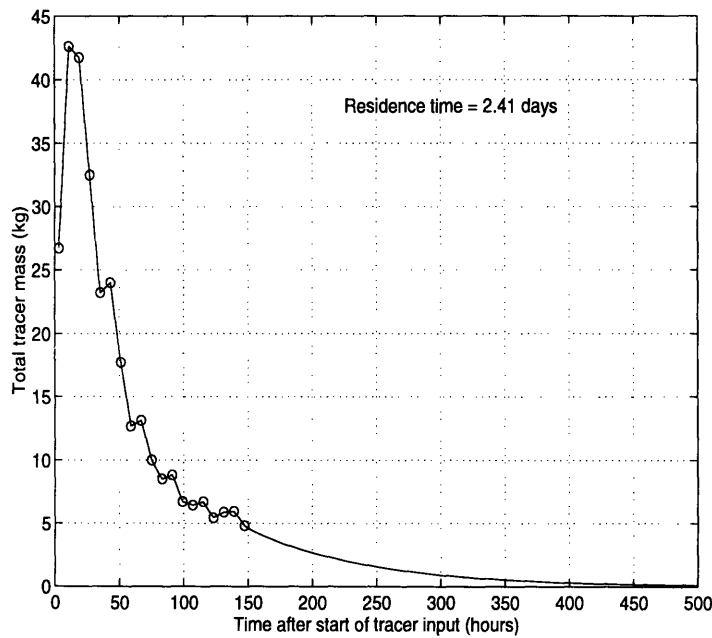


Figure 4-28: Tracer mass extrapolated to zero for the  $u_{m01}=2.5 \times 10^{-5} \text{ m}^2/\text{s}$  case. The circles indicate the model data, and the line beyond  $t = 147$  hours is extrapolated.

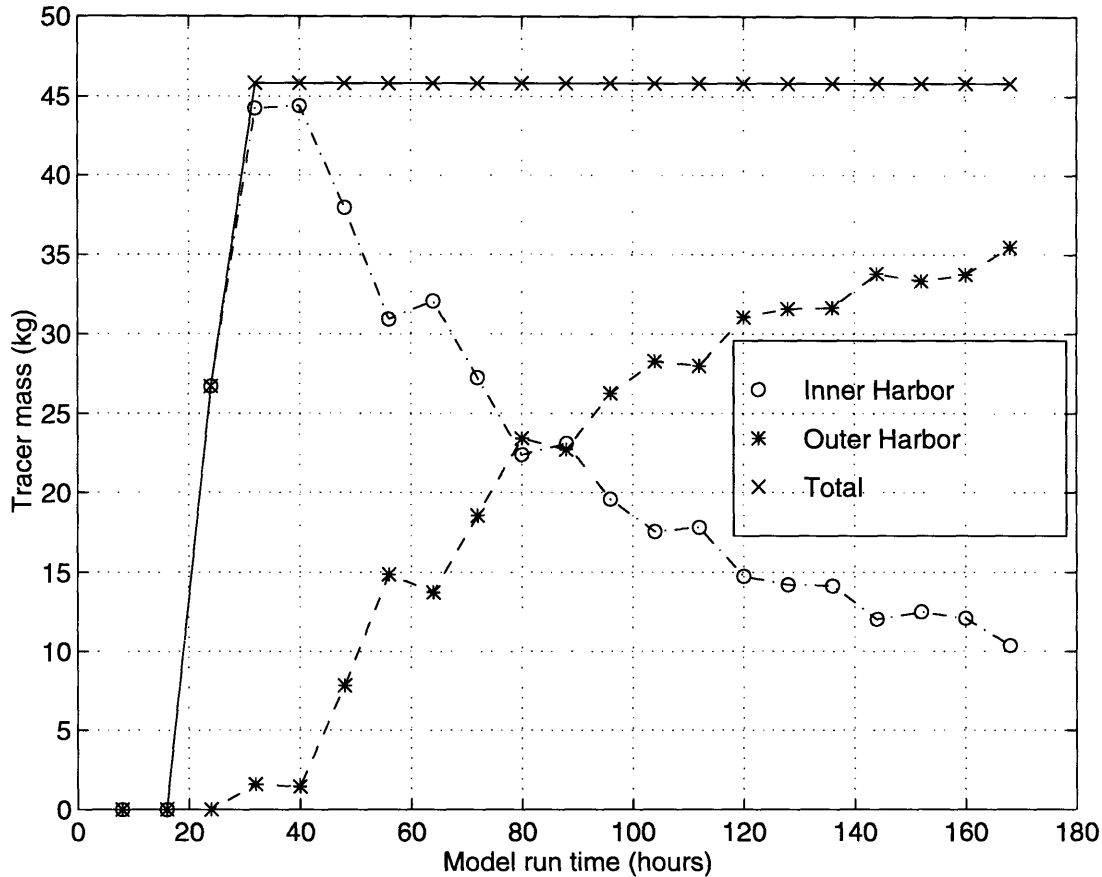


Figure 4-29: Tracer mass varying with time for the  $um_1=7.5 \times 10^{-5} \text{ m}^2/\text{s}$  case.

versus time) starting at 59 hours after the start of the tracer release gave a slope of -0.0088 and y-intercept of 3.64. See Figure 4-30. The calculated residence time was 3.97 days. See Figure 4-31.

Tracer concentration contours for this test case in which  $um_1=7.5 \times 10^{-5} \text{ m}^2/\text{s}$  are located in Appendix Section B.

### 4.4.3 Summary

The results of all of the model simulations are summarized in Figure 4-32. The residence time of the freshwater within the Inner Harbor decreases with increasing freshwater average flow rate. The simulations indicate an exponential relationship between average Charles River flow rate and residence time. Figure 4-32 also shows that varying the average freshwater discharge rate or varying the background ver-



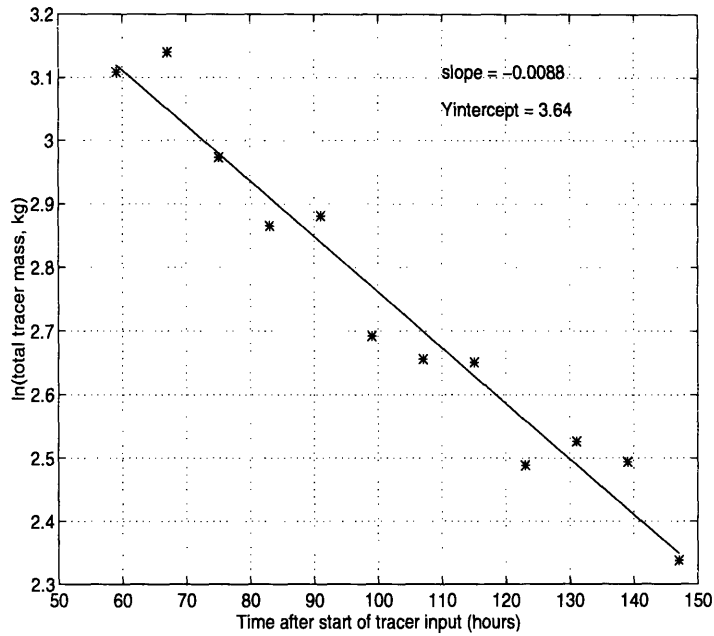


Figure 4-30: Fitting a line through  $\ln(\text{mass})$  vs. time for the  $u_{m01}=7.5 \times 10^{-5} \text{ m}^2/\text{s}$  case.

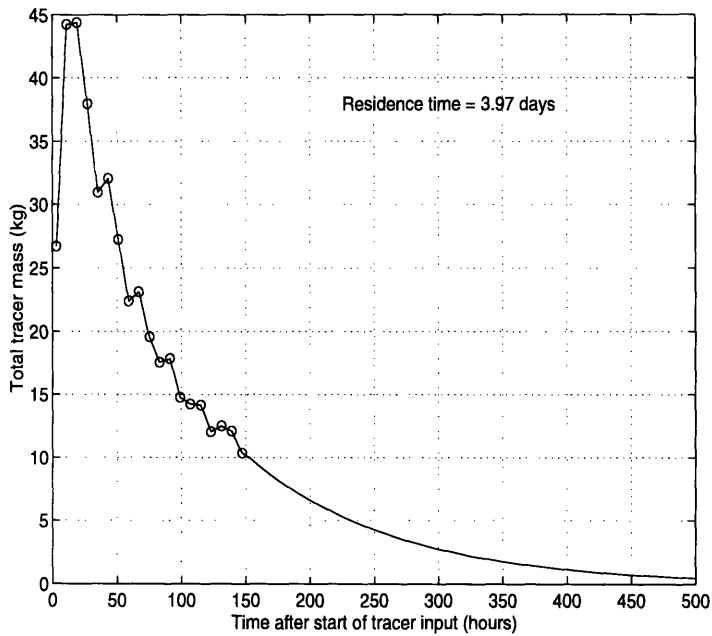


Figure 4-31: Tracer mass extrapolated to zero for the  $u_{m01}=7.5 \times 10^{-5}$  case. The circles indicate the model data, and the line beyond  $t = 147$  hours is extrapolated.

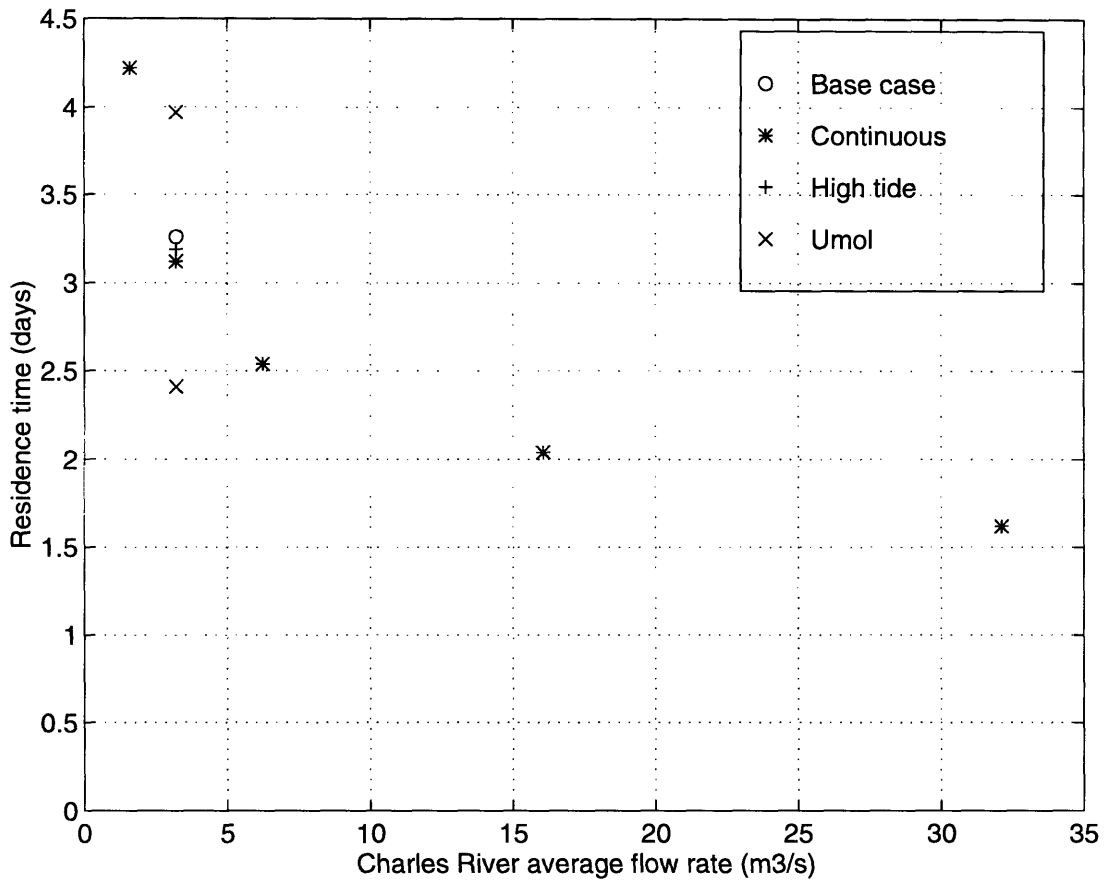


Figure 4-32: Summary of residence times as a function of average Charles River flow rate from model simulations.

tical diffusivity, umol, has a greater effect on the residence time than varying the freshwater discharge sequence.

# Chapter 5

## Discussion

The following sections will compare the field study data from Bumpus *et al.* and Adams *et al.* with the numerical modeling results. Additionally, the effects of varying the freshwater discharge sequence and the flow rate on the residence time will be discussed.

### 5.1 Calibration of numerical model

The numerical model base case was calibrated to the dye study results, as mentioned in Section 4.3.1. The vertical mixing and residence times of the two were compared. In general, there is a good agreement between the dye study data and the model base case results. Figures 5-1 through 5-8 show the local conservative tracer concentration vertical profiles at several times after the start of the tracer discharge for the dye study data, the model base case, and the model case with background vertical mixing coefficient,  $umol$ , set to  $7.5 \times 10^{-5} \text{ m}^2/\text{s}$ . In each of the vertical profiles shown, the data from the dye study are the average concentrations from several sampling locations that are all in a local area. The model results are the concentrations at a location in the model grid that corresponds to an approximate center point of the dye study local area. The solid lines correspond to the Adams *et al.* dye study data, where the letter-number labels are the data sampling locations, as indicated on Figure 1-2, that were averaged. The dashed lines correspond to the model base

case results, where the x-location is the x-coordinate on the model grid. The dot-dash lines correspond to the model simulations in which the background vertical mixing coefficient was  $7.5 \times 10^{-5} \text{ m}^2/\text{s}$ . For the model data, the points are along the center longitudinal cross-section of the model grid for the Inner Harbor ( $j=36$ ,  $y\text{-coordinate}=8040 \text{ m}$ ) were represented.

At 34 hours after the beginning of the tracer release at the Charles River Dam, the model data indicate that the tracer is moving faster out of the Inner Harbor region upstream of the Charles River Dam than for the dye study. See Figures 5-1 and 5-2. The tracer concentrations for the model simulations are less than that in the dye study, especially upstream of the Charles River Dam. Additionally, the model does not produce the clear subsurface maximum concentration that is present in the dye study data at locations near the Mystic and Charles Rivers. This subsurface maximum is due to the freshwater from the Mystic River moving over the denser saltwater. The model base case does closely match the dye study data downstream of the Charles River Dam; although at the location nearest to the Inner Harbor mouth, the model base case and  $um01=7.5 \times 10^{-5} \text{ m}^2/\text{s}$  simulation show more vertical movement of the the tracer mass than the dye study.

Figures 5-3 and 5-4 compare the vertical concentration profiles at 84 hours after the initial release of tracer. The model results show almost uniform concentrations in the vertical direction upstream of the Charles River Dam. Downstream of the Charles River, there is a larger concentration gradient in the model data, which more closely matches that of the dye study for the locations.

Figures 5-5 and 5-6 show a close match between the dye study data and the model base case and  $um01=7.5 \times 10^{-5} \text{ m}^2/\text{s}$  cases 115 hours after the beginning of the tracer release, with the exception of the two areas near the Mystic and Chelsea Rivers. The similarities are more apparent at locations just downstream of the Charles River. At location near the Inner Harbor mouth, the model concentrations for the upper regions are slightly lower than those of the dye study. This indicates that the tracer mass has moved out of the Inner Harbor faster in the model than in the dye study.

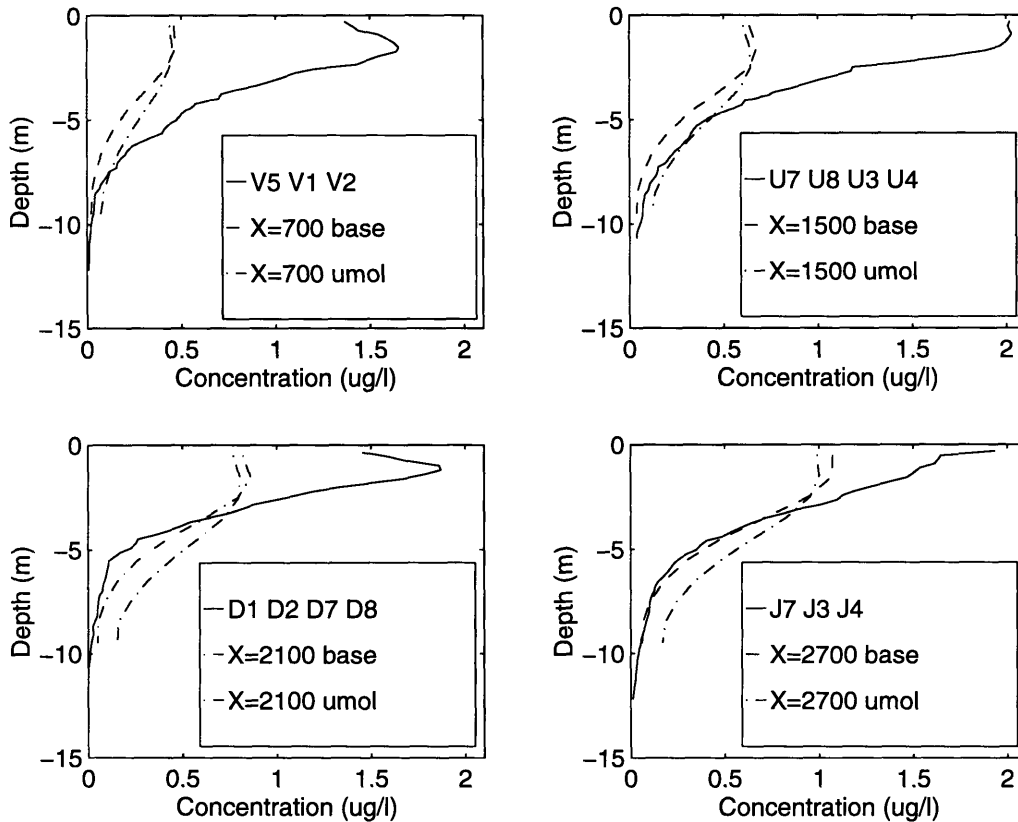


Figure 5-1: Vertical profile of tracer concentration ( $\mu\text{g/l}$ ) at locations upstream and including the Charles River Dam for the dye study by Adams *et al.*, the model base case, and the model  $umol=7.5 \times 10^{-5} \text{ m}^2/\text{s}$  case 34 hrs after the start of dye discharge.

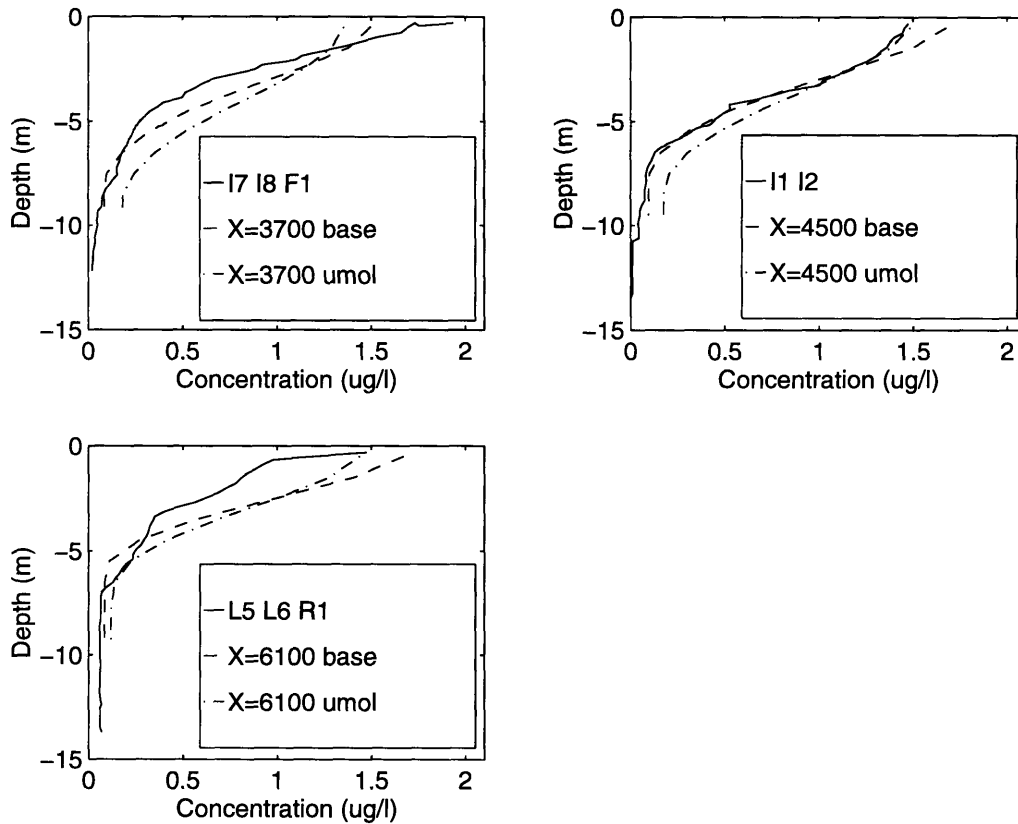


Figure 5-2: Vertical profile of tracer concentration ( $\mu\text{g/l}$ ) at locations downstream of the Charles River Dam for the dye study by Adams *et al.*, the model base case, and the model  $\text{umol}=7.5 \times 10^{-5} \text{ m}^2/\text{s}$  case 34 hrs after start of dye discharge.

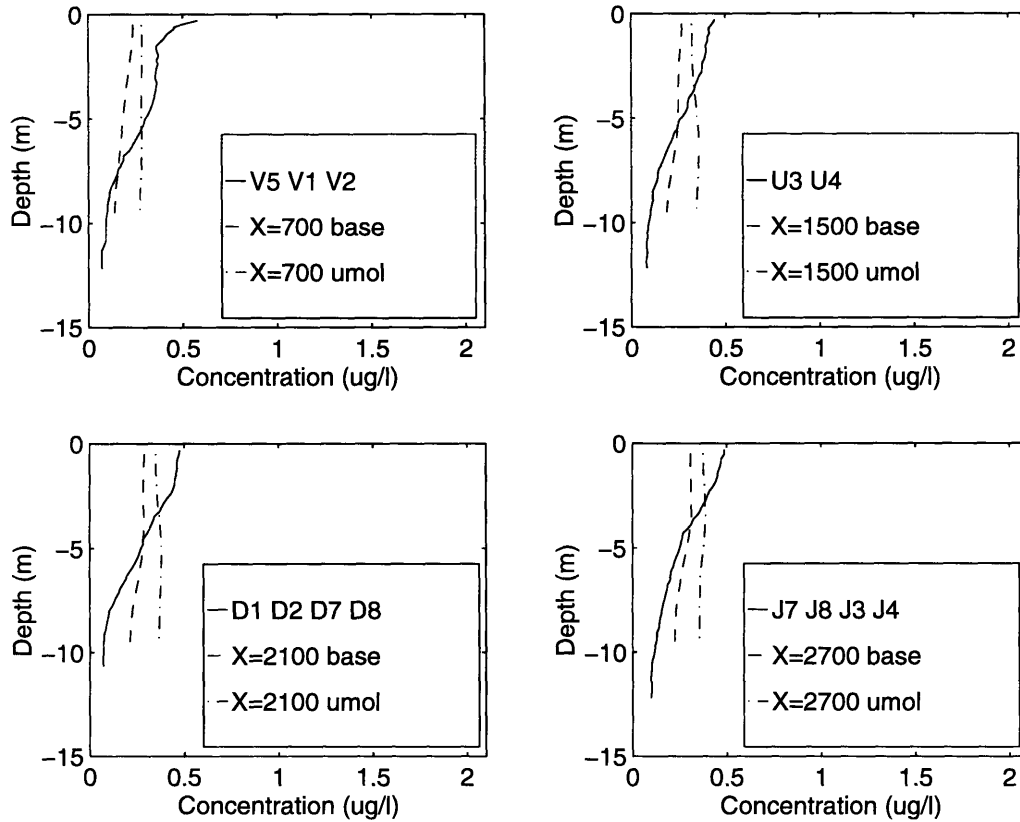


Figure 5-3: Vertical profile of tracer concentration ( $\mu\text{g/l}$ ) at locations upstream and including the Charles River Dam for the dye study by Adams *et al.*, the model base case, and the model  $\text{umol}=7.5 \times 10^{-5} \text{ m}^2/\text{s}$  case 84 hrs after start of dye discharge.

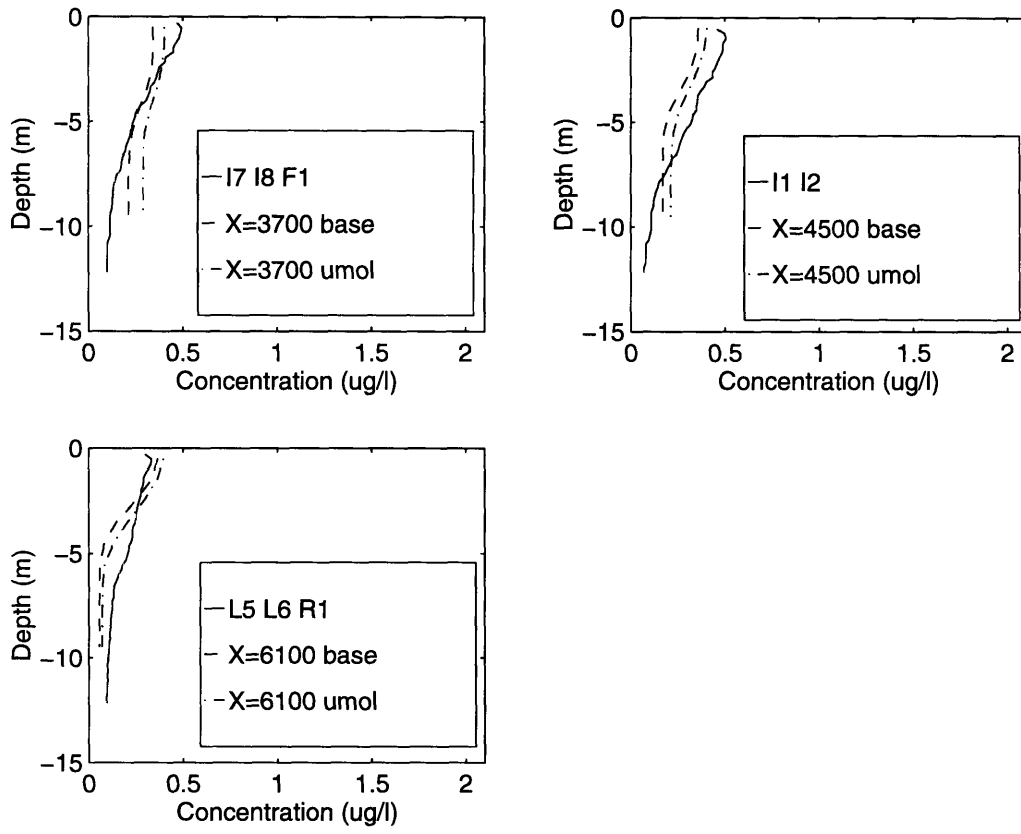


Figure 5-4: Vertical profile of tracer concentration ( $\mu\text{g/l}$ ) at locations downstream of the Charles River Dam for the dye study by Adams *et al.*, the model base case, and the model  $\mu\text{mol}=7.55 \times 10^{-5} \text{ m}^2/\text{s}$  case 84 hrs after the start of dye discharge.



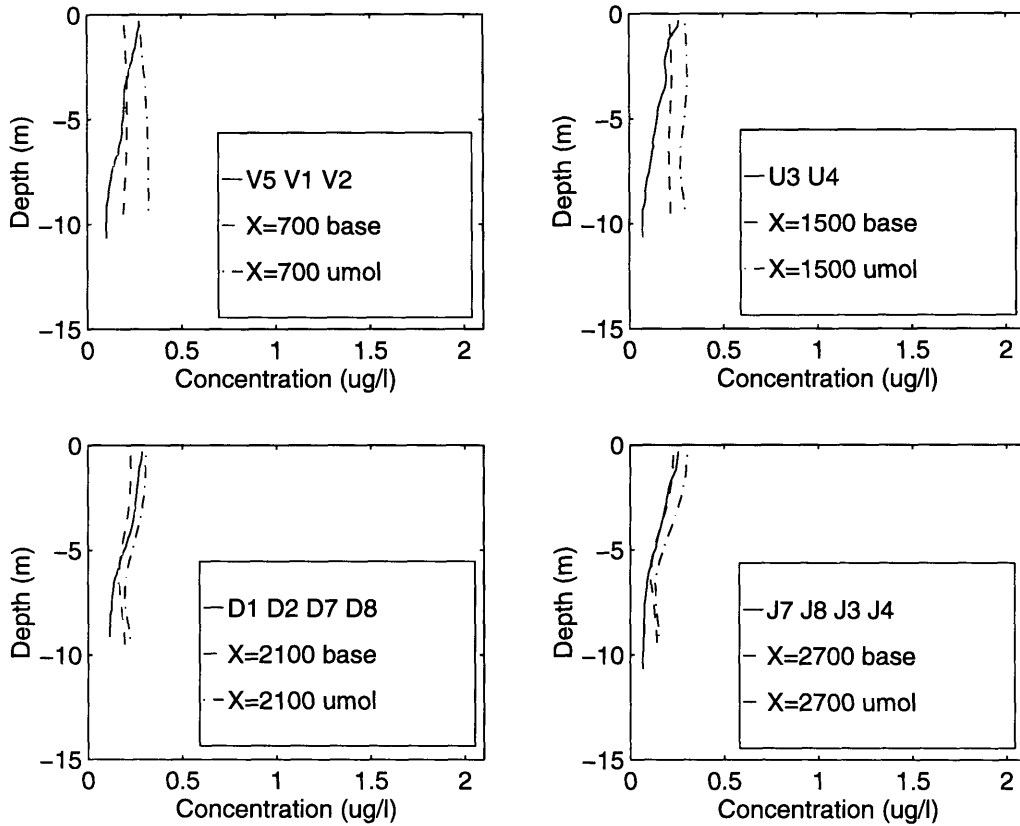


Figure 5-5: Vertical profile of tracer concentration ( $\mu\text{g/l}$ ) at locations upstream and including the Charles River Dam for the dye study by Adams *et al.*, the model base case, and the model  $\text{umol}=7.5 \times 10^{-5} \text{ m}^2/\text{s}$  case 115 hrs after start of dye discharge.

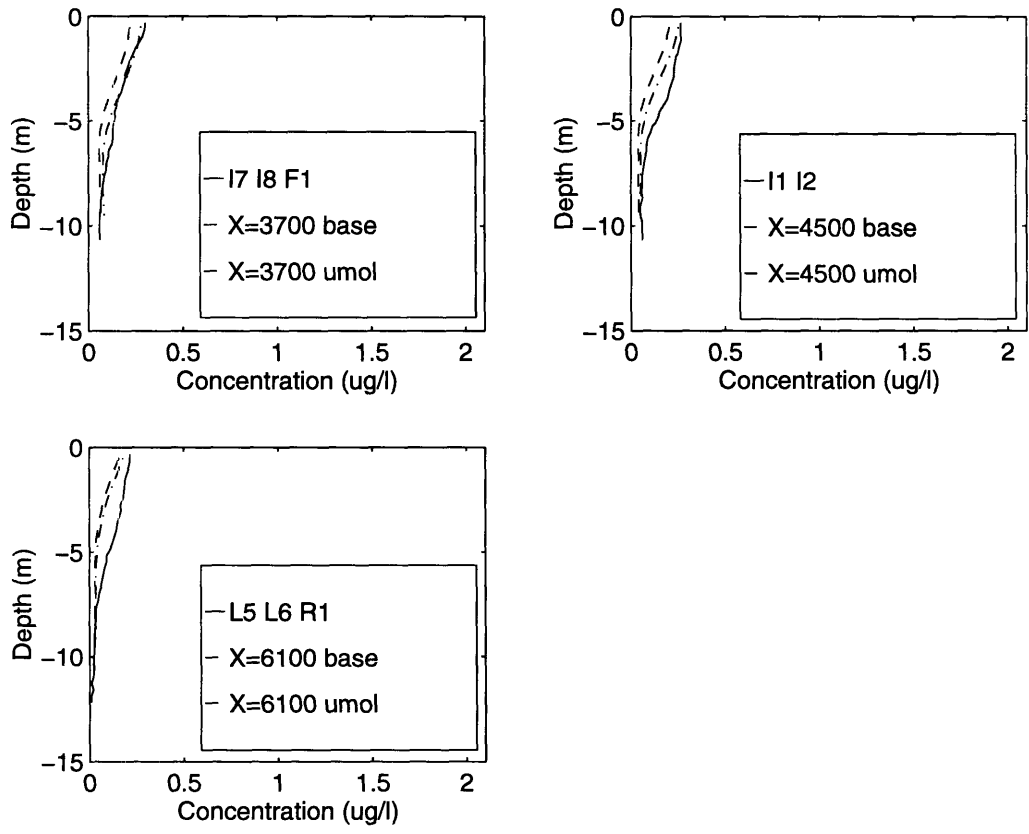


Figure 5-6: Vertical profile of tracer concentration ( $\mu\text{g/l}$ ) at locations downstream of the Charles River Dam for the dye study by Adams *et al.*, the model base case, and the model  $umol=7.5 \times 10^{-5} \text{ m}^2/\text{s}$  case 115 hrs after start of dye discharge.

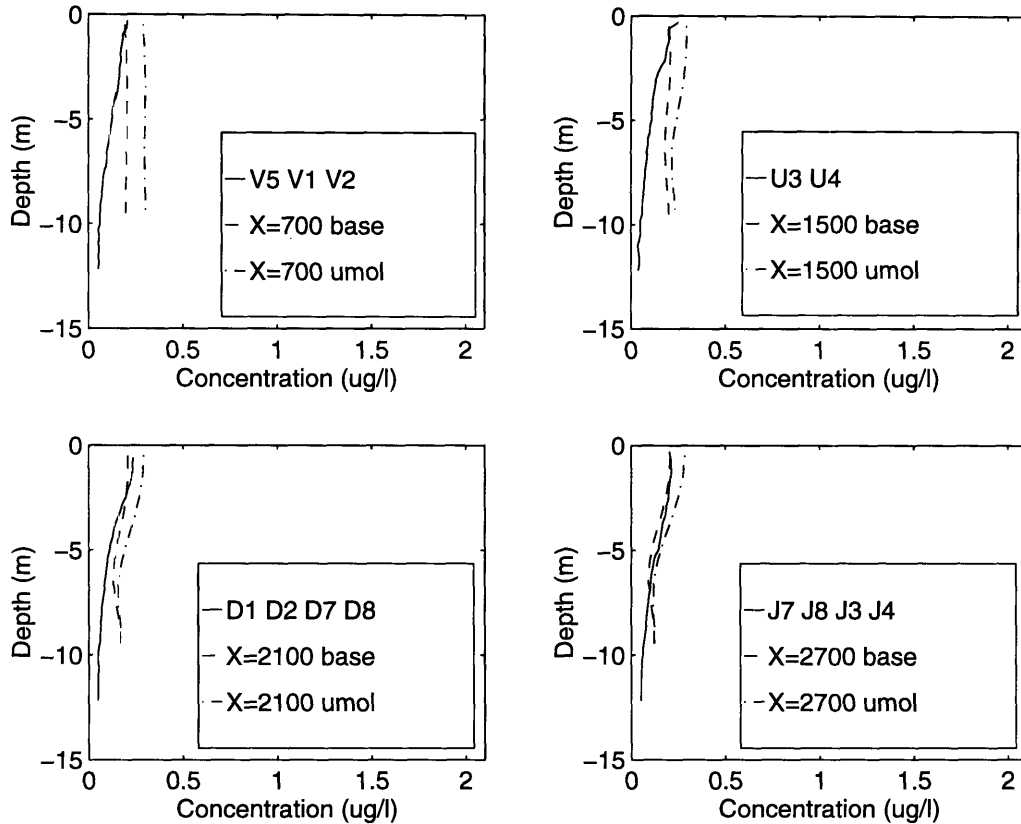


Figure 5-7: Vertical profile of tracer concentration ( $\mu\text{g/l}$ ) at locations upstream and including the Charles River Dam for the dye study by Adams *et al.*, the model base case, and the model  $\text{umol}=7.5 \times 10^{-5} \text{ m}^2/\text{s}$  case 134 hrs after the start of dye discharge.

At 134 hours after the start of the tracer release, in the two regions upstream of the Charles River Dam, the model simulations show nearly well-mixed conditions. Figure 5-5 indicates that directly near the Charles River Dam (at survey locations “D” and “J”) the base case has better agreement to the dye study data than  $\text{umol} = 7.5 \times 10^{-5} \text{ m}^2/\text{s}$  simulation. Downstream, the increased  $\text{umol}$  case has a slightly better match than the base case, as shown in Figure 5-6.

Figure 5-9 shows the Inner Harbor tracer mass variation with time for the dye study and the model base case. Both curves have the same shape, with the exception of a phase lag between the two. The model base case results indicate that the tracer mass leaves the Inner Harbor faster than the dye study data shows. This may be due to the idealization of the Inner Harbor in the numerical modeling. The curves

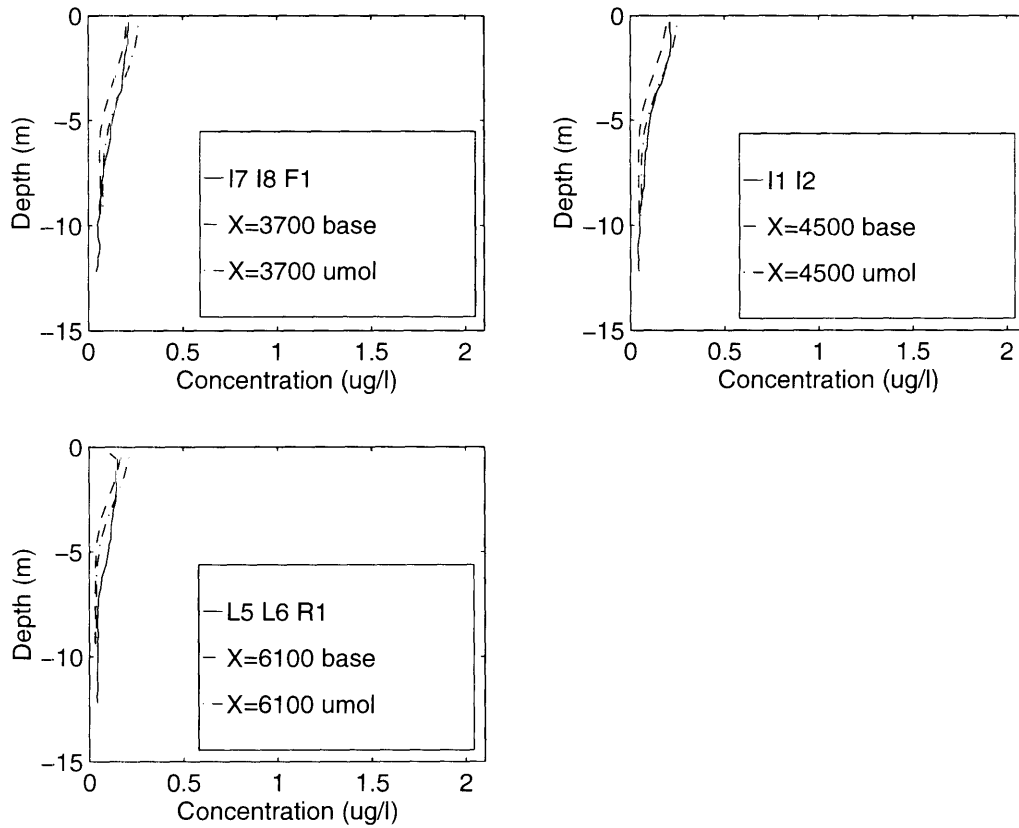


Figure 5-8: Vertical profile of tracer concentration ( $\mu\text{g/l}$ ) at locations downstream of the Charles River Dam for the dye study by Adams *et al.*, the model base case, and the model  $\text{umol}=7.5 \times 10^{-5} \text{ m}^2/\text{s}$  case 134 hrs after start of dye discharge.

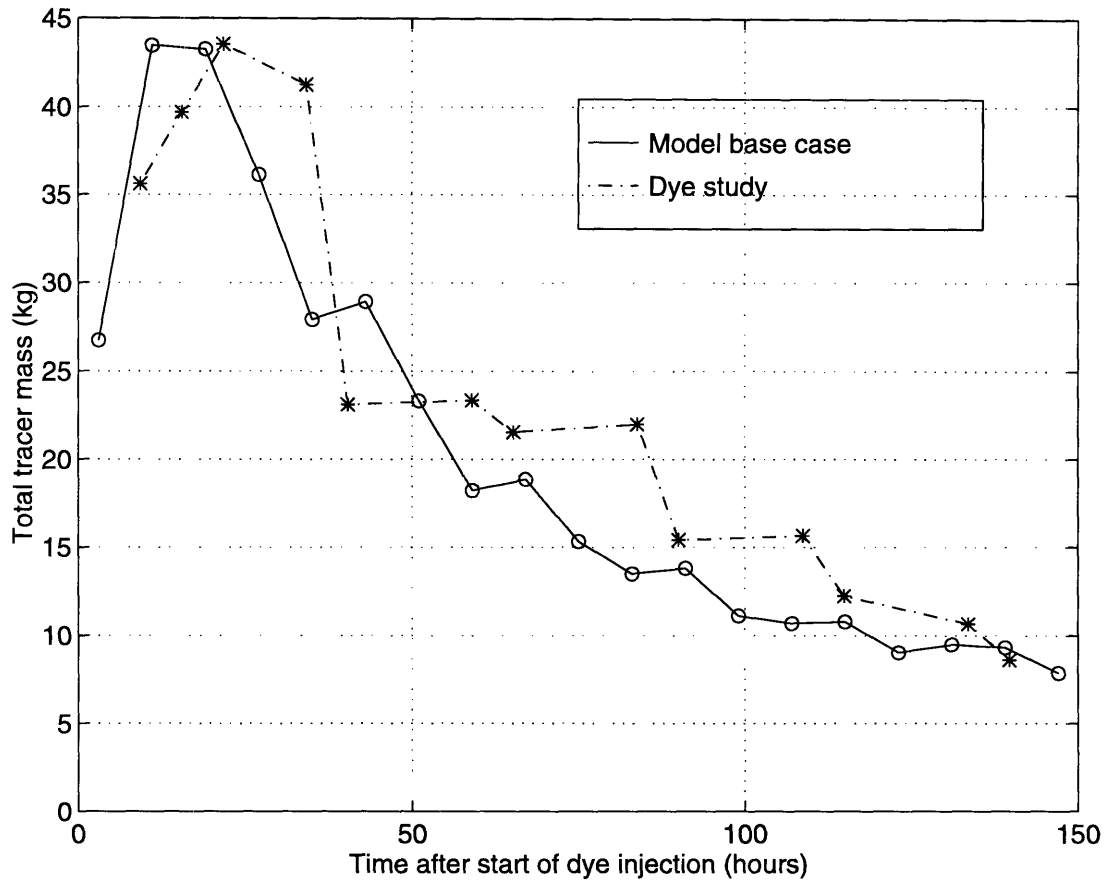


Figure 5-9: A comparison of dye study data and model base case values of tracer concentration ( $\mu\text{g/l}$ ) in the Inner Harbor as a function of time

and irregular shorelines of the Inner Harbor were omitted, as well as the variation in the bottom bathymetry along the shores. Mass would have more difficulty leaving the Inner Harbor with the presence of an irregular bathymetry and protrusions and small embayments, such as Fort Point and Reserved Channels, along the shoreline.

A background vertical mixing coefficient  $\text{umol}$  value of  $5 \times 10^{-5} \text{ m}^2/\text{s}$  was chosen for the numerical simulations because it more closely simulates the vertical mixing of the conservative tracer and freshwater in the Adams *et al.* dye study than the  $\text{umol} = 7.5 \times 10^{-5} \text{ m}^2/\text{s}$  case. This chosen value resulted in a residence time (3.26 days) shorter than that of the dye study (3.75 days). On the other hand, the  $\text{umol} = 7.5 \times 10^{-5} \text{ m}^2/\text{s}$  resulted in a residence time (3.95 days) that was closer to the dye study residence time although the vertical mixing it produced was not as good of a match. A molecular vertical diffusivity value for  $\text{umol}$  of  $1 \times 10^{-6} \text{ m}^2/\text{s}$  grossly

underpredicted the vertical mixing, resulting in a much smaller residence time than the two aforementioned cases. As a result, the chosen value of  $5 \times 10^{-5} \text{ m}^2/\text{s}$  was a compromise of the two deciding factors (residence time and vertical mixing). A value between  $5 \times 10^{-5} \text{ m}^2/\text{s}$  and  $7.5 \times 10^{-5} \text{ m}^2/\text{s}$  would probably be a more precise value.

## 5.2 Comparison between field studies and model

There is a general agreement between the field data and the model results. Figure 5-10 indicates that the trend of decreasing residence time with increasing average freshwater flow rate is followed. More discussion on the effects of freshwater on the residence time will be presented in Section 5.3. The field data and model results also indicate that with increasing freshwater discharge rate, there are less significant effects on decreasing the residence time. There is a better match between the field data and model results at higher total freshwater flow rates; whereas at lower flow rates, the model results gave shorter residence times than those of the field data. Moreover, the residence time calculated from the Adams *et al.* data is shorter than the residence time of the Bumpus *et al.* data for a similar total flow rate. This may be due to the method used by Bumpus *et al.* to estimate the Charles River flow rates from the unsteady Waltham gage data during their sampling.

Ketchum computed a theoretical residence time of six days for Inner Harbor waters between the Charles River and the mouth with the modified tidal prism technique. [17] Using the regular tidal prism method, with high tide volume of  $7.8 \times 10^7 \text{ m}^3$ , a tidal period of 12.42 hours, and a tidal prism volume of  $2.2 \times 10^7 \text{ m}^3$ , as computed by Bumpus *et al.*, the residence time of Charles River freshwater in Boston's Inner Harbor is 1.8 days.

From Figure 4-32, the summertime average flow rate of the Charles River at the Waltham gage ( $3.4 \text{ m}^3/\text{s}$ ) corresponds to a residence time between 2.7 and 4.3 days. For the Charles River annual average flow rate at Waltham ( $8.6 \text{ m}^3/\text{s}$ ), the residence time would be about 2.4 days. From Figure 5-10, the sum of the Charles

River annual average flow rate and the average flow rate of the Mystic River during the model simulations ( $0.68 \text{ m}^3/\text{s}$ ), corresponds to a residence time between 3.4 and 5 days. For the summertime Charles River average and the Mystic average, the residence time is between 2.2 and 2.6 days.

## 5.3 Effects of freshwater inflow on flushing

The effects of changing the continuous freshwater discharge situation will be discussed in the following section.

### 5.3.1 Varying continuous freshwater flow rates

Figure 5-11 compares the tracer mass variation with model run time for the simulations in which the freshwater flow rate (and total freshwater volume released) were varied. After model run time  $t = 72$  hours, all five scenarios behave in the same manner, following the same trend in variation. Figures 4-32 and 5-10 show that increasing the freshwater flow rate has a significant effect on decreasing the residence time. This is especially true for discharge rates that are within the range of annual average rates at the Charles River Waltham gage, *i.e.* less than  $10 \text{ m}^3/\text{s}$ , as can be seen in Figures 4-32 and 5-11 for the simulations of half of base case average flow rate and same flow rate as the base case average. With larger flow rates, the increase in the discharge rate has a smaller effect on reducing the residence time of the freshwater in the Inner Harbor.

### 5.3.2 Varying freshwater input sequence

Figure 5-12 compares the tracer mass as a function of model run time between the base case (in which freshwater is released around low tide), the case in which freshwater is released continuously, and the case in which freshwater is released during the two hours around high tide. There is little difference between the base case and the high tide input simulations, and discharging freshwater continuously

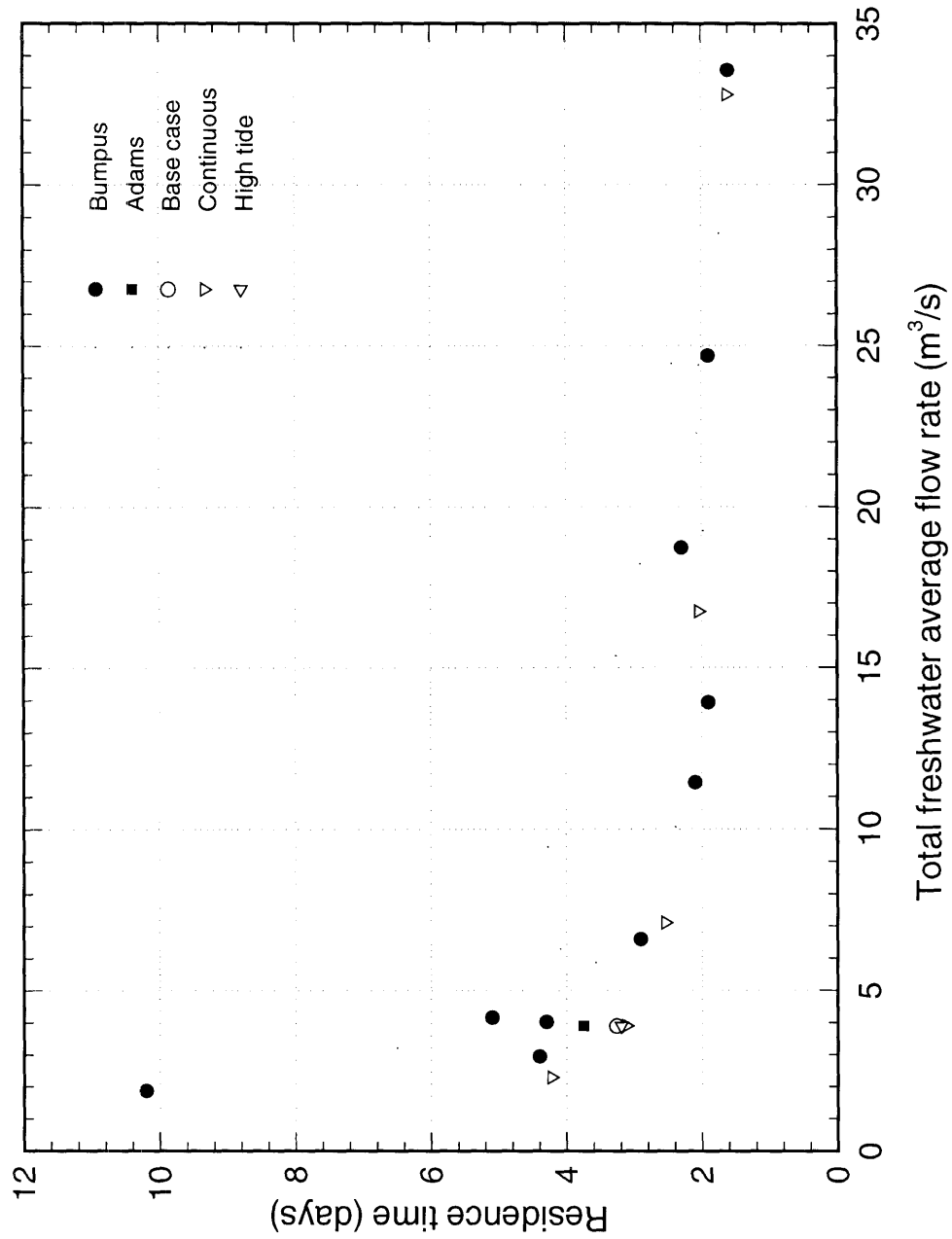


Figure 5-10: Residence time as a function of average flow rate from field study and model results.



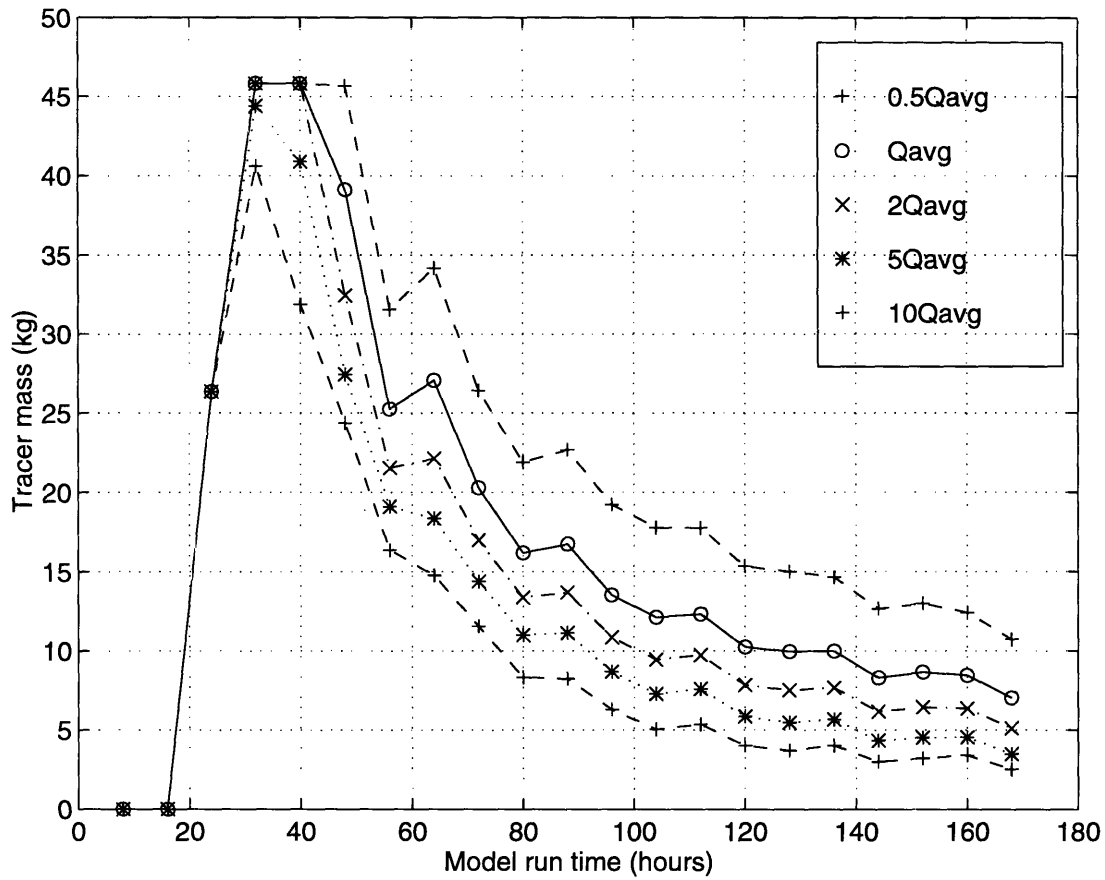


Figure 5-11: Time variation of tracer concentration ( $\mu\text{g}/\text{l}$ ) in the Inner Harbor for various constant freshwater discharge rates.

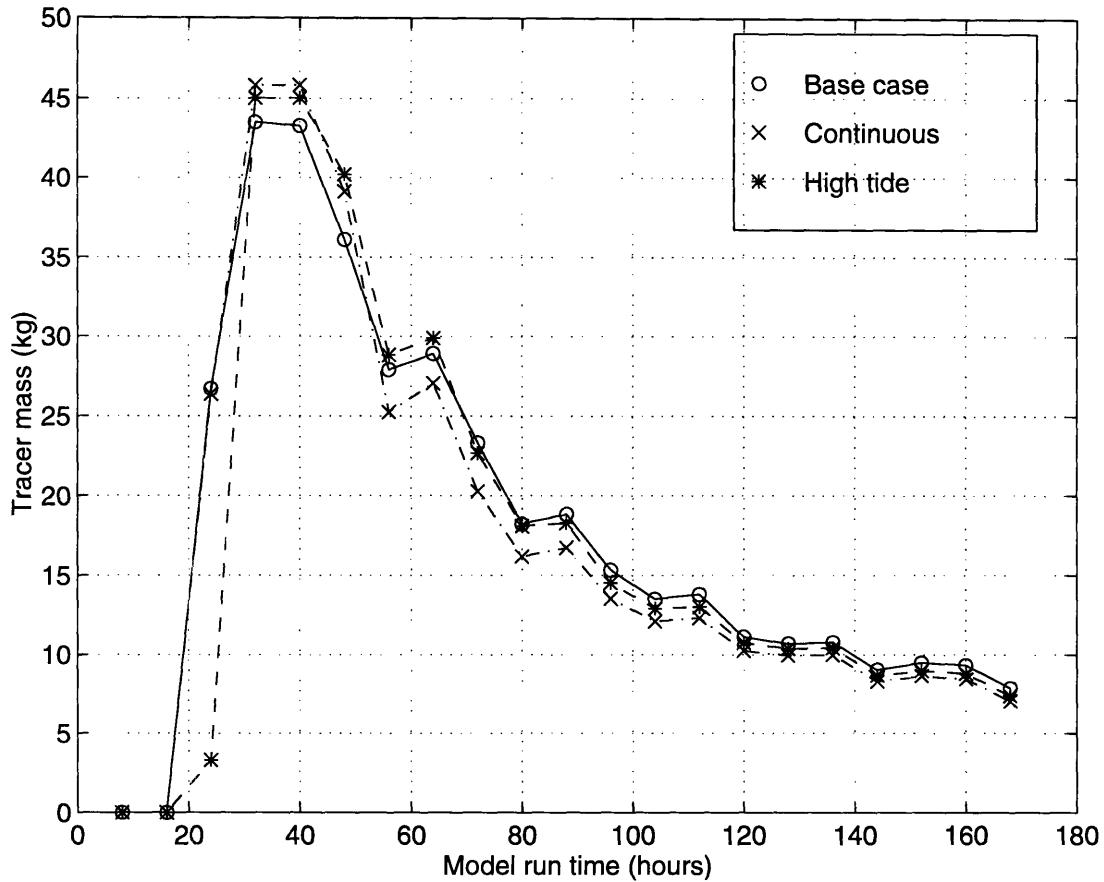


Figure 5-12: Time variation of tracer concentration ( $\mu\text{g/l}$ ) in the Inner Harbor for the base case, continuous discharge, high tide simulations.

rather than intermittently slightly increases the flushing rate. Figures 4-32 and 5-10 show that discharging the freshwater around high tide only slightly decreases the residence time. This is surprising since theoretically, there would be more outward momentum pushing mass out of the Inner Harbor when the freshwater is released during high tide. Nevertheless, this situation is not practical in reality at the New Charles River Dam since flows are gravity-driven at the dam sluice gates. The expected ranking of residence times from the three different discharge scenarios, from shortest to longest residence times, are high tide, continuous, and low tide. However, this was not the case according to the numerical modeling results. The increased vertical stability from the continuous discharge scenario helped flush the freshwater because this led to less turbulence, which in turn resulted in less vertical mixing.

### 5.3.3 Vertical diffusivity model sensitivity

From the results in Section 4.4, it can be seen that the model ECOM-si is sensitive to the given value for the background vertical diffusivity,  $um01$ . Figures B-7 through B-12 and Figures B-13 through B-18 show that the increase in the value of  $um01$  increases the vertical mixing. At model time  $t = 32$  hours, the tracer mass moved down to a maximum depth of 6 meters for the base case ( $um01 = 5 \times 10^{-5} \text{ m}^2/\text{s}$ ), as compared to 7 meters for the  $um01 = 7.5 \times 10^{-5} \text{ m}^2/\text{s}$  case.

The smaller value of background vertical diffusion coefficient,  $um01$ , causes the tracer (and also the freshwater that it marks) to remain at the upper layers of the water column. Therefore the majority of the mass moves out of the Inner Harbor more quickly, as shown in Figure 5-13. And conversely, the increased vertical mixing causes the mass to move out slower in the longitudinal direction. At model time  $t = 168$  hours, the tracer mass travelled to the Outer Harbor to a distance  $x=1.68 \times 10^4$  meters in the base case, and to a distance  $x= 1.7 \times 10^4$  meters for the  $um01=7.5 \times 10^{-5} \text{ m}^2/\text{s}$  case, according to Figures B-12 and B-18, respectively. As a result, the residence time changes with the variation of  $um01$ , which is noted in Figures 4-32 and 5-10. Doubling the  $um01$  value from  $2.5 \times 10^{-5} \text{ m}^2/\text{s}$  to  $5.0 \times 10^{-5} \text{ m}^2/\text{s}$  results in a 35 percent increase in freshwater residence time, from 2.24 days to 3.26 days; and increasing  $um01$  50 percent, from  $5.0 \times 10^{-5} \text{ m}^2/\text{s}$  to  $7.5 \times 10^{-5} \text{ m}^2/\text{s}$ , results in a 22 percent increase in the residence time, from 3.26 days to 3.97 days.

With the increase of freshwater flow rate, there is an increased shear produced by the freshwater moving over the Harbor saltwater. There is additional turbulence associated with this. The question is then raised as to whether the background vertical mixing coefficient,  $um01$ , should vary with each simulation, depending on the freshwater discharge scenario. Figures 5-14 and 5-15 show the variation of  $K_h$  with time for several locations in the Inner and Outer Harbor in the model grid, at near-surface depths at two locations in the Inner Harbor, (30,36,2) and (37,36,2), and two locations in the Outer Harbor, (45,36,2) and (55,36,2). Comparing the variation of  $K_h$ , calculated from the turbulence model, with time for the base case

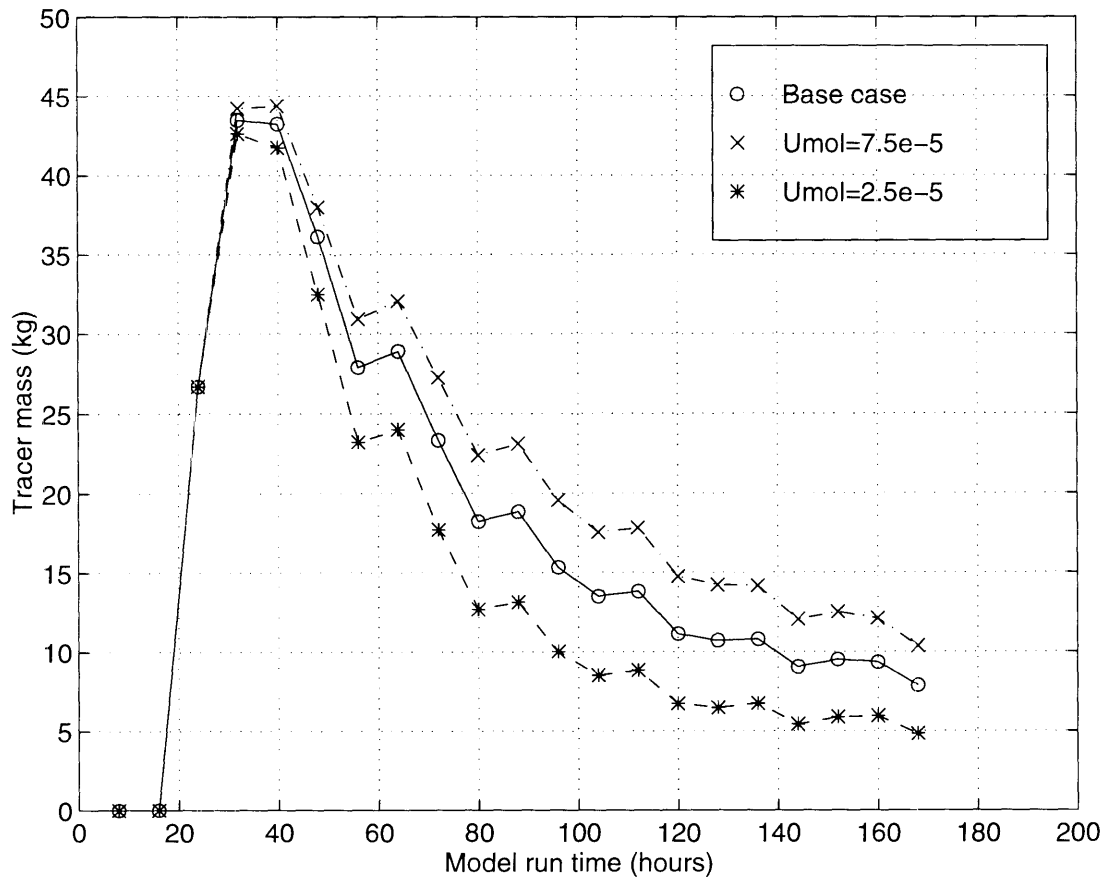


Figure 5-13: Time variation of tracer concentration ( $\mu\text{g}/\text{l}$ ) in the Inner Harbor for various  $\text{umol}$  values.

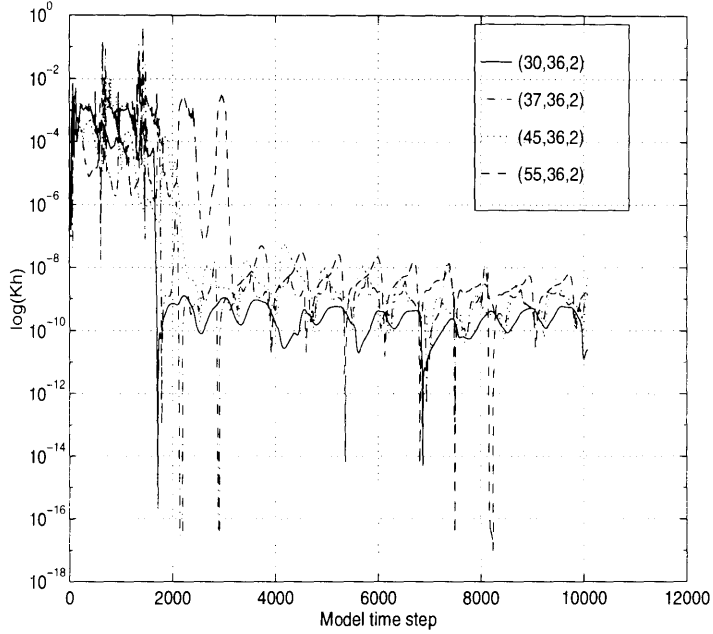


Figure 5-14:  $K_h$  variation with time for base case.

and the case in which the freshwater was discharged at a continuous flow rate ten times greater than the average flow rate of the base case, it can be seen that the base case results in values of  $K_h$  one to two orders of magnitude greater than those for the ten times greater flow rate case at time steps after around 2000. However, the  $K_h$  values computed in both simulations are many orders of magnitude smaller than the background vertical mixing coefficient,  $umol = 5.0 \times 10^{-5} \text{ m}^2/\text{s}$ , at these time steps. The  $K_m$  and  $K_q$  values are similar to the  $K_h$  values. This indicates that the turbulence model does not produce significant vertical mixing in the near-surface layers for the model simulations. However, it is this upper region, in which the conservative tracer and freshwater vertically mix, that is particularly important to the flushing rate and residence time of the tracer and freshwater in the Inner Harbor.

In order to explore this situation further, the vertical distribution of  $K_h$ , longitudinal velocity,  $u$ , and tracer concentration (when relevant) were plotted at several locations in the Inner and Outer Harbor at a few times during the base case model simulation. Figure 5-16 indicates that the values of  $K_h$  are greater than the  $umol$  value near the surface and middepth at model time  $t = 8$  hours, before any dis-

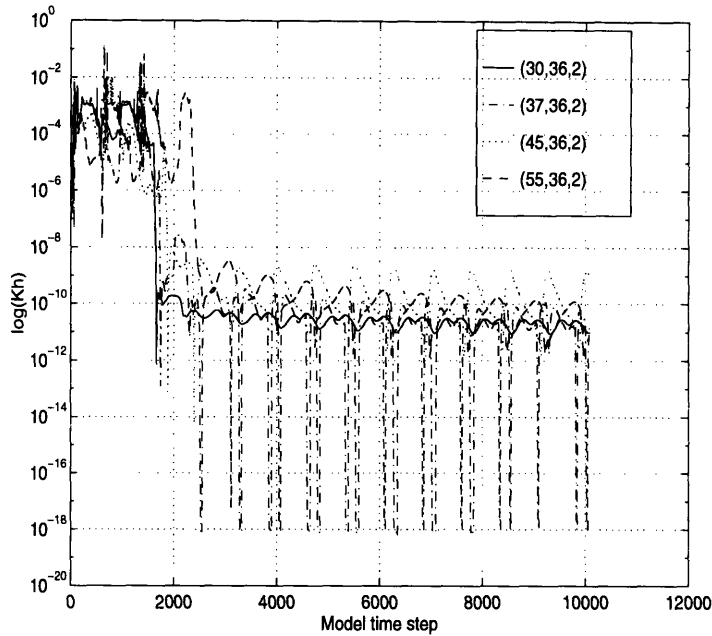


Figure 5-15:  $K_h$  variation with time for ten times the base case average flow rate.

charge of Charles River freshwater and conservative tracer. However, Figures 5-17 and 5-18 show that the  $K_h$  values in the top portion of the Inner and Outer Harbors were approximately zero at model times  $t = 72$  and 80 hours (timesteps 4320 and 4800, respectively), as is indicated in Figure 5-14. It is also noted that the maximum values of  $K_h$  were located further towards the bottom of the water column as time progressed. This corresponds to vertical diffusion and thus the movement of tracer mass (and freshwater since the tracer was used to tag the Charles River freshwater) towards the bottom over time, as well as a decreased density gradient near the bottom. Therefore, the near-zero  $K_h$  values corresponds to depths where there were strong salinity and tracer concentration gradients. Figures 5-17 and 5-18 indicate that the  $K_h$  values increased to values that dominated over the  $umol$  value where there were small gradients in the tracer concentration and where there was little tracer mass or freshwater.

Therefore, the turbulence closure model in ECOM-si, which calculated the  $K_h$ ,  $K_m$ , and  $K_q$  values, produced mixing coefficients several orders of magnitude smaller than the  $umol$  value of  $5 \times 10^{-5} \text{ m}^2/\text{s}$  at depths where the freshwater and tracer moved vertically. However, it is at these depths that it is most important for the

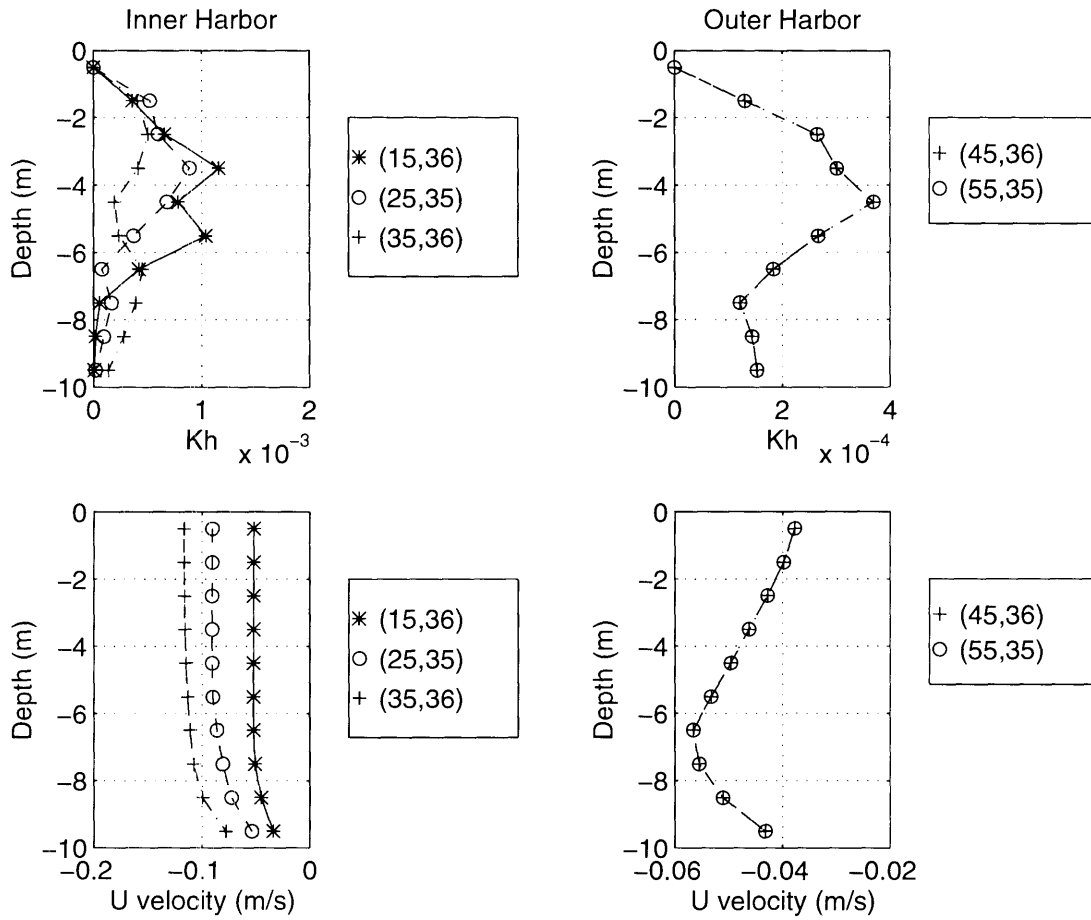


Figure 5-16: Vertical profiles of  $K_h$  and  $u$  at model time  $t = 8$  hrs.





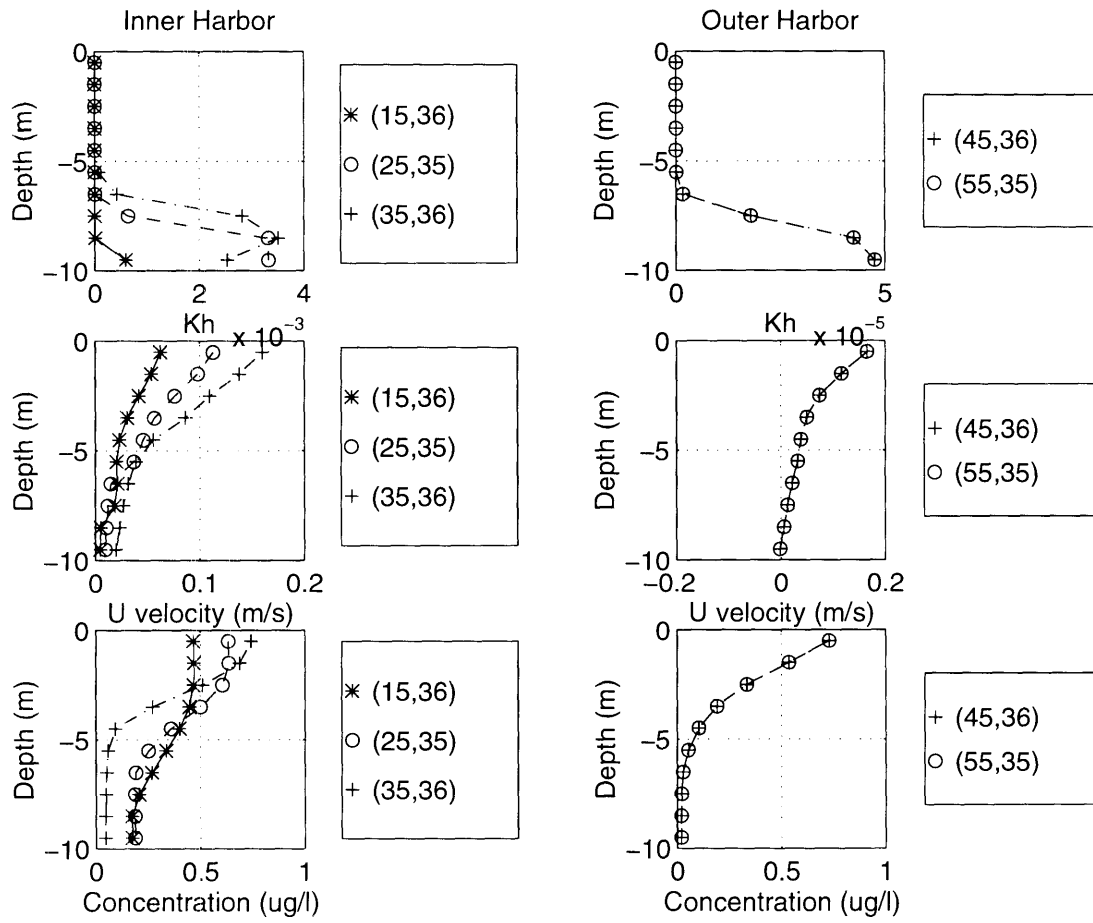


Figure 5-18: Vertical profiles of  $K_h$ ,  $u$ , and tracer concentration at model time  $t = 80$  hrs.

numerical model to realistically reproduce the turbulence due to the density currents and shearing at the freshwater-saltwater interface that are relevant to the vertical mixing and consequently the turbulent mixing coefficients.

# Chapter 6

## Conclusion

The overall relationship between the residence time of freshwater in Boston's Inner Harbor and the average flow rate of the freshwater is summarized in Figure 5-10. Residence time decreases with increasing average discharge rate. This relationship is one such that the effect of decreasing the residence time with increasing the freshwater flow rate is reduced at higher flow rates.

The field studies by Bumpus *et al.* calculated residence times of the freshwater in Boston's Inner Harbor to be between 1.6 days and 10.2 days, for average combined freshwater discharge rates from the Charles, Mystic, and Chelsea Rivers of  $33.6 \text{ m}^3/\text{s}$  ( $1185 \text{ ft}^3/\text{s}$ ) and  $1.9 \text{ m}^3/\text{s}$  ( $66 \text{ ft}^3/\text{s}$ ), respectively. The numerical model simulations indicate that the residence time varies with the average flow rate in the same manner as in the field studies. The model simulations, in which the average freshwater flow rates were varied, resulted in residence times between 1.62 days and 4.22 days for Charles River average flow rates of  $32.1 \text{ m}^3/\text{s}$  and  $1.6 \text{ m}^3/\text{s}$ , respectively. Therefore according to the model results, pollutants associated with the freshwater discharges from the rivers, such as chemical and biological contaminants found in CSOs and storm water runoff, have between 1.62 and 4.22 days to react, settle, or decay while traveling through the Inner Harbor. The majority of contaminants with reaction or settling times or decay rates similar to these calculated residence times will not reach the Outer Harbor.

Adams *et al.* dye study data was used to help calibrate the numerical model. The

background vertical mixing coefficient,  $umol$ , was used to simulate vertical mixing and a freshwater residence time as closely possible to the field data. A  $umol$  value of  $5 \times 10^{-5} \text{ m}^2/\text{s}$  was chosen. Using a molecular vertical diffusivity value of  $1 \times 10^{-6} \text{ m}^2/\text{s}$  for  $umol$  was inadequate since it produced much less vertical mixing, and thus a shorter residence time, than the dye study or the base case. For the base case, which is modeled after the dye study, the resulting residence time for an average Charles River flow rate of  $3.2 \text{ m}^3/\text{s}$  is 3.26 days. Adams *et al.* dye study data show that the residence time of Charles River freshwater in the Inner Harbor, with the same average flow rate, is 3.75 days.

The model simulations sometimes resulted in slightly lower values for the residence time of freshwater in the Inner Harbor than those determined by Bumpus *et al.* and Adams *et al.* field study data. The cause of the differences may be the simplifications in defining the domain and its forcings, as well as the boundary condition imposed at the open boundary, in the numerical modeling. Additionally, Bumpus *et al.* did not explicitly consider the unsteady flow rates of the Charles River when calculating their residence times.

The model simulations show that the magnitude of the average freshwater discharge rate into the Inner Harbor had the greatest effect on the residence time of the freshwater. The trend of the model results is similar to that of the Bumpus *et al.* data. At higher freshwater flow rates, the residence times from the field data and the model results were in very close agreement. Freshwater discharges associated with storms and CSO runoff are usually characterized by instantaneous high flow rates. Therefore pollutants from these runoffs will likely have shorter residence times than those of normal dry weather conditions because of the increased flow rates.

Changing the time sequence at which the freshwater is discharged, such as around high tide or low tide or continuously, affected the freshwater residence time only slightly in the simulations. Nevertheless, discharging the freshwater continuously rather than intermittently produced the fastest flushing rates, and thus the shortest residence times. This is because there is more vertical stability in the continuous discharges than in the intermittent ones; and therefore there is less turbulence and

vertical mixing, which results in shorter residence times.

The numerical model is sensitive to the user-specified background mixing value,  $um_01$ , which often dominated over the vertical mixing coefficients calculated by the turbulence closure submodel in the simulations. This is especially true in the upper layers of the water column, where the conservative tracer and freshwater reside and where there are stronger concentration and density gradients. Therefore, the turbulence model is often insufficient in the region in which the vertical mixing is important.

# Chapter 7

## Further study

A better turbulence submodel may need to be implemented for these numerical simulations because the turbulence closure submodel in ECOM-si underpredicts the turbulence and vertical mixing in the upper layers of the water column, where there are larger density and concentration gradients than the near-bottom region. The background vertical mixing coefficient,  $umol$ , which is supposed to behave as the molecular vertical diffusivity essentially becomes the user-specified constant value for these upper layers in the model simulations. Since the degree of turbulence varies with the discharge scenarios (high versus low flow rates and continuous versus intermittent releases) the turbulence submodel should be sensitive enough to adapt to the situations and provide significant vertical mixing coefficients that are not dominated by  $umol$  in the regions of turbulence.

# Appendix A

## Dye study concentration contours

Figures A-1 through A-4 show the longitudinal-vertical conservative tracer concentrations for the 13 surveys during the Adams *et al.* dye study. These contours were made by projecting the measured concentrations at the sampling locations to a regular 600-foot (horizontal) by 1-foot (vertical) grid using inverse-distance-squared weighting and the fitting a two-dimensional quadratic surface.

Figure A-1 indicates that the dye is initially concentrated at the surface. Subsequent figures show the dye moving vertically downwards and longitudinally outwards towards the Inner Harbor mouth. Because of this spreading and mixing, the concentrations decrease in value. After about 140 hours, the dye in the Inner Harbor is fairly well-mixed vertically and longitudinally, as shown in Figure A-4.

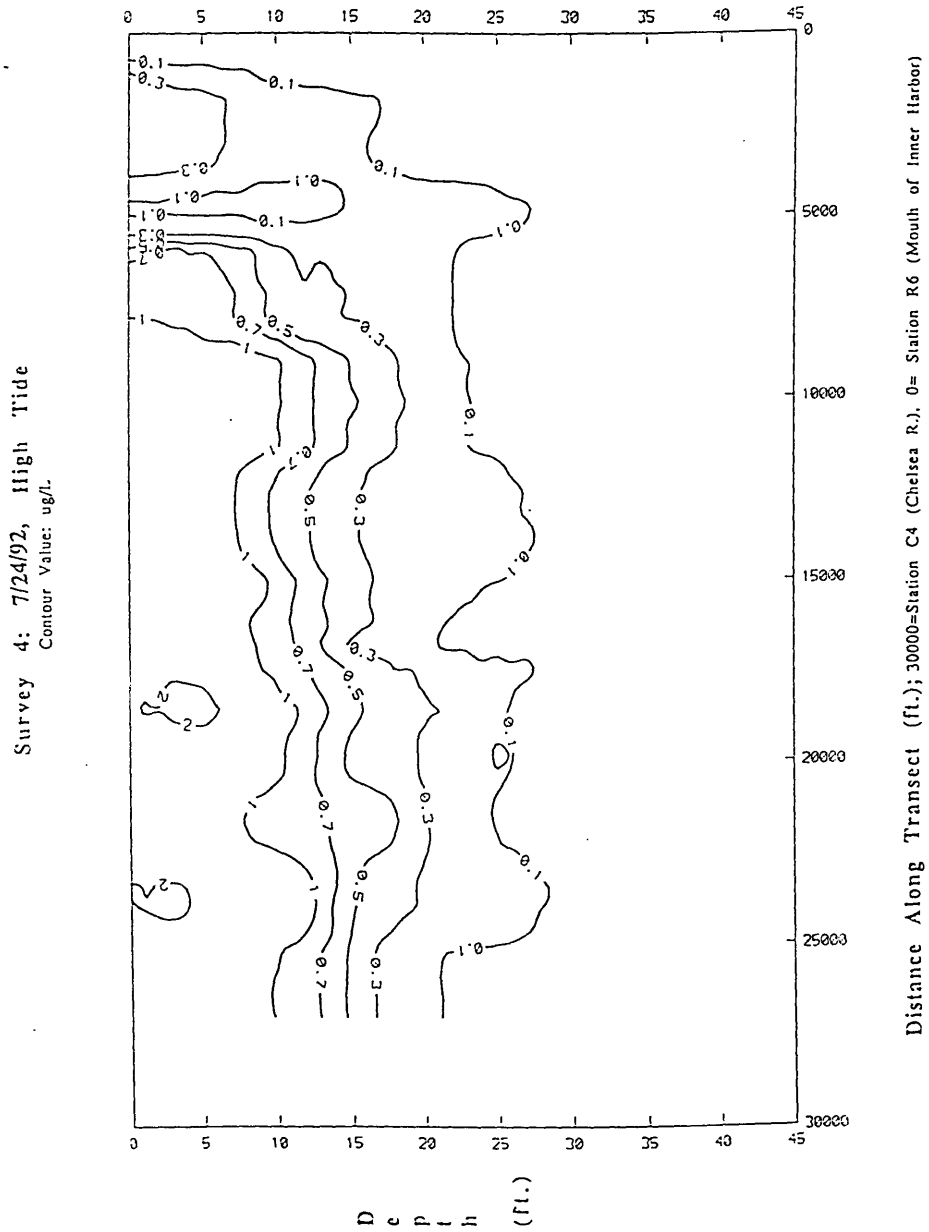


Figure A-1: Longitudinal-vertical contours of tracer concentration ( $\mu\text{g}/\text{l}$ ) for dye study at 34 hours after the initial release of tracer. Charles River Dam located at approximately 19,000 ft in the longitudinal direction.



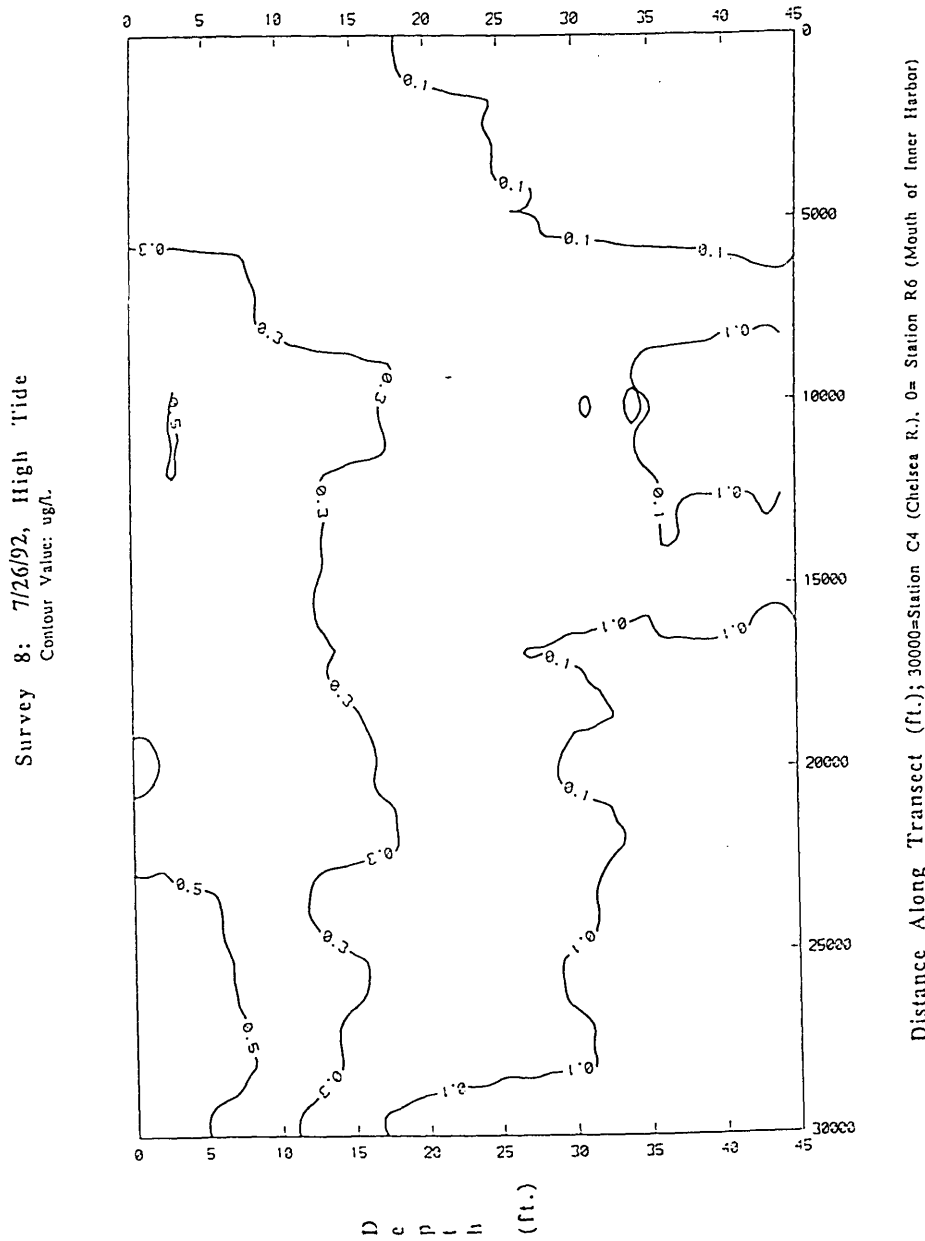


Figure A-2: Longitudinal-vertical contours of tracer concentration ( $\mu\text{g/l}$ ) for dye study at 84 hours after the initial release of tracer. Charles River Dam located at approximately 19,000 ft in the longitudinal direction.

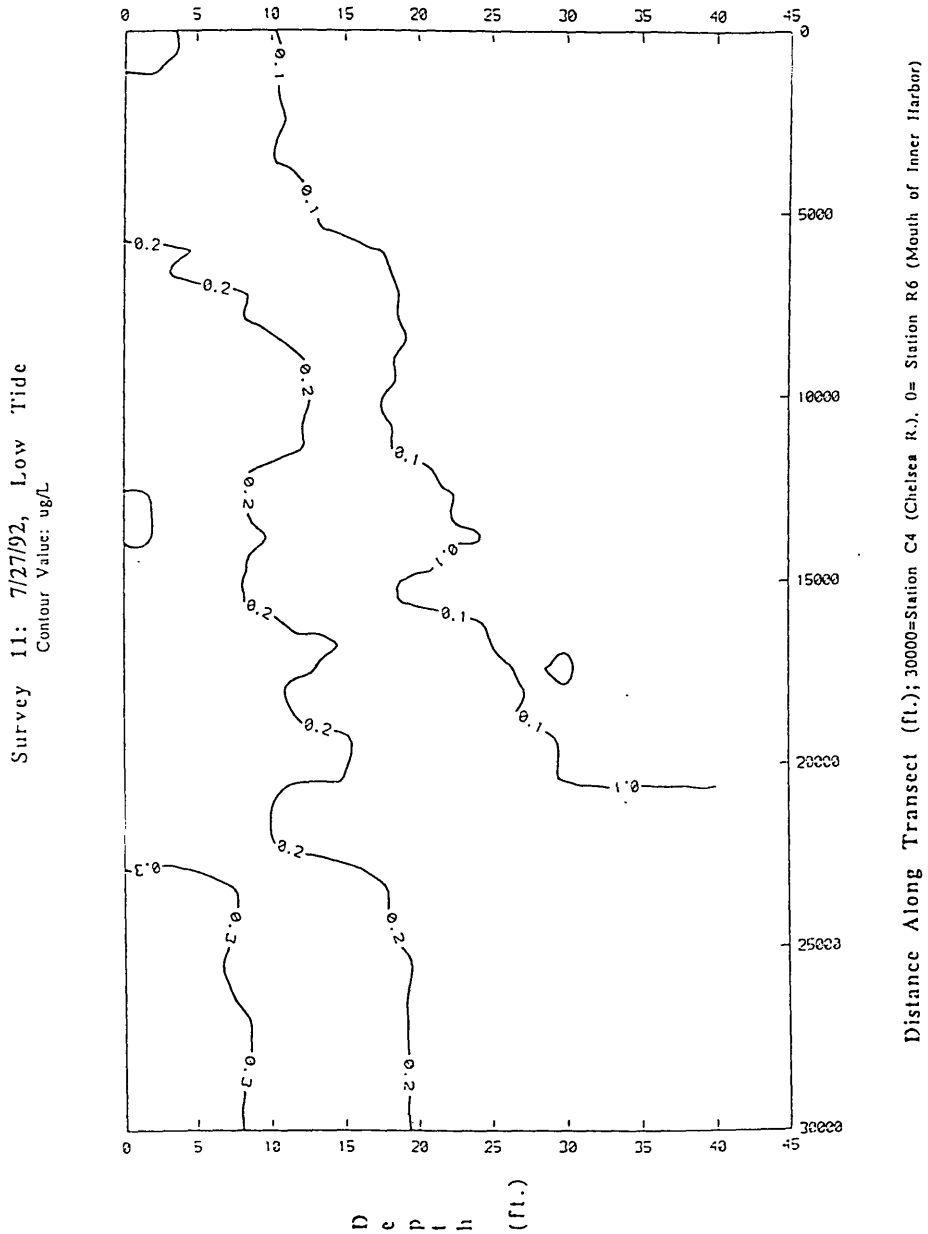


Figure A-3: Longitudinal-vertical contours of tracer concentration ( $\mu\text{g/l}$ ) for dye study at 115 hours after the initial release of tracer. Charles River Dam located at approximately 19,000 ft in the longitudinal direction.

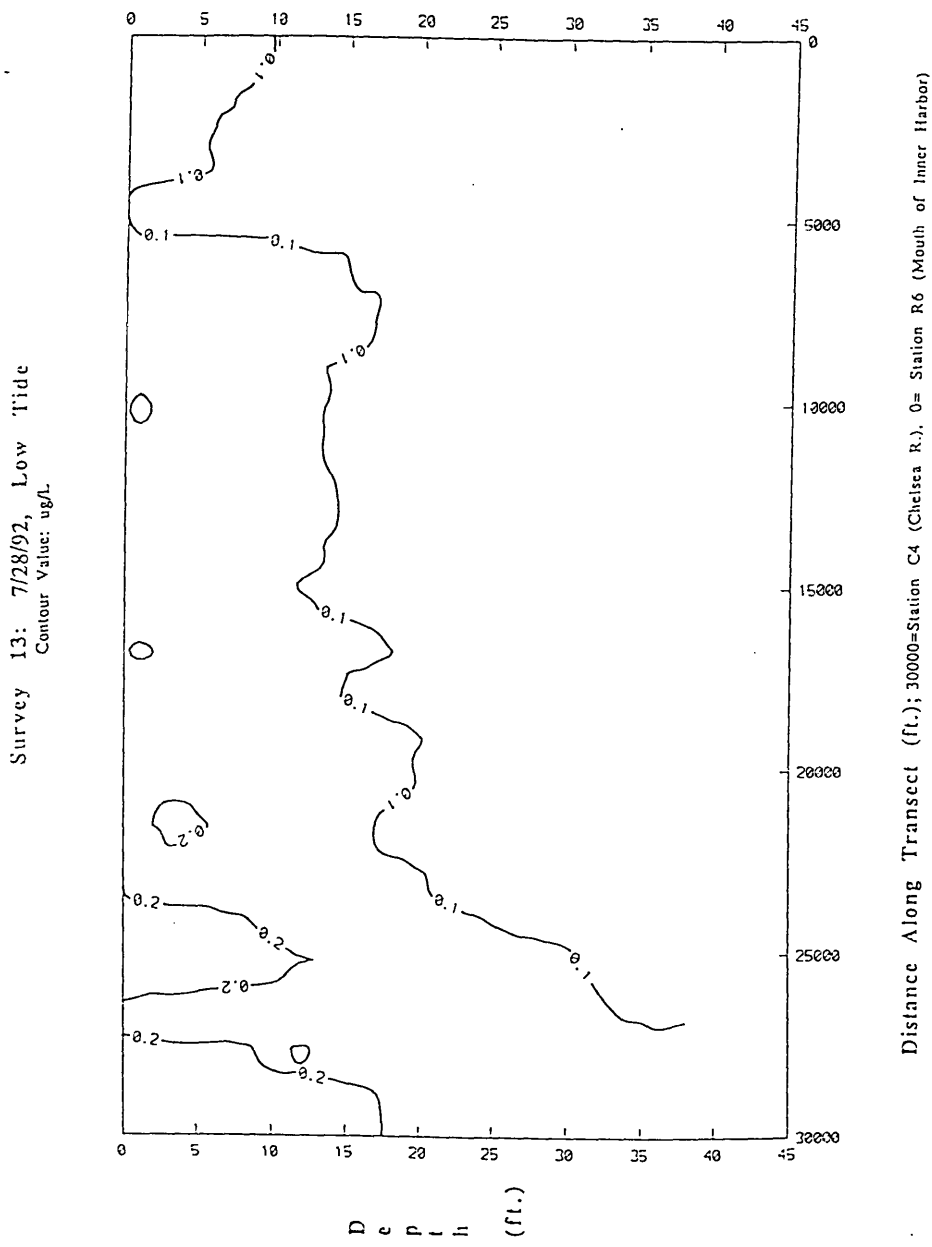


Figure A-4: Longitudinal-vertical contours of tracer concentration ( $\mu\text{g/l}$ ) for dye study at 140 hours after the initial release of tracer. Charles River Dam located at approximately 19,000 ft in the longitudinal direction.

# Appendix B

## Model simulation plots

The following sections will show the variation of the flow field and the the movement of the conservative tracer with time for the model base case and for the case in which the background vertical mixing coefficient,  $um_1$ , is increased to a value of  $7.5 \times 10^{-5} \text{ m}^2/\text{s}$ .

### B.1 Base case

The flow fields and concentration contours, at various time steps during the model simulation and at longitudinal and vertical cross-sections, for the base case are shown in the sections below.

#### B.1.1 Base case velocity vectors

The flowfield of the model domain for every 8 eight hours of simulation time are shown in Figures B-1 through B-6. The top figures are slices through the middle row of the Inner Harbor (j-index of 36, corresponding to  $y=8030 \text{ m}$ ) showing the longitudinal (x) and vertical (z) axes. Note that because of the small x-z aspect ratio (1:690), the direction and magnitude of the vertical velocity components of these velocity vectors are greatly exaggerated. The bottom figures are plan views of the surface layer of the domain, showing the longitudinal (x) and lateral (y) directions.

It can be seen that the flowfield is fairly uniform, both for the longitudinal and lateral cross-sections, especially in the Outer Harbor region. The strong vertical velocities are associated either with the freshwater discharges from the Mystic and Charles Rivers, the river plume fronts, or the sudden expansion/contraction at the Inner Harbor mouth. The fronts produced by the model are in agreement with field studies on fronts and river plumes. [9] [12] [13] [14] [18] [27] Both experimental results and the numerical modeling show a downward circulation at the fronts and a slight rising in the lower region near the front.

Small circular, vortex-like, flow patterns are produced in the Outer Harbor region, near the Inner Harbor mouth; examples of these are in Figures B-1 and B-6. Because these patterns occur approximately every 24 hours, it can be deduced that they are induced by tidal currents. The incoming flood tide is in opposition with the river plume, creating a shear.

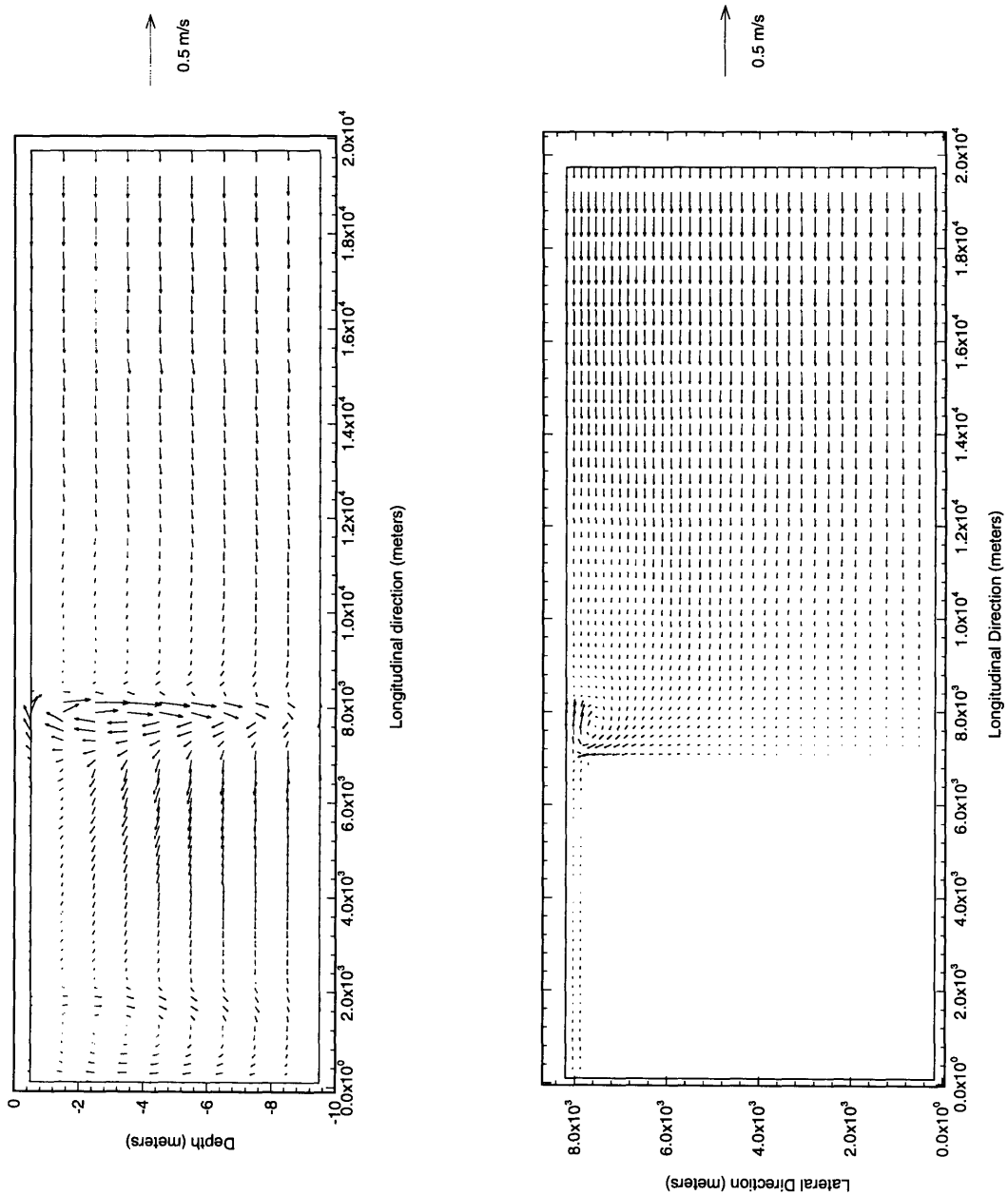


Figure B-1: Velocity vectors for the base case at model time  $t = 32$  hrs (11 hrs after initial injection of tracer)

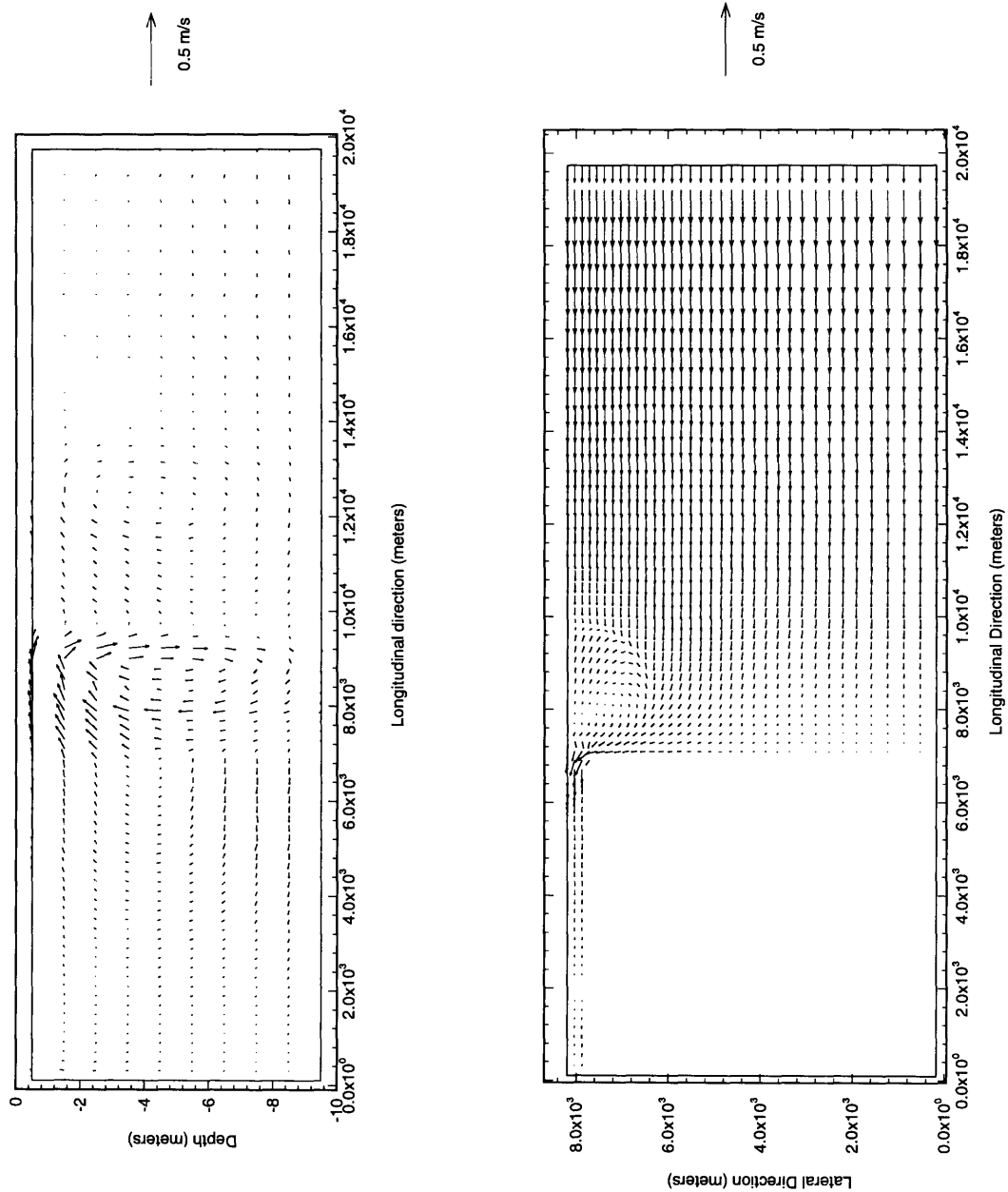


Figure B-2: Velocity vectors for the base case at model time  $t = 56$  hrs (35 hrs after initial injection of tracer)

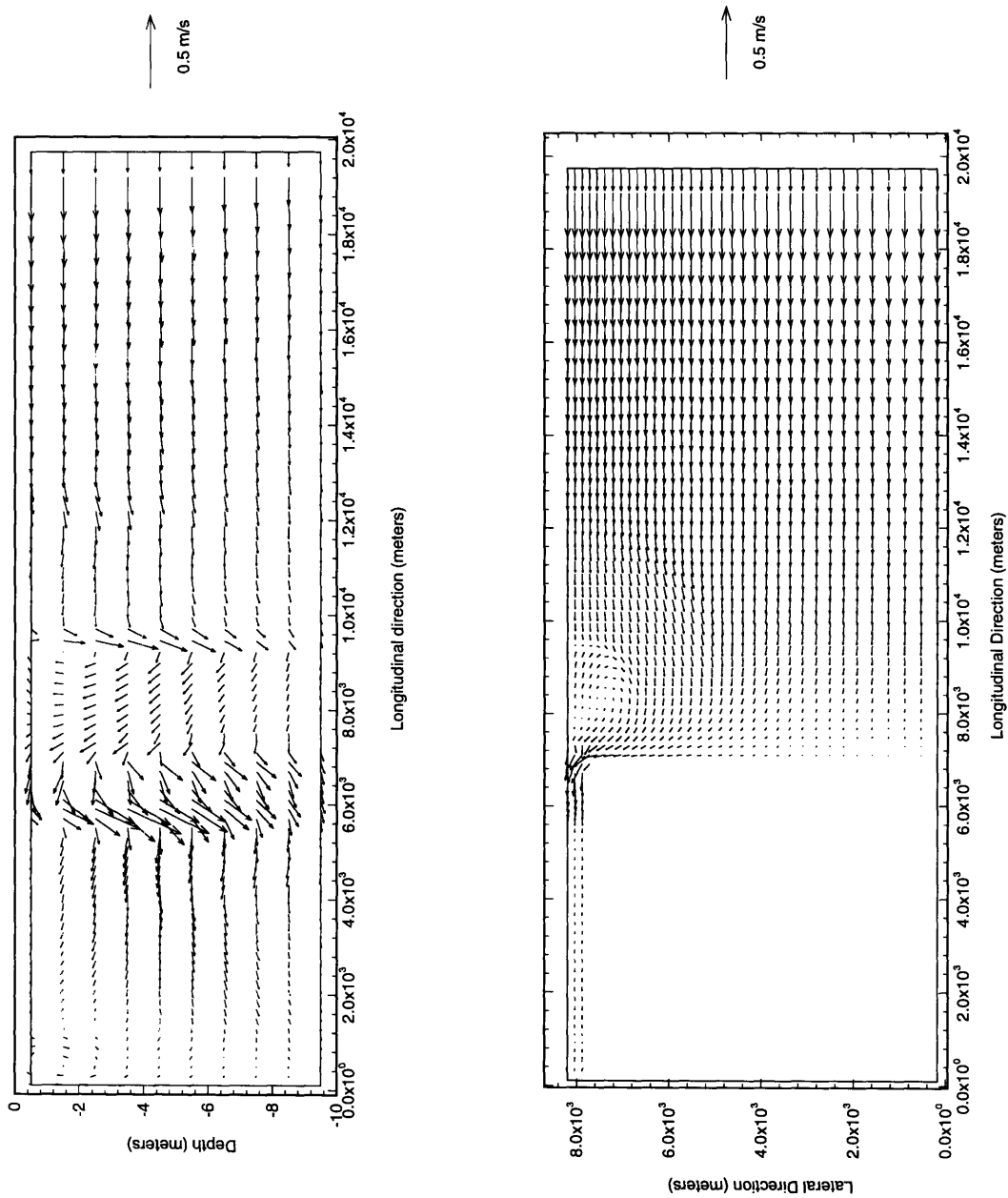


Figure B-3: Velocity vectors for the base case at model time  $t = 72$  hrs (51 hrs after initial injection of tracer)



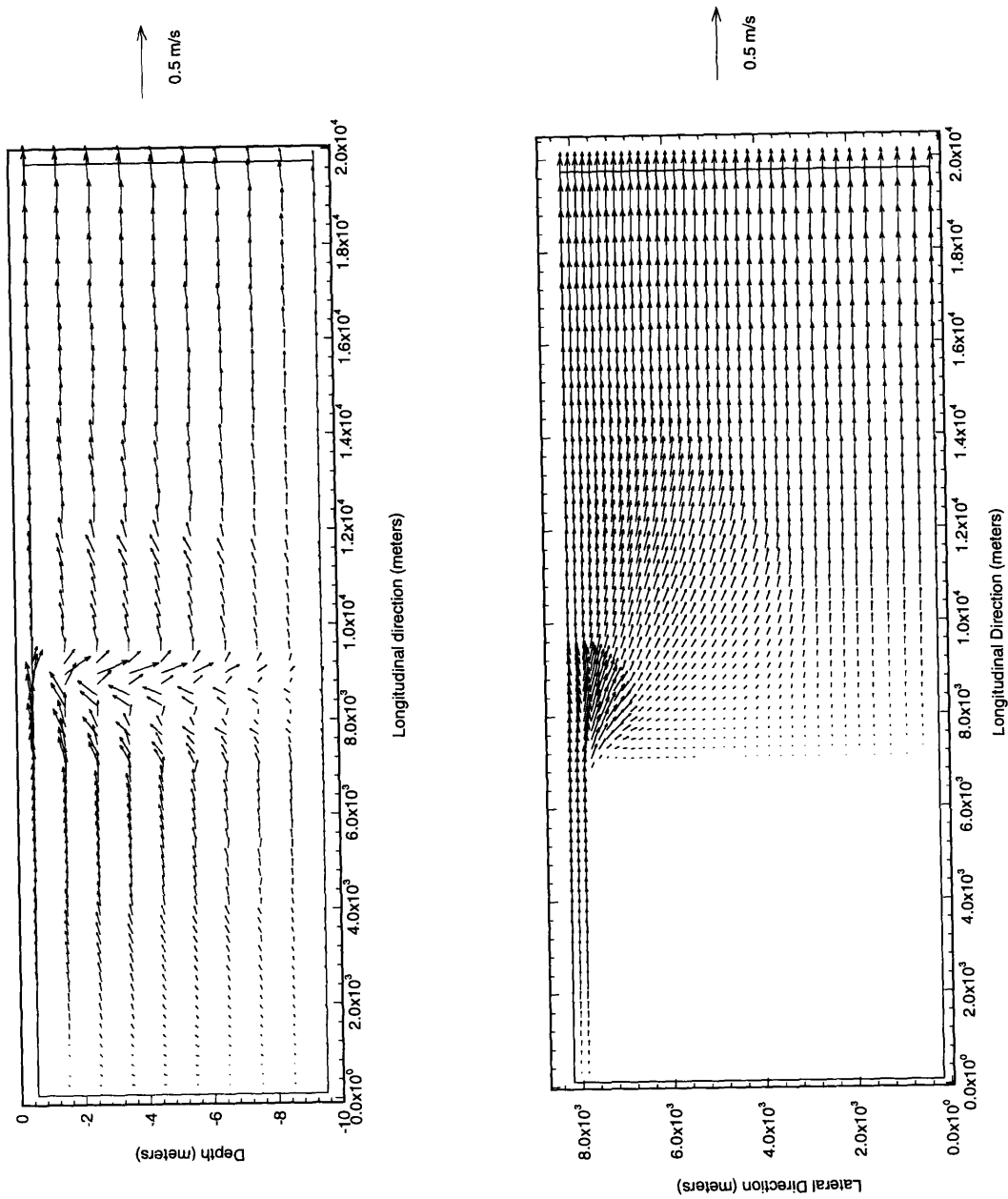


Figure B-4: Velocity vectors for the base case at model time  $t = 104$  hrs (83 hrs after initial injection of tracer)

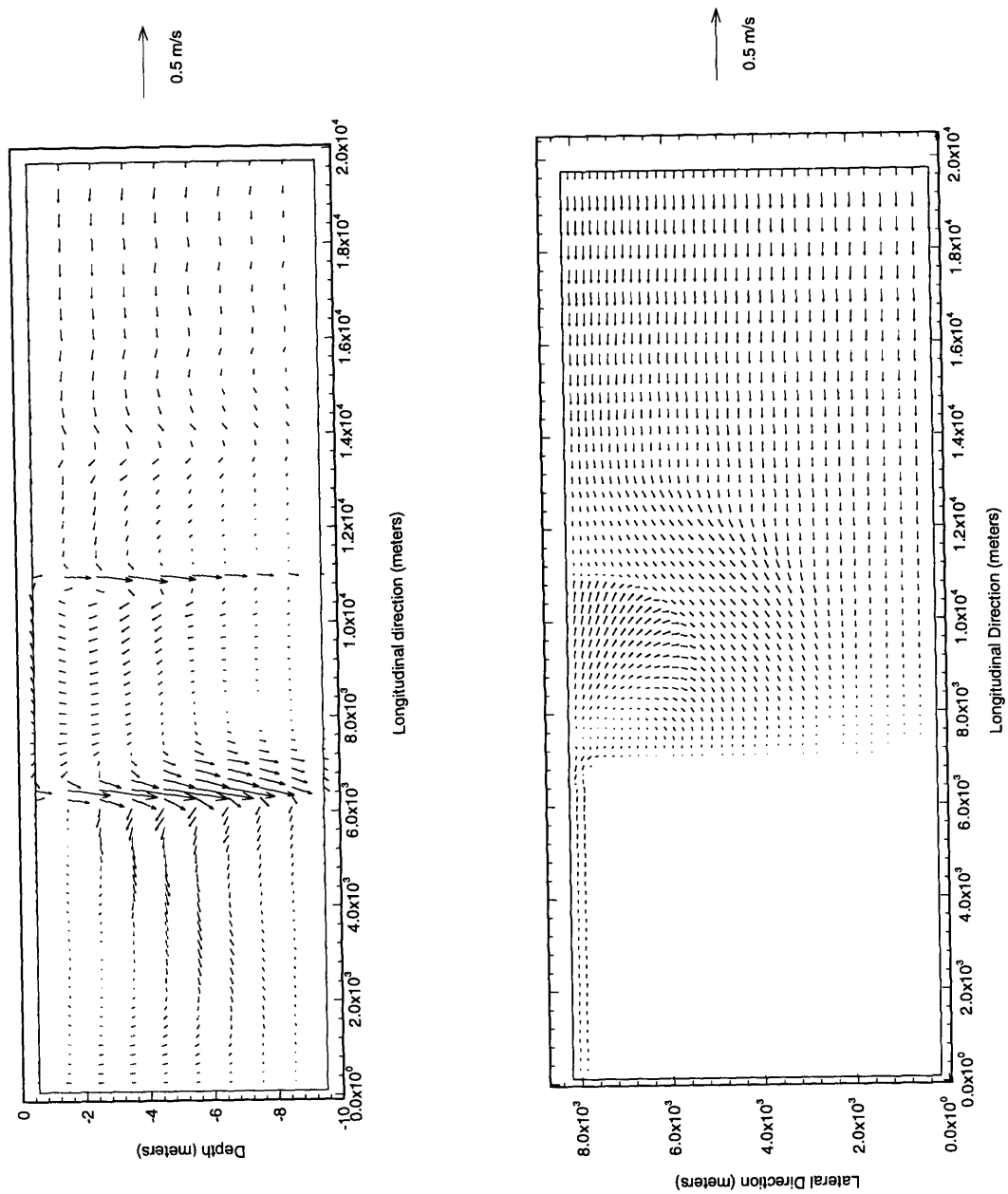


Figure B-5: Velocity vectors for the base case at model time  $t = 136$  hrs (115 hrs after initial injection of tracer)

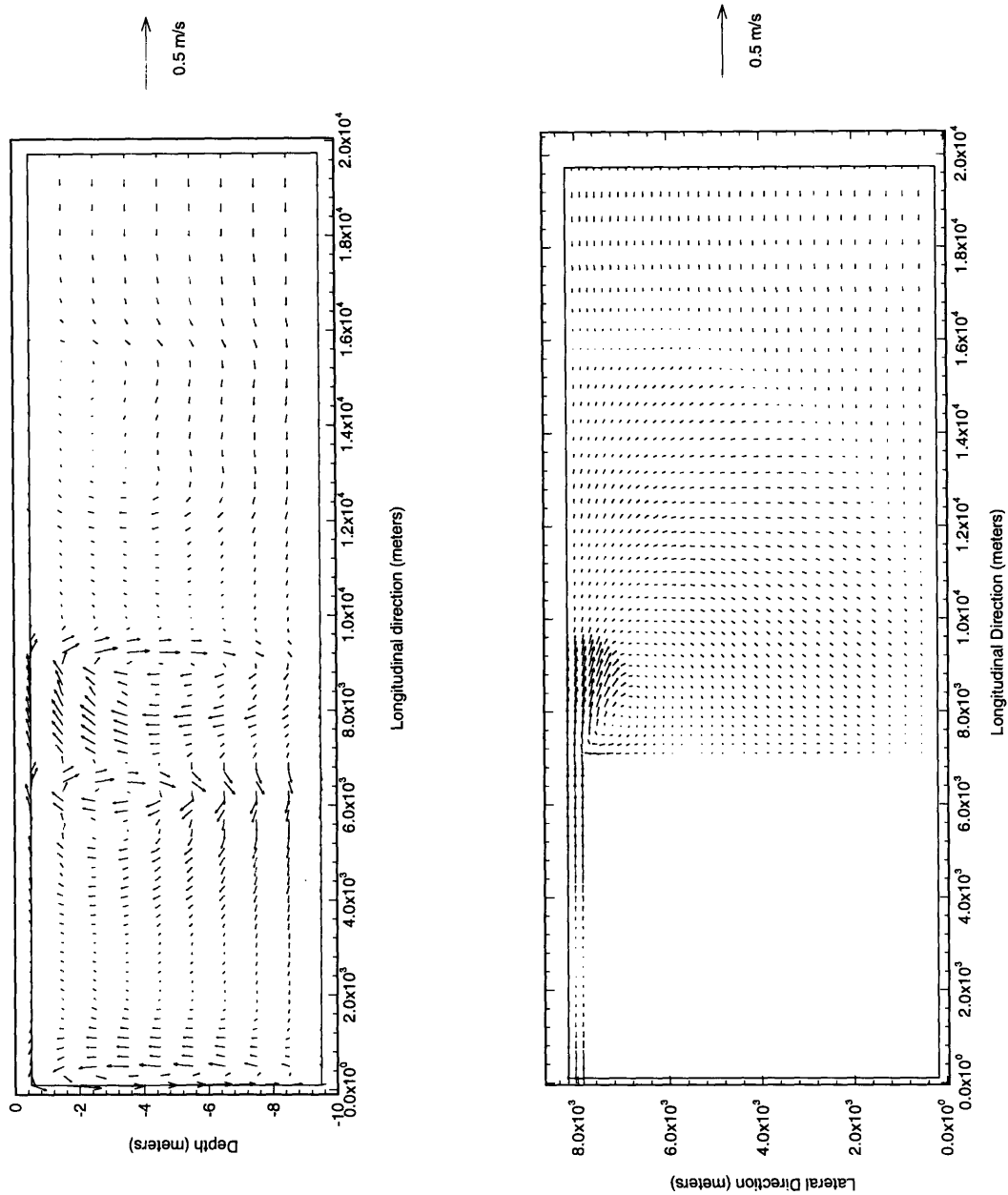


Figure B-6: Velocity vectors for the base case at model time  $t = 168$  hrs (147 hrs after initial injection of tracer)

### B.1.2 Base case concentration contours

The tracer concentration contours of the model domain for every eight hours of simulation time, starting from  $t = 24$  hours, are shown in Figures B-7 through B-12. The top figures are slices through the middle row of the Inner Harbor (j-index of 36, corresponding to  $y=8030$  m) showing the longitudinal (x) and vertical (z) axes. Note that because of the small x-z aspect ratio (1:690), the horizontal concentration gradients are greatly exaggerated. Note also that the contour scale is exponential. The bottom figures are plan views of the surface layer of the domain, showing the longitudinal (x) and lateral (y) directions.

Figures B-7 through B-10 show stratification in the tracer concentration in most of the Inner Harbor. Subsurface maximum concentrations may also be seen in Figures B-8, which are due to the surface discharge of freshwater from the Mystic River. Separation of the concentration contour intervals is observed at model  $t = 72$  hours, as indicated in B-9. This separation in the Outer Harbor, near the Inner Harbor mouth, is due to the circular flow field in this region interacting with the ebbing and flooding tide. Starting at model time  $t = 104$ , it can be seen that the tracer mass is fairly well-mixed laterally in the Outer Harbor.

There is a significant rise in the tracer mass when it reaches the Outer Harbor, as indicated in Figures B-8 through B-12. This is due to the lateral expansion in the Outer Harbor, which allows the mass to move laterally outward and therefore decreases the vertical spreading of the mass. The sloping structure of fronts and river plumes can also be seen in these concentration contours.

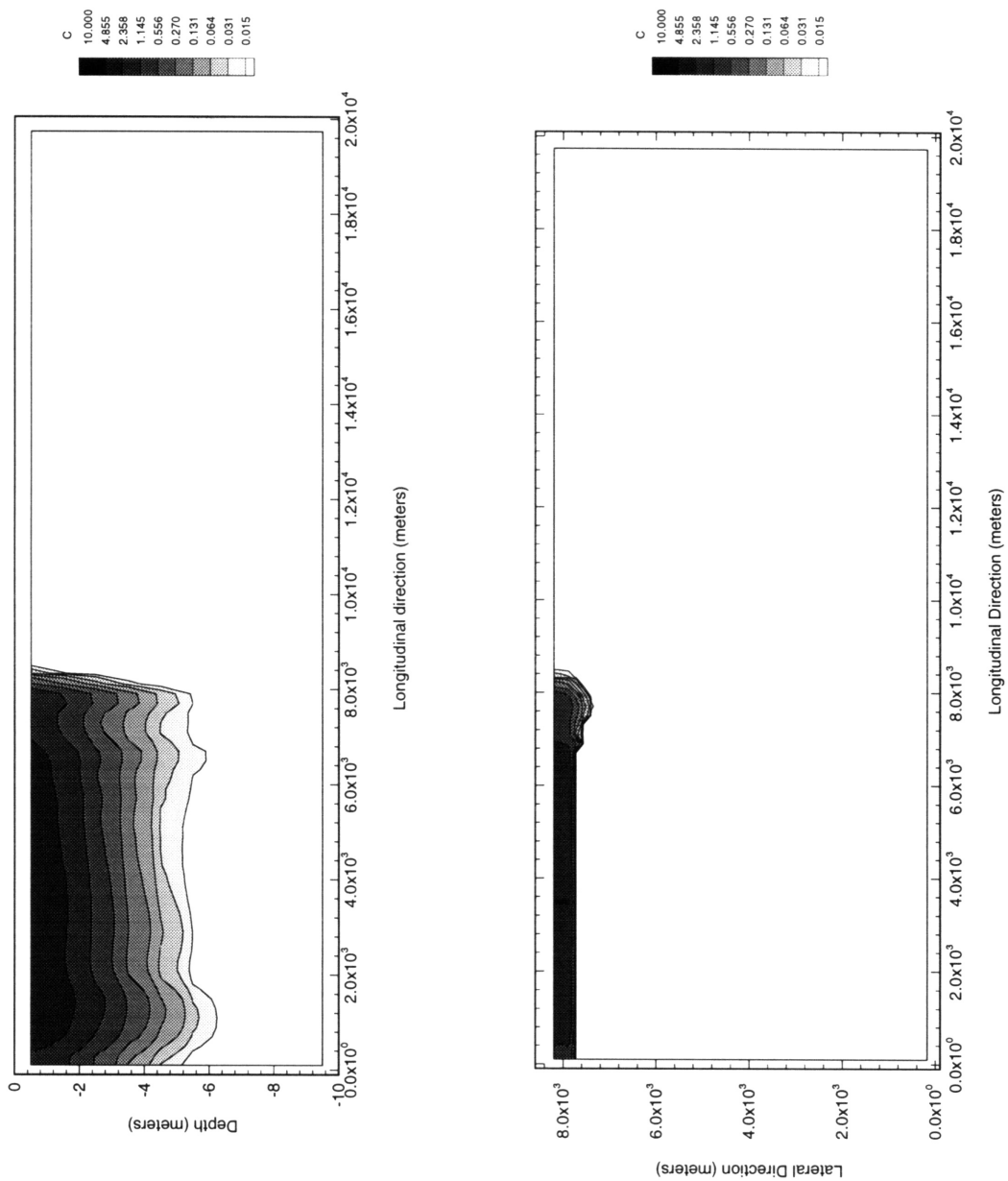


Figure B-7: Tracer concentration ( $\mu\text{g/l}$ ) contours for the base case at model time  $t = 32$  hrs (11 hrs after initial injection of tracer)

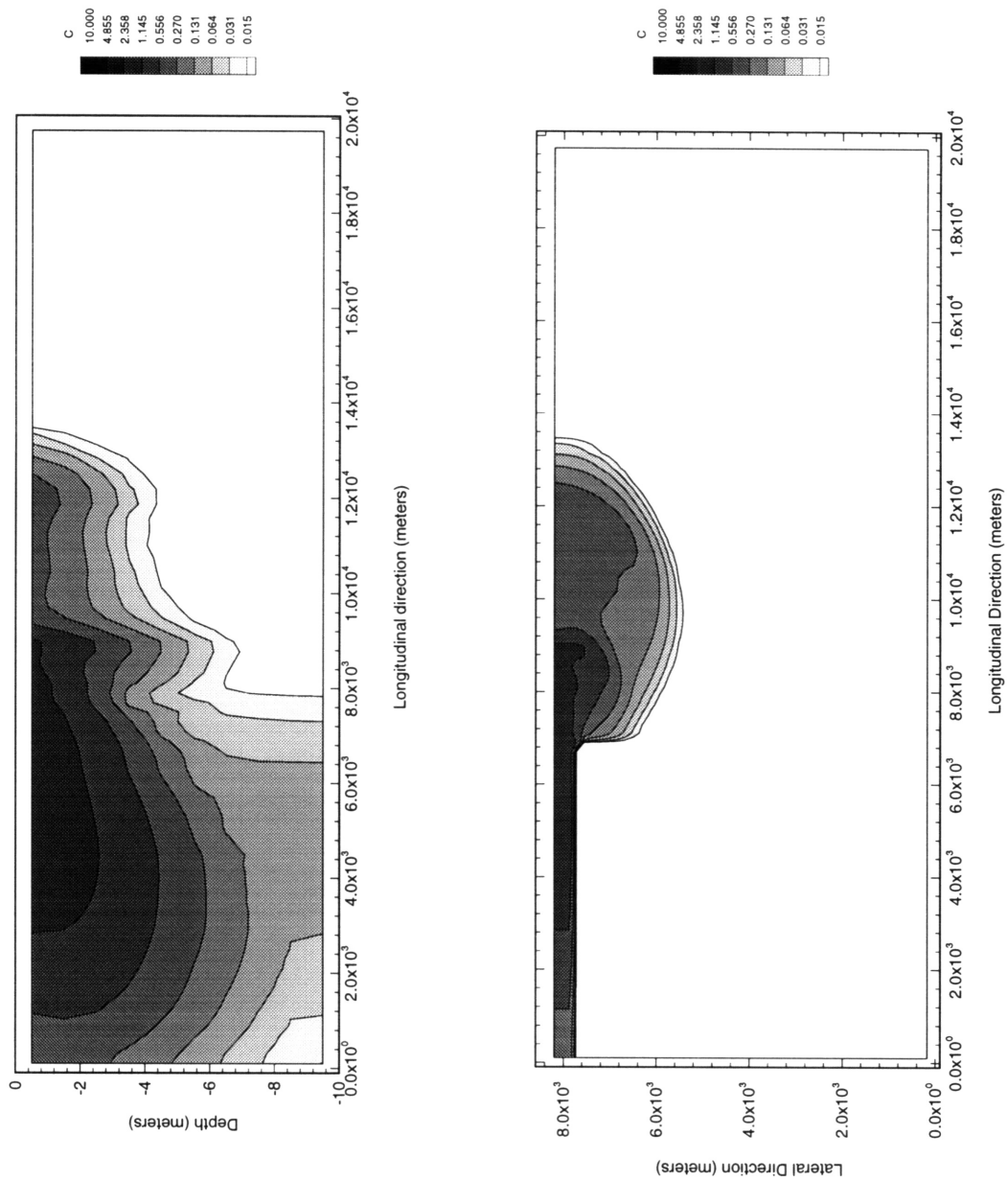


Figure B-8: Tracer concentration ( $\mu\text{g}/\text{l}$ ) contours for the base case at model time  $t = 56$  hrs (35 hrs after initial injection of tracer)

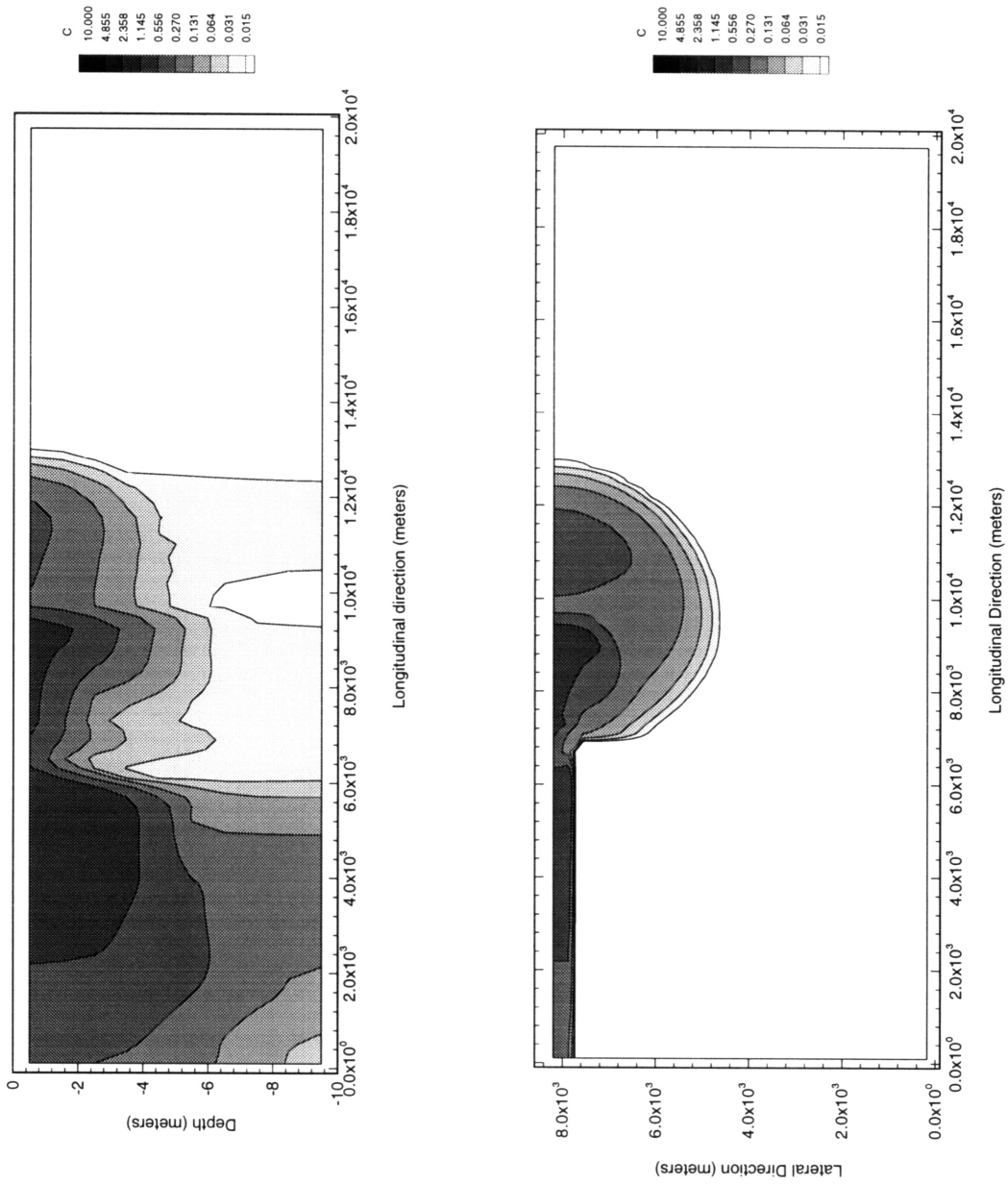


Figure B-9: Tracer concentration ( $\mu\text{g/l}$ ) contours for the base case at model time  $t = 72$  hrs (51 hrs after initial injection of tracer)

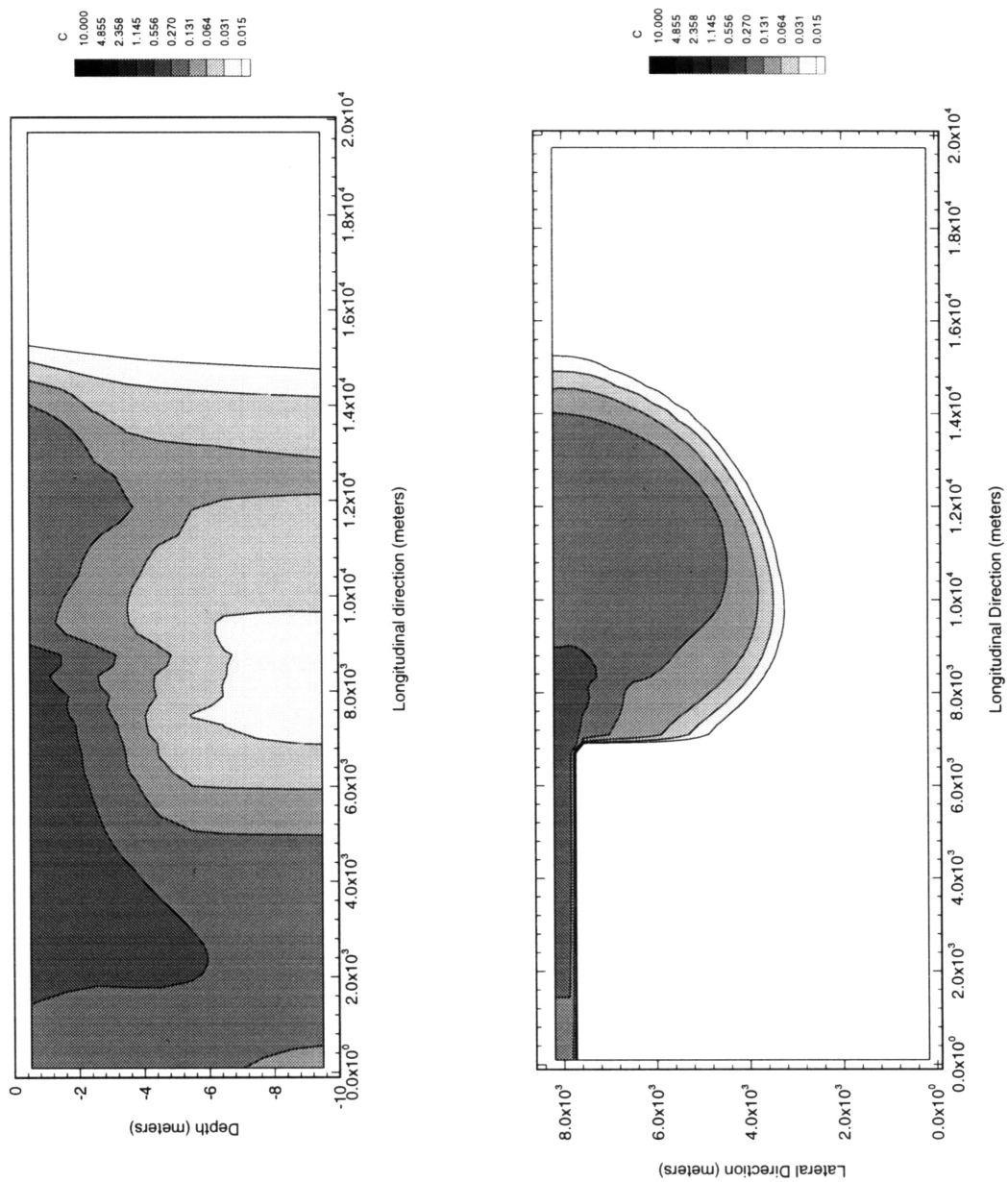


Figure B-10: Tracer concentration ( $\mu\text{g/l}$ ) contours for the base case at model time  $t = 104$  hrs (83 hrs after initial injection of tracer)



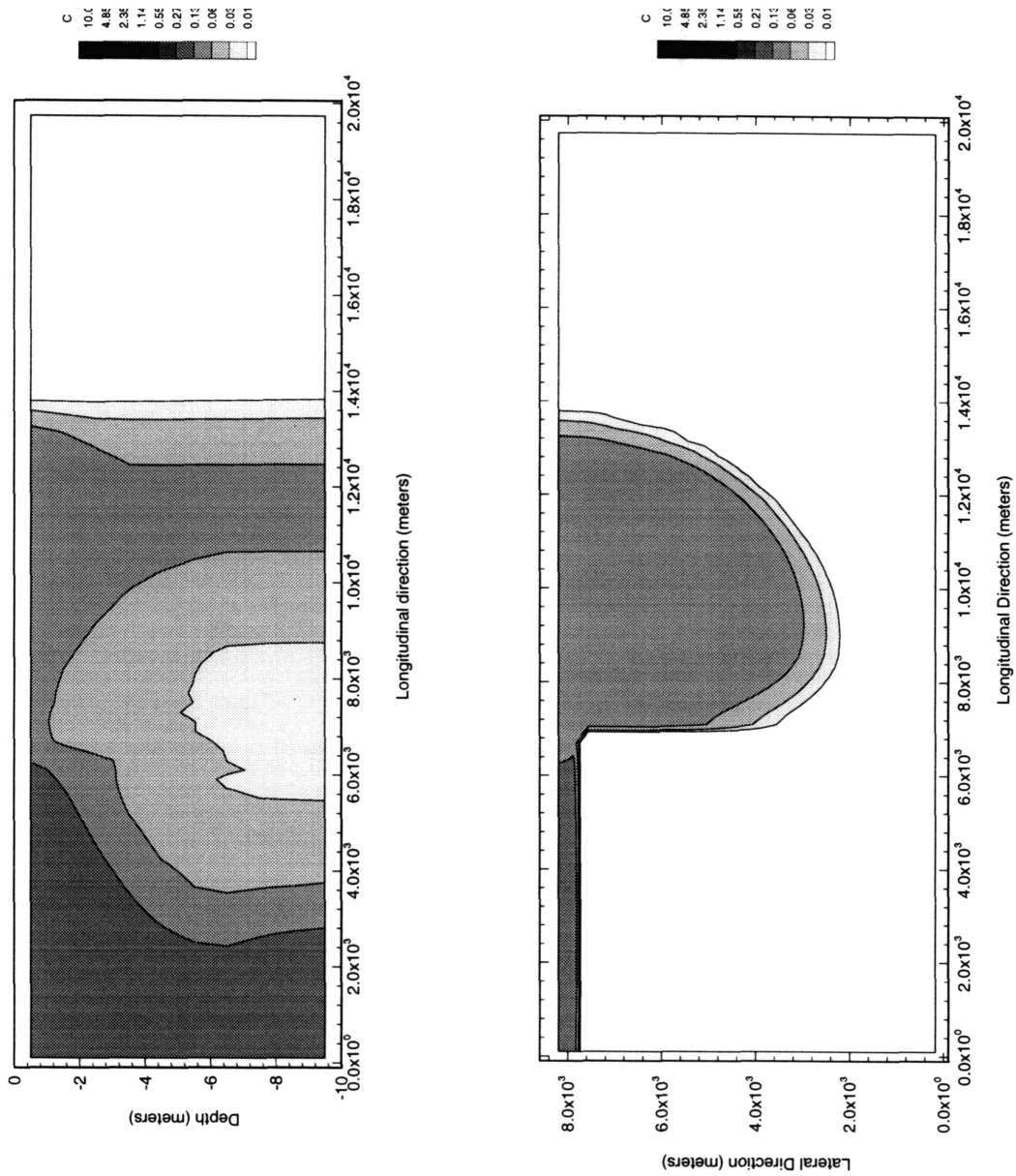


Figure B-11: Tracer concentration ( $\mu\text{g/l}$ ) contours for the base case at model time  $t = 136$  hrs (115 hrs after initial injection of tracer)

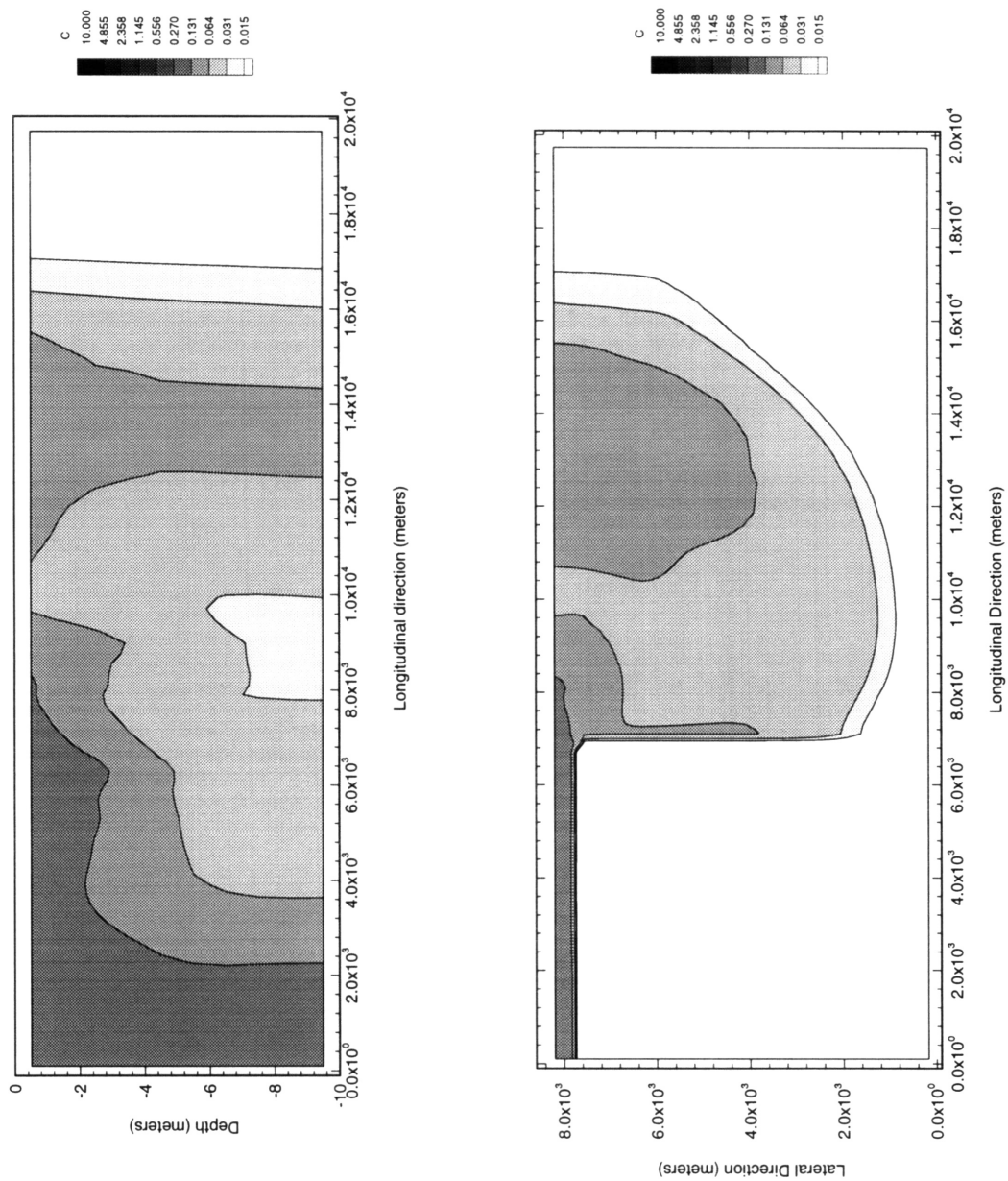


Figure B-12: Tracer concentration ( $\mu\text{g}/\text{l}$ ) contours for the base case at model time  $t = 168$  hrs (147 hrs after initial injection of tracer)

## B.2 Variation in vertical diffusivity

The tracer concentration contours of the model domain for every eight hours of simulation time, starting from  $t = 24$  hours, are shown in Figures B-13 through B-18. The top figures are slices through the middle row of the Inner Harbor (j-index of 36, corresponding to  $y=8030$  m) showing the longitudinal (x) and vertical (z) axes. Note that because of the small x-z aspect ratio (1:690), the horizontal concentration gradients are greatly exaggerated. Note also that the contour scale is exponential. The bottom figures are plan views of the surface layer of the domain, showing the longitudinal (x) and lateral (y) directions.

There is a significant vertical variation in the tracer mass in the Inner Harbor region up until model time  $t = 104$  hours. A subsurface maximum in the tracer concentration, which is caused by the discharge of freshwater from the Mystic River at the surface, at model times  $t = 56$  hours, as seen in Figures B-14. The tracer concentration contours separate in the Outer Harbor region near the Inner Harbor mouth at model time  $t = 56$  hours. Again, this separation in the Outer Harbor, near the Inner Harbor mouth, is due to the circular flow field in this region interacting with the ebbing and flooding tide. Starting at model time  $t = 136$ , it can be seen that the tracer mass is fairly well-mixed laterally in the Outer Harbor.

A significant rise in the tracer mass when the tracer reaches the Outer Harbor, as indicated in Figures B-14 through B-16. This is due to the lateral expansion in the Outer Harbor, which allows the mass to move laterally outward and therefore decreases the vertical spreading of the mass. The sloping structure of fronts and river plumes can also be seen in these concentration contours.

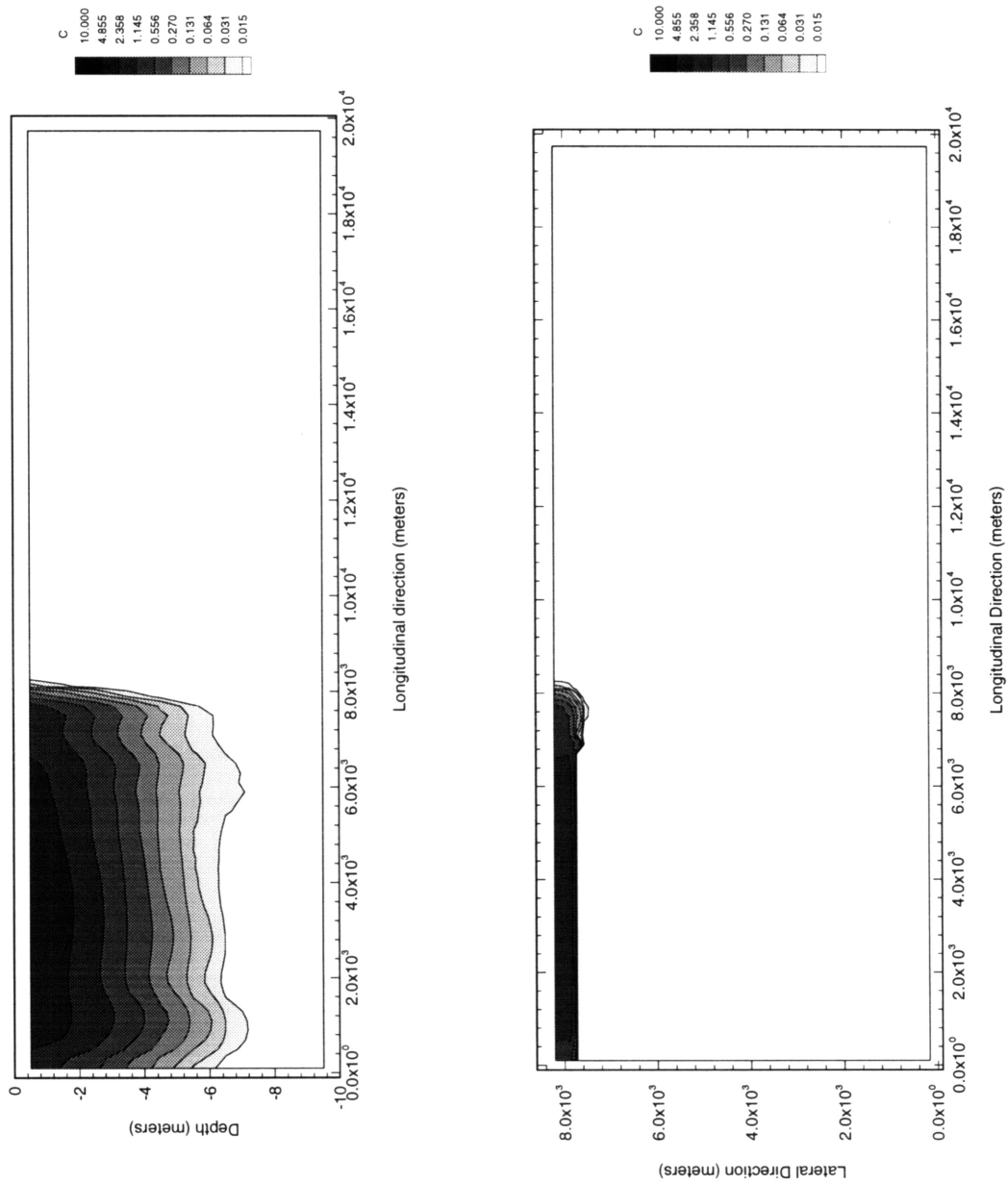


Figure B-13: Tracer concentration ( $\mu\text{g/l}$ ) contours for  $u_{m01} = 7.5 \times 10^{-5} \text{ m}^2/\text{s}$  at model time  $t = 32 \text{ hrs}$  (11 hrs after initial injection of tracer)

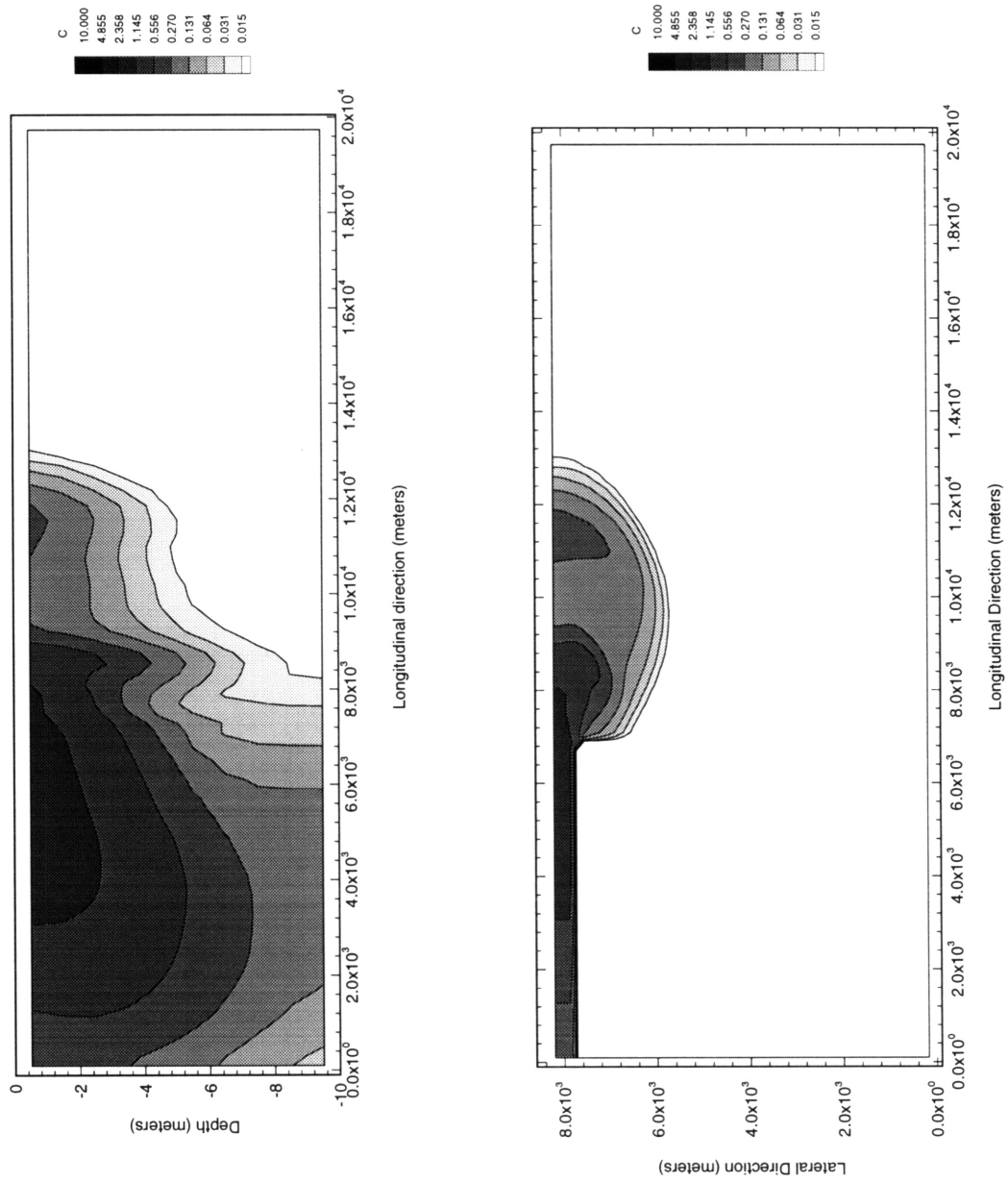


Figure B-14: Tracer concentration ( $\mu\text{g/l}$ ) contours for  $u_{\text{mol}}=7.5 \times 10^{-5} \text{ m}^2/\text{s}$  at model time  $t = 56 \text{ hrs}$  (35 hrs after initial injection of tracer)

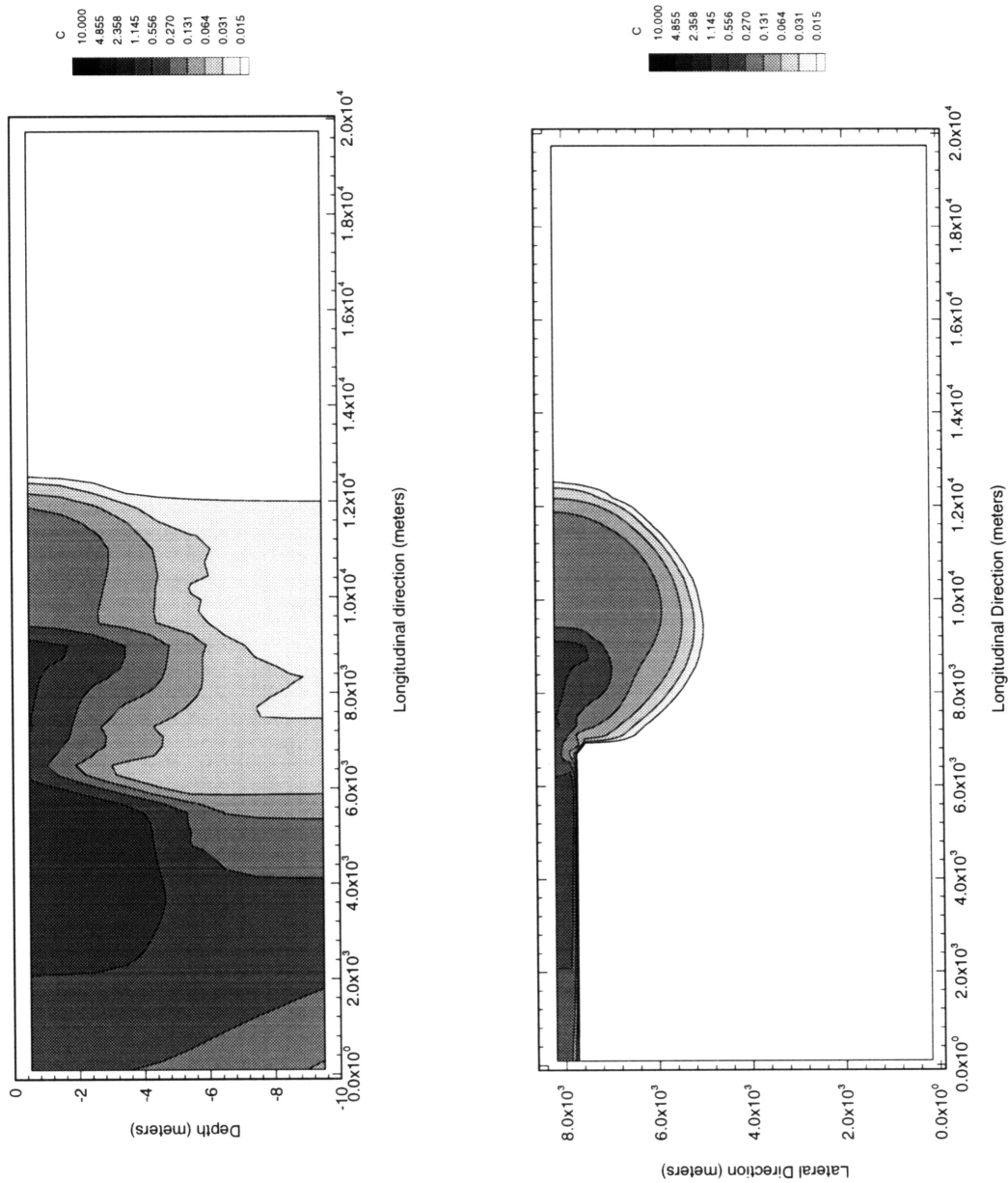


Figure B-15: Tracer concentration ( $\mu\text{g/l}$ ) contours for  $u_{\text{mol}}=7.5 \times 10^{-5} \text{ m}^2/\text{s}$  at model time  $t = 72 \text{ hrs}$  (51 hrs after initial injection of tracer)

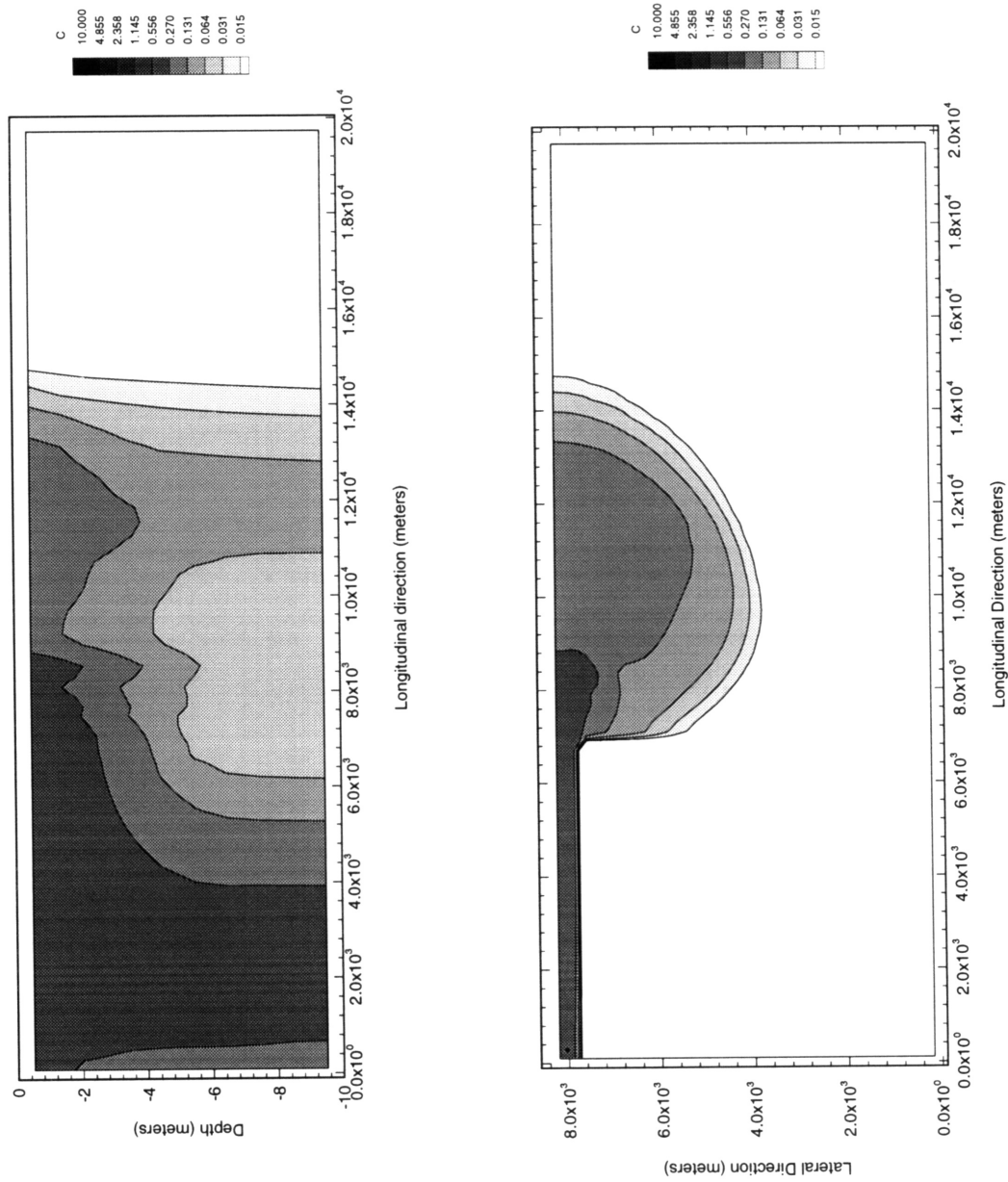


Figure B-16: Tracer concentration ( $\mu\text{g/l}$ ) contours for  $u_{m01} = 7.5 \times 10^{-5} \text{ m}^2/\text{S}$  at model time  $t = 104$  hrs (83 hrs after initial injection of tracer)

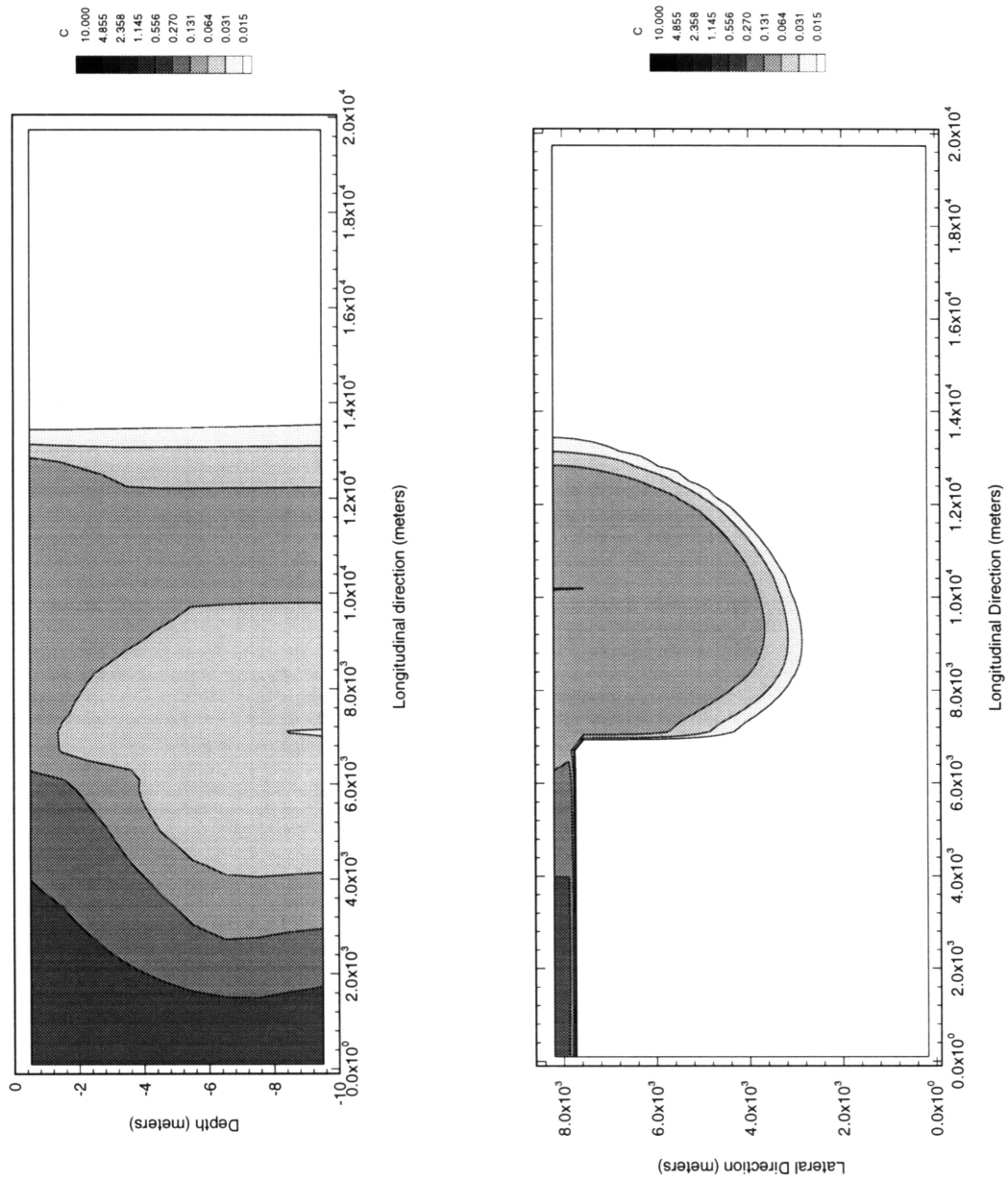


Figure B-17: Tracer concentration ( $\mu\text{g/l}$ ) contours for  $u_{\text{mol}}=7.5 \times 10^{-5} \text{ m}^2/\text{s}$  at model time  $t = 136 \text{ hrs}$  (115 hrs after initial injection of tracer)



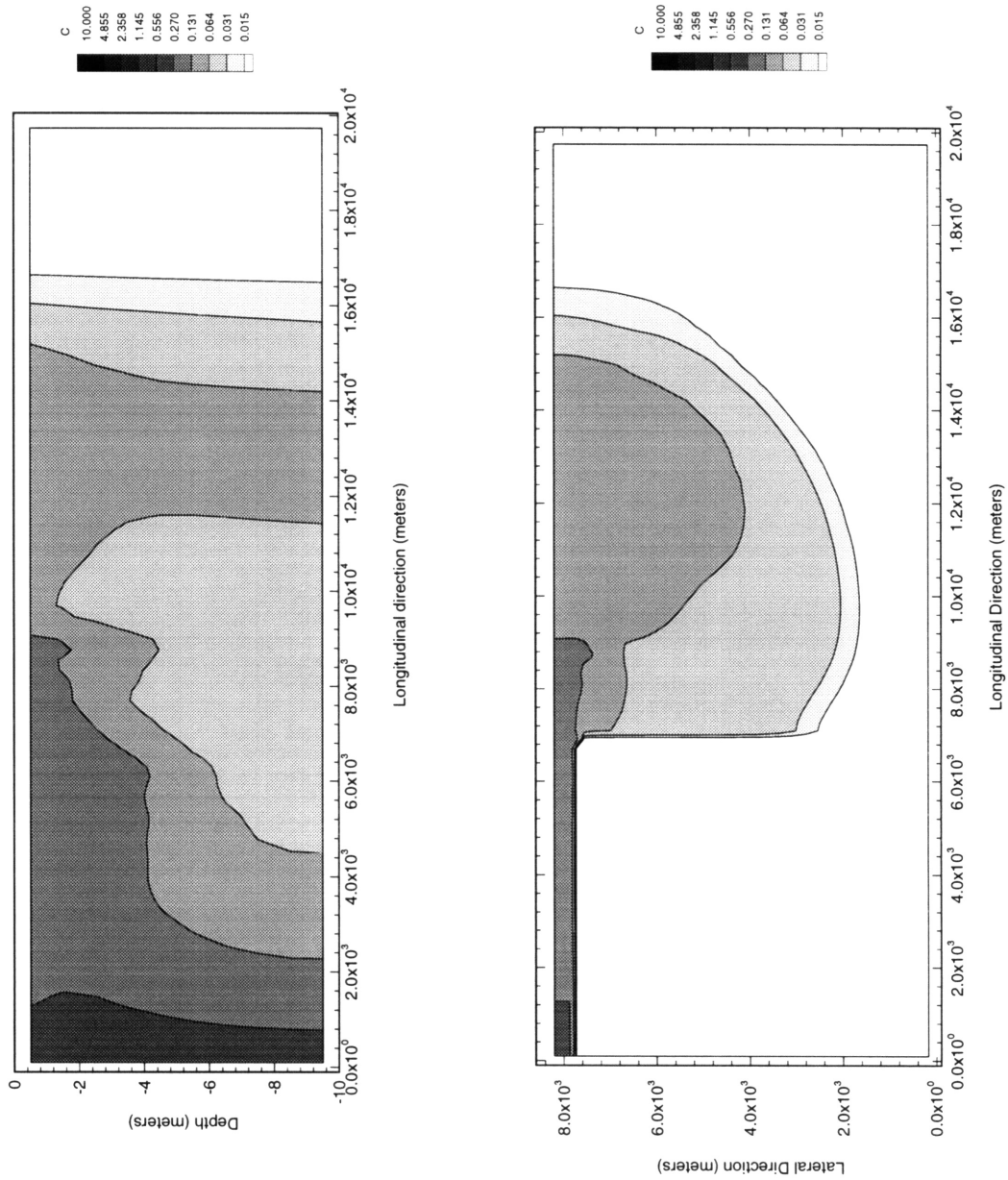


Figure B-18: Tracer concentration ( $\mu\text{g/l}$ ) contours for  $u_{m01} = 7.5 \times 10^{-5} \text{ m}^2/\text{s}$  at model time  $t = 168 \text{ hrs}$  (147 hrs after initial injection of tracer)

# Bibliography

- [1] Adams, E. E., D. L. McGillivray, S. W. Suh, R. R. Luxenberg. 1993. Analysis of Boston Inner Harbor Dye Study.
- [2] Alber, M. and A. B. Chan. 1994. Sources of contaminants to Boston Harbor: Revised loading estimates. Technical Report 94-1. Environmental Quality Department, Massachusetts Water Resources Authority, Charlestown, Massachusetts.
- [3] Blumberg, A. F. and G. L. Mellor. 1980. A Coastal Ocean Numerical Model, in *Mathematical Modelling of Estuarine Physics, Proceedings of an International Symposium*, Hamburg, 24-26 August 1978. J. Sundermann and K. P. Holz, eds., Springer-Verlag, Berlin.
- [4] Blumberg, A. F. and G. L. Mellor. 1987. A Description of the Circulation in the Gulf of Mexico, *Israel Journal of Earth Sciences*, **34**, 122-144.
- [5] Bowden, K. F. 1963. The mixing processes in a tidal estuary. *International Journal of Air Water Pollution*. **7**, 343-356.
- [6] Bowden, K. F. 1967. Stability effects on mixing intidal currents. *Phys. Fluids Supplement*. **10**, S278-S280.
- [7] Bumpus, D. F., W. S. Butcher, W. D. Athern, and C. G. Day. 1953. Inshore survey project, Boston, Final harbor report. Ref. 53-20, Woods Hole Oceanographic Institution, Woods Hole, Massachusetts.

- [8] Casulli, V. 1990. Semi-implicit Finite Difference Methods for the Two-dimensional Shallow Water Equations. *Journal of Comput. Physics*, **86**, 56-74.
- [9] Cromwell, T. and J. L. Reid, Jr. 1956. A Study of Ocean Fronts, *Tellus*, **8**(1), 94-101.
- [10] Fischer, H. B., E. J. List, R. C. Y. Koh, J. Imberger, and N. H. Brooks. *Mixing in Inland and Coastal Waters*, Academic Press, Inc., San Diego.
- [11] Galperin, B., L. H. Kantha, S. Hassid, and A. Rosati. 1988. A Quasi-equilibrium Turbulent Energy Model for Geophysical Flows, *Journal of Atmospheric Science*, **45**, 55-62.
- [12] Garvine, R. W. 1974a. Physical Features of the Connecticut River Outflow During High Discharge, *Journal of Geophysical Research*, **79**(6), 831-846.
- [13] Garvine, R. W. 1974b. Dynamics of Small-Scale Oceanic Fronts, *Journal of Physical Oceanography*, **4**, 557-569.
- [14] Garvine, R. W. and J. D. Monk. 1974. Frontal Structure of a River Plume, *Journal of Geophysical Research*, **79**(15), 2251-2259.
- [15] Harleman, D. R. F. 1966. Pollution in estuaries, in *Estuary and Coastline Hydrodynamics*, McGraw-Hill, New York, pp. 630-647.
- [16] HydroQual. 1991. A Primer for ECOM-si. HydroQual, Inc., Mahwah, New Jersey 07430.
- [17] Ketchum, D. A. 1951. The flushing of tidal estuaries. *Sewage and Industrial Wastes*, **23**, 189-209.
- [18] Knauss, J. A. 1957. An Observation of an Oceanic Front, *Tellus*, **9**(2), 234-237.
- [19] Mellor, G. L. and T. Yamada. 1982. Development of a Turbulence Closure Model for Geophysical Fluid Problems, *Rev. Geophysical Space Physics*, **20**, 851-875.

- [20] Munk, W. and E. R. Anderson. 1948. Notes on a theory of the thermocline. *Journal of Marine Research*. **7**, 276-295.
- [21] Officer, C. B. 1976. *Physical Oceanography of Estuaries (and Associated Coastal Waters)*. John Wiley and Sons, Inc., New York.
- [22] Partch, E. N. and J. D. Smith. 1978. Time dependent mixing in a salt wedge estuary. *Estuarine Coastal Marine Science*. **6**, 3-19.
- [23] Phillips, N. A. 1957. A Coordinate System Having Some Special Advantages for Numerical Forecasting, *Journal of Meteorology*, **14**, 184-185.
- [24] Rao, G. V. and T. S. Murty. 1973. Some Case Studies of Vertical Circulations Associated with Oceanic Fronts, *Journal of Geophysical Research*, **78**(3), 549-557.
- [25] Roache, P. 1982. *Computational Fluid Dynamics*. Revised printing, Hermosa, Albuquerque, New Mexico, Appendix A.
- [26] Sanford, L. P., W. C. Boicourt, and S. R. Rives. 1992. Model for Estimating Tidal flushing of Small Embayments, *Journal of Waterways, Port, Coastal and Ocean Engineering*, ASCE, **118**(6): 635-654.
- [27] Stommel, H. and H. G. Farmer. 1952. Abrupt Change in Width in Two-Layer Open Channel Flow, *Journal of Marine Research*, **9**(2), 205-214.
- [28] U. S. Geological Survey. 1992. Water resources data, Massachusetts and Rhode Island Water Year 1992.